

Theo yêu cầu của khách hàng, trong một năm qua, chúng tôi đã dịch qua 16 môn học, 34 cuốn sách, 43 bài báo, 5 sổ tay (chưa tính các tài liệu từ năm 2010 trở về trước) Xem ở đây

**DỊCH VỤ
DỊCH
TIẾNG
ANH
CHUYÊN
NGÀNH
NHANH
NHẤT VÀ
CHÍNH
XÁC
NHẤT**

Chỉ sau một lần liên lạc, việc dịch được tiến hành

Giá cả: có thể giảm đến 10 nghìn/1 trang

Chất lượng: Tao dựng niềm tin cho khách hàng bằng công nghệ 1. Bạn thấy được toàn bộ bản dịch; 2. Bạn đánh giá chất lượng. 3. Bạn quyết định thanh toán.

Tài liệu này được dịch sang tiếng việt bởi:

www.mientayvn.com

Tìm bản gốc tại thư mục này (copy link và dán hoặc nhấn Ctrl+Click):

<https://drive.google.com/folderview?id=0B4rAPqlxIMRDSFE2RXQ2N3FtdDA&usp=sharing>

Liên hệ để mua:

thanhlam1910_2006@yahoo.com hoặc frbwrthes@gmail.com hoặc số 0168 8557 403 (gặp Lâm)

Giá tiền: 1 nghìn /trang đơn (trang không chia cột); 500 VND/trang song ngữ

Dịch tài liệu của bạn: http://www.mientayvn.com/dich_tiang_anh_chuyen_nghanh.html

FUNDAMENTAL ELECTROMAGNETIC CONCEPTS FOR RAM

In Chapter I, the concept of RAM was introduced as a means for reducing the RCS of aerospace vehicles. Numerous RAM were also introduced in that chapter; many of which still find extensive use in stealth, antenna engineering and microwave related technologies. It was also mentioned that these RAM vary considerably in their absorption characteristics. An enhancement in the absorption due to the RAM coating on a target results in lower scattered EM fields and hence radar cross section reduction (RCSR) of the target.

It is possible in principle to predict the electromagnetic fields at an observation point, i.e., the receiving radar, by the application of EM field theory. In this chapter, we first introduce Maxwell's equations in their most general form. These equations constitute the starting point for F.M wave propagation analysis. The wave analysis involves not only free space propagation and interaction at the interface of two media, but also through bounded material medium. EM wave propagation equations are set up in this chapter for the three most common cases of free space, homogeneous, and inhomogeneous propagation.

Wave propagation through a material medium is governed by the intrinsic physical parameters of the medium, viz. its permittivity, permeability and conductivity. The well known classes of dielectric and

CÁC KHÁI NIỆM ĐIỆN TỪ CƠ BẢN VỀ RAM

Trong chương I, chúng tôi đã đưa ra khái niệm RAM như một cách để làm giảm RCS của các phương tiện hàng không vũ trụ. Một số lượng lớn RAM cũng được trình bày trong chương đó. Nhiều RAM trong số đó vẫn được sử dụng rộng rãi trong các công nghệ tàng hình, kỹ thuật anten và các công nghệ liên quan đến vi sóng. Nhiều nghiên cứu cho thấy rằng các đặc tính hấp thụ của các RAM khác nhau rất khác nhau. Lớp phủ RAM trên mục tiêu giúp tăng cường khả năng hấp thụ, dẫn đến giảm trường EM tán xạ và từ đó làm giảm tiết diện radar của mục tiêu.

Về nguyên tắc, chúng ta có thể dự đoán trường điện từ tại một điểm quan sát, tức là ở radar thu bằng cách áp dụng lý thuyết trường EM. Trong chương này, đầu tiên, chúng tôi giới thiệu các phương trình Maxwell dưới dạng tổng quát nhất của chúng. Những phương trình này là bước khởi đầu để tiếp tục phân tích sự lan truyền sóng F.M. Việc phân tích sóng không chỉ liên quan tới truyền sóng trong chân không và sự tương tác tại mặt phân cách của hai môi trường, mà chúng ta còn phải phân tích các sóng qua môi trường vật chất hữu hạn. Các phương trình truyền sóng EM được thiết lập trong chương này cho ba trường hợp phổ biến nhất là chân không, môi trường truyền sóng đồng nhất và không đồng nhất.

Sóng lan truyền qua một môi trường vật chất bị chi phối bởi các tham số vật lý nội tại của môi trường đó, tức là, hằng số điện môi, độ từ thẩm, và độ dẫn của môi trường. Về cơ bản, các loại RAM điện môi và từ phổ biến nhất thể hiện

magnetic RAM are essentially a manifestation of these intrinsic EM parameters of the medium. It is also possible to explain the various properties, such as isotropy, linearity and reciprocity of the medium in terms of the nature of these parameters.

In the optical region one frequently encounters the phenomena of optical activity and circular dichroism. Drawing upon a microwave analog of these, one may visualize chiral materials, which are in fact highly effective absorbers. The electromagnetic parameters corresponding to chirality are defined in Section 2.4.

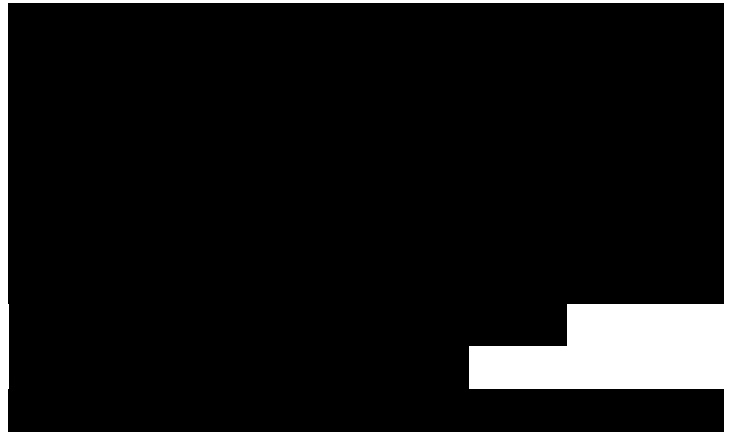
2.1 MAXWELL'S EQUATIONS

The most fundamental laws of electromagnetics are Maxwell's equations which originate from Faraday's law, Ampere's law, and Gauss's law. These are expressed in differential form as

In the equations above, E and H are the electromagnetic field vectors. The wave propagation analysis is often carried out in terms of these. E and H refer to the electric field strength and the magnetic field strength, respectively. D is known as the electric displacement density whereas its analog, B , is called the magnetic flux density. The partial derivative in eqs. (2.1) and (2.2) is with respect to the time t . Finally, the symbols J and ρ appearing in the right hand side of eqs (2.2) and (2.3) refer to the electric current density and the volume charge density, respectively.

Equation (2.1) follows from the Faraday induction law, while eq. (2.2) is a generalization of the Ampere circuital law by Maxwell and is also referred to as the

các tham số EM nội tại của môi trường. Chúng ta cũng có thể giải thích những tính chất khác, chẳng hạn như tính đẳng hướng, tuyến tính, và thuận nghịch của môi trường theo bản chất của những thông số này.



Maxwell-Ampere law. Equation (2.3) is the differential form of Gauss's law for the electric displacement density. Finally, eq. (2.4) merely states that magnetic monopoles are non-existent. It is in fact the **magnetic analog** of Gauss's law, and can be readily derived from the Biot-Savart law.

Although one is accustomed to four Maxwell equations, two of these, namely, the divergence relations (2.3) and (2.4) can be derived from the curl equations (2.1) and (2.2) (Corson & Lorrain, 1962). The alternate representation of the Maxwell's equations is in the integral form and can be obtained by suitably integrating eqs. (2.1) through (2.4). The integration in the case of eqs. (2.1) and (2.2) is with respect to the **area element da** , whereas in the case of eqs. (2.3) and (2.4) it is with respect to the volume element dv . The Maxwell equations in the integral form are:

The derivation of eqs. (2.5) and (2.6) is carried out by resorting to Stokes' theorem. Stokes' theorem is a well known result of vector calculus which establishes an equivalence between the surface integrals and the line integrals; the curl of a vector A over a surface area is thus related to the vector on the curve enclosing that area.

$$\int_V \nabla \times A \, da = \oint A \, dl \quad (2.9)$$

Likewise, in the case of volume integrals, the area contour integral appearing on the left hand side of (2.7) and (2.8) follow from Gauss's divergence theorem which relates the divergence of a vector A from a volume, to the vector over the surface area enclosing that volume,

Both the differential and integral forms of Maxwell's equations are extensively used in the EM wave propagation analysis. For example, the differential form of these equations forms the starting point for the finite difference time domain (FDTD) analysis, and EM wave propagation in free space and other continuous media. On the other hand, as shall be shown in the next section, the integral form of Maxwell's equations are used to derive the boundary conditions at the interface between two media.

2.2 SURFACE BOUNDARY CONDITIONS

Equations (2.1) through (2.4) describe the spatial value of EM vectors E , H , D and B . These vectors are continuous along the direction of propagation within a medium. It is of interest to examine whether these vectors remain continuous across the interface of two different media.

We begin the discussion with eqs. (2.1) and (2.2). Hence for the corresponding integral forms (2.5) and (2.6), it is possible to visualize a surface area enclosed by a curve.

Boundary Condition I

Let an area completely enclosed by a curve be intersected by an interface of the two media as shown in Fig. 2.1. By applying Farad's law of eq. (2.5), one can visualize the electric fields E_1 and E_2 , very close to the media interface along the v -direction. Similarly, E_{1v} , E_{2v} , E_{1n} and E_{2n} are along the v -direction. The exact values for these



vectors are not known a priori. Integrating along the closed curve we get,
(2.11)

The assumption that \mathbf{r}_1 and \mathbf{r}_2 are very close to the interface, requires that A_y tends to zero. Thus
$$\oint (\mathbf{r}_1 - \mathbf{r}_2) \cdot \mathbf{A} \cdot \mathbf{v} = 0$$

(2.13)

Since E_x and \mathbf{r}_1 are tangential to the interface, eq. (2.13) is generalized as:

The first boundary condition therefore requires that the tangential component of the electric field be continuous at the interface of two arbitrary media. Without loss of generalization, let us assume that Medium 2 is a perfect conductor. For such a case, it can be shown that E_{tan} is zero, so that
(2.15)

Hence in those cases where one of the media is a conductor, the electric field can only be normal to the interface.

Figure 2.1 The boundary condition for the electric field vectors at the interface between two media

Boundary Condition 2

As mentioned above, the Maxwell-Ampere law of eq. (2.6) is also implicitly a curl relation so that the corresponding boundary condition can be analyzed in a similar manner, as shown by Fig. 2.2. Once again, integrating along the closed curve, we get
(2.16)



With reference to Fig. 2.2, it is possible to define a linear current density J , for perfectly conducting surfaces.
(2.17)

It may be noted that a Finite linear current density is generated only when the current density J is infinitely large. Equation (2.16) can then be written as

Medium 2

Figure 2.2 The boundary condition for the magnetic field vectors at the interface between two media The linear current density J_s is at the surface boundary Since A_y tends to zero (vide Fig. 2.2), that is

In cases where the current density J is finite, J_s tends to zero, and one obtains
 $\nabla_t = H_{x1}$ (2.21)

Once again since the magnetic field H_{x1} and H_{x2} , in the limit are directed along the interface to the two media, eqs. (2.20) and (2.21) may be written as

for a perfect conductor

Figure 2.3 The boundary condition for the electric displacement density at the interface The condition on the normal component of D is obtained by assuming ϵ_0 to be infinitesimally small

The second boundary condition therefore states that if there exists a linear current density at the interface as in the case of a perfect conductor, the tangential component of the magnetic field is discontinuous; in the



absence of this linear current density between two arbitrary media, the tangential component of magnetic field is continuous at the surface.

The first and second of Maxwell's equations are curl relations giving rise to the tangential boundary relations. On the other hand, eqs. (2.3) and (2.4) are divergence equations. For the corresponding integral equations (2.7) and (2.8), a finite volume completely enclosed by a surface is assumed. Such a visualization permits elegant derivation of the boundary conditions for the normal components of D and B.

Boundary Condition 3

Gauss's law (2.3) is a divergence relation which could be used to arrive at the normal boundary condition for D at the surface. Consider an infinitesimal volume $\Delta r \Delta y \Delta z$ in the rectangular coordinate system. With reference to Fig. 2.3, we obtain:

As Δy tends to zero, an elemental surface area A ($=\Delta y \Delta z$) may be defined, which is at the interface of the two media. It is then possible to define a surface charge density to describe the charge enclosed within the elemental volume

(2.25)

Substituting eq. (2.25) in eq. (2.24), we obtain the relation

$$\epsilon_0 (E_1 - E_2) \cdot \hat{n} = \rho_s$$

or

$$\epsilon_0 (E_1 - E_2) \cdot \hat{n} = \rho_s$$

Since D_{1n} and D_{2n} are normal to the surface boundary, eq. (2.26b) may be expressed as

$$\oint \mathbf{D} \cdot d\mathbf{l} = Q_{\text{free}}$$

If surface charges do not exist at the interface, as is usually the case when both the media are dielectric in nature,

$$\oint \mathbf{D} \cdot d\mathbf{l} = 0$$

Finally, if Medium 2 is a perfect conductor, the field inside, i.e., \mathbf{D}_2 is zero, and eq. (2.27) reduces to
for a perfect conductor

Thus the third boundary condition, in its general form (2.27) states that if there are free charges residing at an interface between two media, the normal components of electric displacement density on either side of the interface differ by an amount equal to the surface charge density at the interface. As a corollary, if there are no charges at the interface, the normal component of the electric displacement density is continuous across the media. Finally, if one of the media is a perfect conductor, the normal component of the electric displacement exterior to the conductor is equal to the surface charge density at its boundary.

Boundary Condition 4

The fourth boundary condition follows from the last of Maxwell's equations. Once again this is a divergence relation, so that the integral equation (2.8) yields a normal boundary condition. The boundary condition here (in Fig. 2.4) is analogous to the one in Fig. 2.3 but for the fact that there cannot be a magnetic charge density within

an enclosed volume. This follows from the well known observation that magnetic monopoles do not exist. Hence applying eq. (2.8) with reference to the Fig. 2.4, we get (2.30)

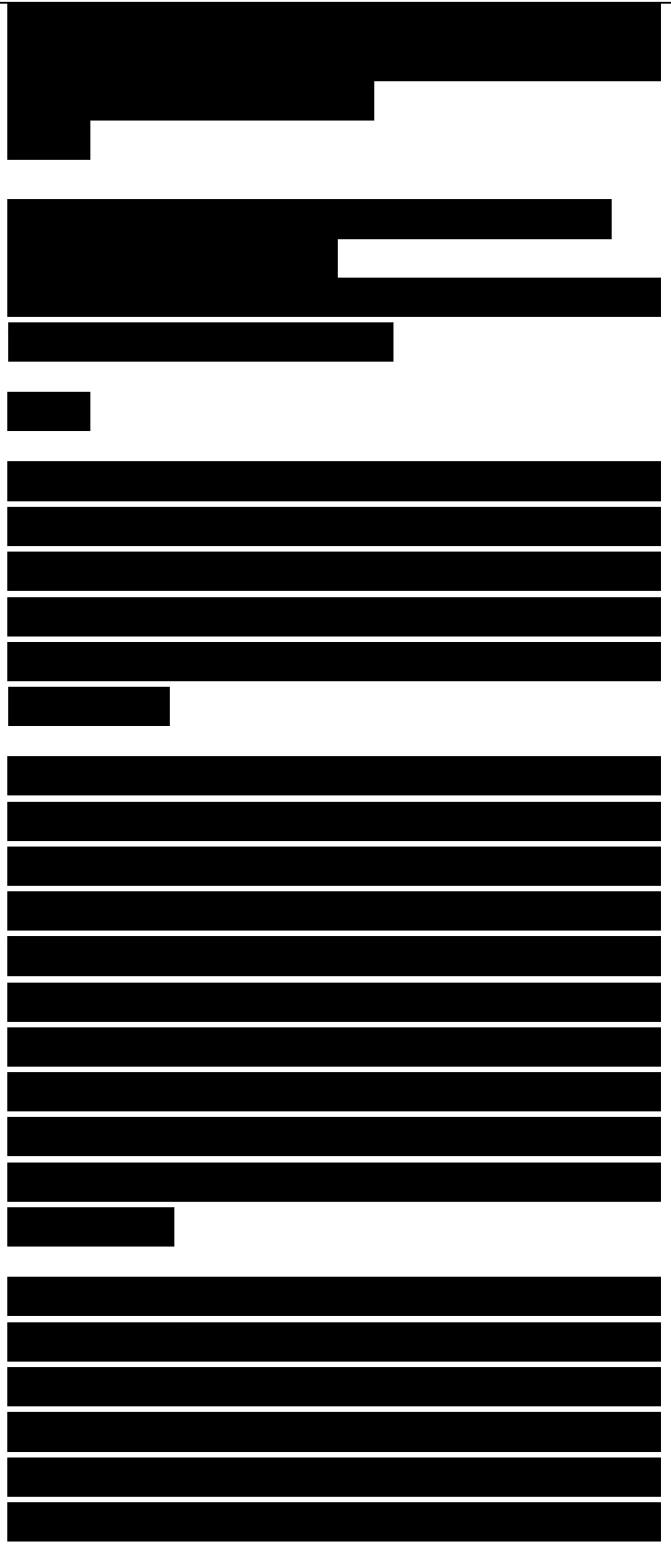
As A_y tends to zero, eq. (2.30) yields (2.31)

Once again, since the v -component is normal to the surface, we can write (2.32)

Equation (2.32) is essentially a statement of conservation of the magnetic flux lines with respect to any enclosed volume. The fourth boundary condition therefore states that the normal components of the magnetic flux density are continuous across the junction of two media.

The four boundary conditions discussed above are of relevance to stealth-type applications. To begin with, they constitute an important step in the determination of the RCS of aircraft. Aircraft surfaces are often metallic, and hence are conducting in nature. Tangential and normal boundary conditions can be applied to the problem of interaction of radar waves with the aircraft surface, where the boundary is idealized as a conductor-free space interface.

These boundary conditions, in fact, form the starting point for the EM Held analysis, even if the aerospace target is partially conducting or dielectric in nature. The method of moments (MoM) and the finite difference time domain method (FDTD) are two well known approaches applied in such cases; they are discussed in detail in Chapter

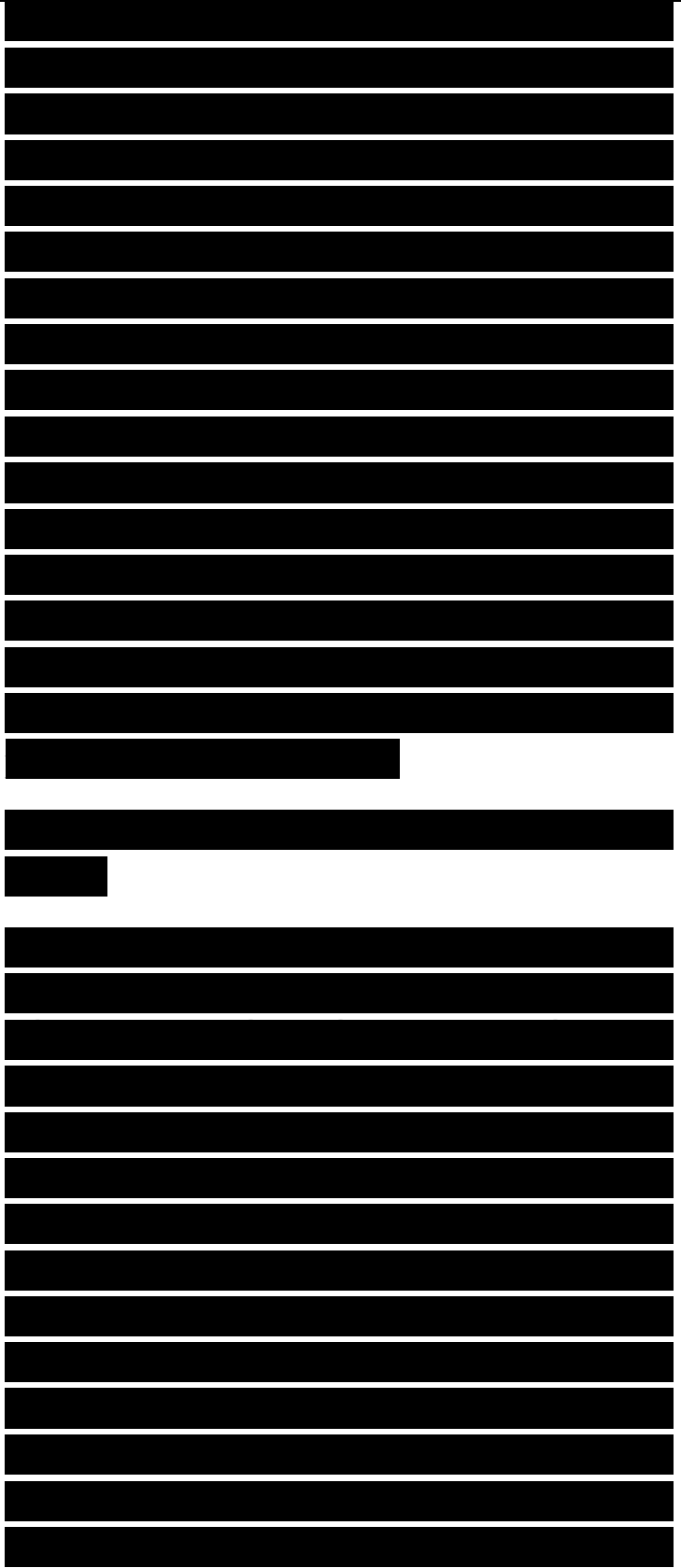


3.

These methods rely extensively on the application of the proper boundary conditions. Finally, the application of RAM coating onto the aircraft surfaces can be handled in two stages. The EM wave first impinges on the free space-RAM interface. This is a dielectric-dielectric interface, for which the normal and tangential boundary' conditions have been derived here. The RAM coating is often on the metallic surface of the aircraft. The boundary conditions outlined here also help analyze the aircraft metal surface-RAM boundary which may be a dielectric-conductor interface.

2.3 CONSTITUTIVE RELATIONS AND FEATURES OF THE MEDIUM

The Maxwell equations in Section 2.1 describe four EM vectors, viz. F., D. H, and B; the corresponding tangential and normal boundary conditions due to the curl and divergence equations are derived in Section 2.2. It is however customary to express wave propagation through free space and other material media, in terms of the electric and magnetic field strengths, F. and H, respectively. This is rendered possible by resorting to the constitutive relations of the medium which relate the electric displacement density D and the current density J to E, and the magnetic flux density B to H. This may be symbolically expressed for a general medium as



where \mathbf{r} is the position vector, and ω is the angular frequency which is related to the operational frequency f as $\omega = 2\pi f$. In eqs. (2.33) through (2.35), t denotes the time instant.

In the case of free space, \mathbf{D} is collinear with \mathbf{E} , and \mathbf{B} with \mathbf{H} . The constitutive relations are of the form

The symbols ϵ_0 , μ_0 , and σ_0 appearing in eqs. (2.36) and (2.37) are known as the permittivity and permeability of the free space. These are fundamental constants of electromagnetics with values

$$\epsilon_0 = 8.854 \times 10^{-12} \text{ Farad/meter} \quad (2.39)$$

and

$$\mu_0 = 4\pi \times 10^{-7} \text{ Henry/meter} \quad (2.40)$$

There are a wide class of materials within which the above mentioned collinearity relations of the vectors \mathbf{D} and \mathbf{J} with \mathbf{E} , and \mathbf{B} with \mathbf{H} are still valid, but they cannot be related by ϵ_0 and μ_0 alone. They can nevertheless be expressed as scalar relations:

where ϵ , μ , and σ are the permittivity, permeability and conductivity of the medium. In this book we refer to these collectively as the intrinsic EM parameters of the medium. Quite often, the permittivity and permeability of the material are expressed relative to the free space constants and ϵ_r .

where ϵ_r is the relative permittivity or the dielectric constant, and μ_r is called the relative permeability.

The magnitudes of the EM vectors D , B and J in eq. (2.41) through (2.43) are in general different from those obtained in eqs. (2.36) through (2.38). At the macroscopic level this is explained by the fact that ϵ and μ of a material medium are different from those for free space. However at the microscopic level this is explained by the fact that the medium is constituted by charged particles. When an electric or magnetic field is applied on a medium, the molecules and the atomic particles tend to align along the impressed field. This leads to the concepts of electric and magnetic polarizations of materials. The electric polarization P is defined as

$$P = \epsilon_0 \chi_e E \quad (2.46)$$

where χ_e is the electric susceptibility of dielectric medium. The magnetic polarization, or magnetization is similarly defined in terms of the magnetic susceptibility of the medium as

$$M = \chi_m H \quad (2.47)$$

The electric (or magnetic) polarization of the materials alters the electric displacement (or magnetic flux) density within a medium due to an impressed field. Thus the electric displacement density within a dielectric medium may be expressed as the superposition of the electric polarization on the free space field,

$$D = \epsilon_0 E + P \quad (2.48)$$

Substituting the electric polarization vector definition (2.46) in (2.48). we obtain

$$D = \epsilon_0 E + \epsilon_0 \chi_e E = \epsilon_0 (1 + \chi_e) E$$

From eqs. (2.41), (2.44) and (2.49), we conclude that

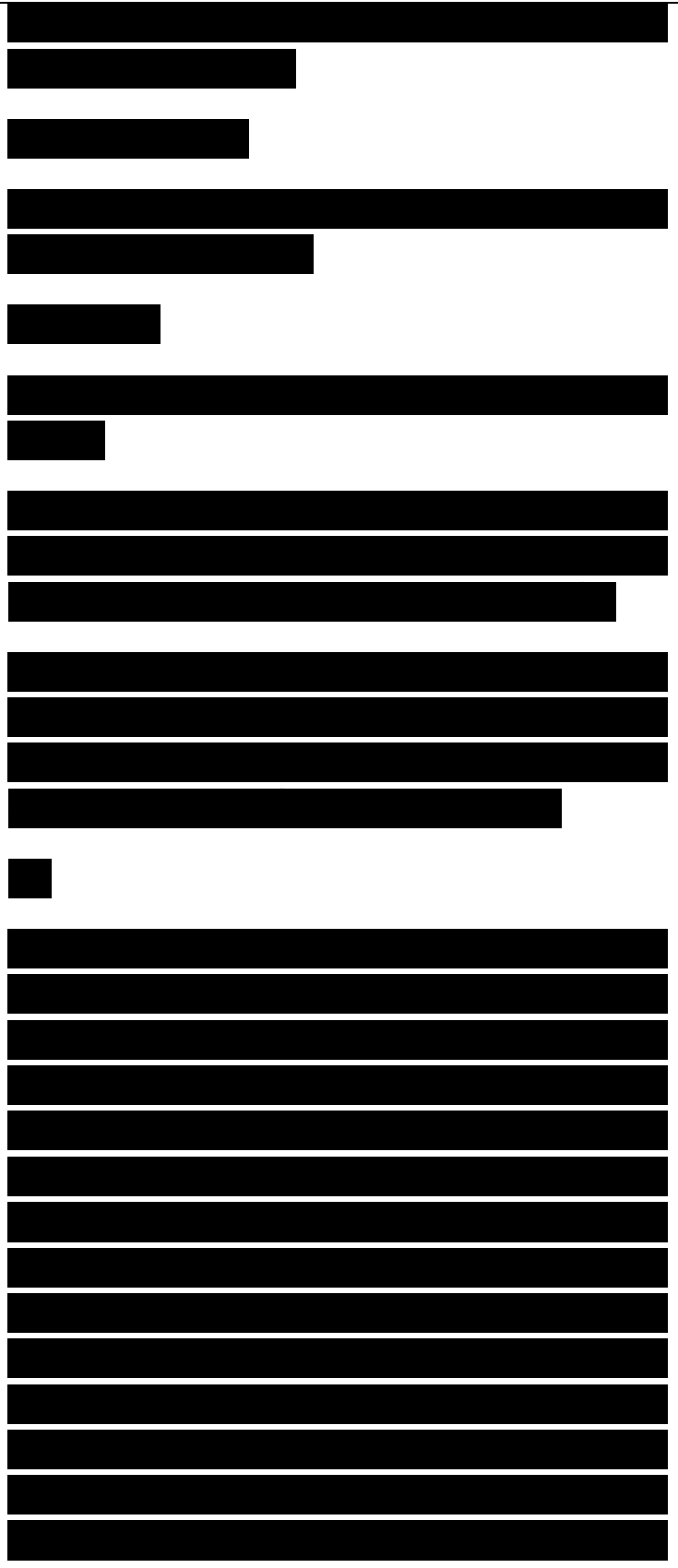
$$\chi_e = \epsilon_r - 1 \quad (2.50)$$

It follows that just as ϵ_r / ϵ_0 is a dimensionless parameter.

An analogous definition is employed in case of the superposition of free space magnetic field on the magnetic polarization field to give

Once again, a similar comparison with respect to eqs. (2.42) and (2.45), relates the dimensionless physical parameter the magnetic susceptibility to the relative permeability of the medium as:

It is apparent from eqs. (2.36) and (2.37) that the electric displacement density and the magnetic flux density vectors, D and B , corresponding to the free space fields are linear. Hence, if the electric polarization P is linear with respect to E , and so also the magnetization M with respect to H , the corresponding expressions for D and B in eqs. (2.48) and (2.51) are also linear. Media obeying these conditions are said to be linear media. It is also possible that the polarization resulting from the applied field is not linear. Such media are identified as nonlinear in which ϵ_r and μ_r become nonlinear functions of E and H , respectively. Examples of such nonlinearity are frequently encountered in the cases of the



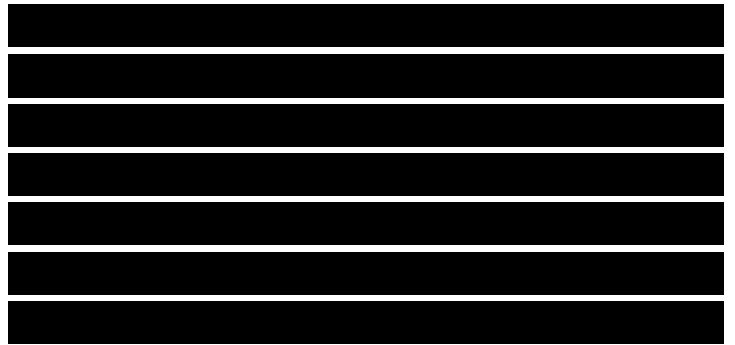
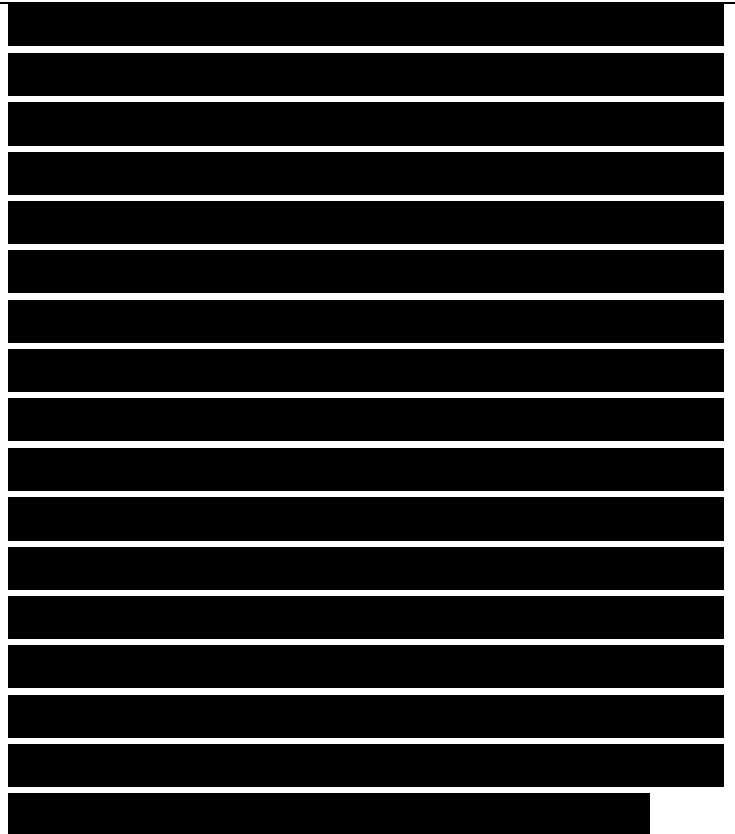
ferroelectric materials, e.g. barium titanate and Rochelle salt (Havt. 1989).

Digressing slightly, it may be mentioned that in engineering one often makes use of bulk properties, such as density to characterize a medium. A material is said to be uniform if its density remains the same throughout a specified volume. In contrast, the density of air in atmosphere varies at different layers. Hence the atmosphere is an example of a nonuniform medium. Drawing upon this analog for electromagnetics, we identify a medium as a homogeneous one, if its characteristic properties, namely // and a remain invariant. If these parameters become a varying function of the space coordinates, the material is said to be inhomogeneous.

The electric polarization P resulting from an impressed electric field E in a medium tends to lag behind it. This can be mathematically represented by assuming a complex form for the electric susceptibility and hence the dielectric constant of the medium.

A similar expression can be obtained from the magnetic polarization M as
$$\text{fr} = K - j\text{Pr} \quad (2.54)$$

The imaginary parts of the eqs. (2.53) and (2.54) are related to the polarization losses within the medium. Vet another loss mechanism is due to the finite but small conductivity of the dielectric medium. All those materials where either of the two mechanisms results in an appreciable loss of energy are said to be dissipative. Otherwise the medium is a nondissipative one.



The materials in which ϵ and μ are frequency-dependent are known as dispersive media. The idea that the intrinsic characteristics of a medium could vary with frequency is not as incongruous as it might appear in the first place. Many common phenomena are explained by these. For example, it is well known that a light ray bends when it traverses from air to glass. The bending of light in glass is proportional to the frequency of light of different colors. Hence it is due to dispersion that white light is resolved into various colors by a glass prism. Glass is a dispersive material in the optical region. A medium where the variations in ϵ and μ as functions of ω are not apparent, is called a nondispersive medium.

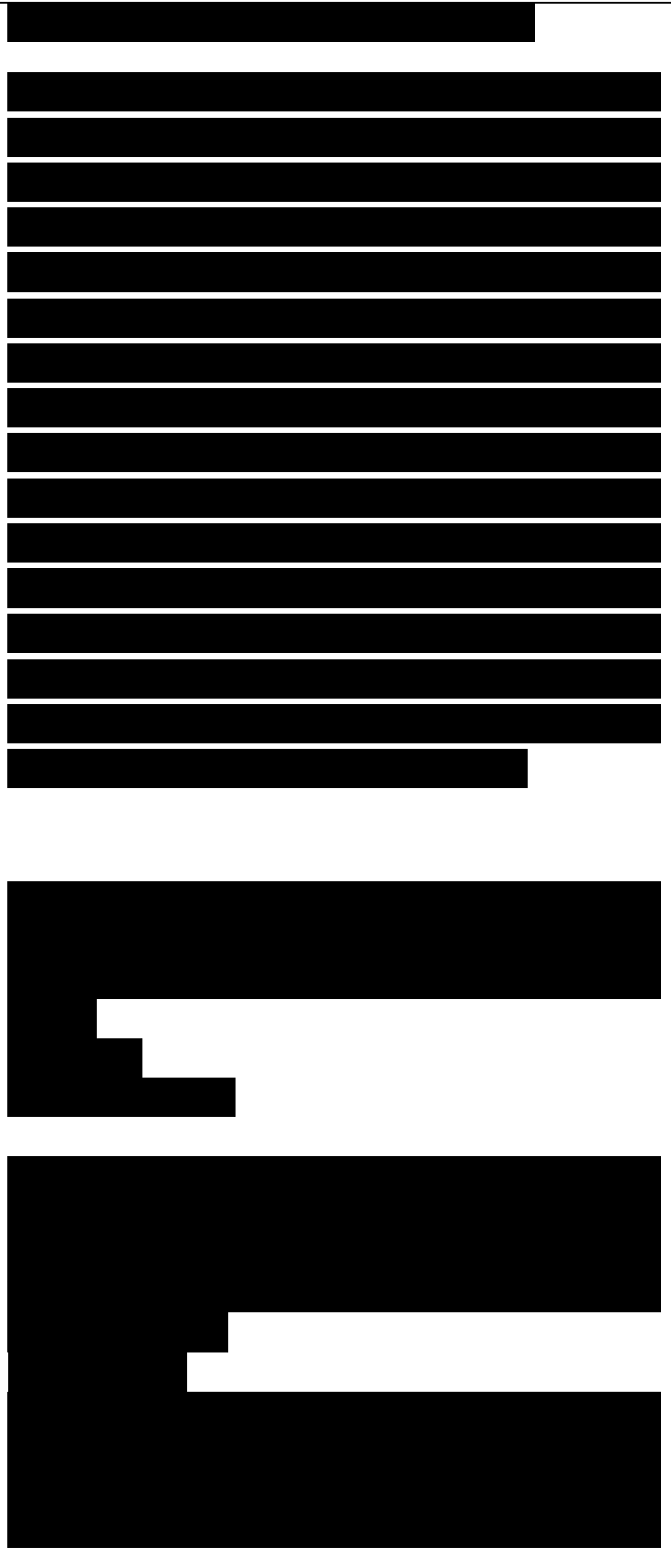
For a dispersive medium, the real and imaginary parts of the relative permittivity are given by the Kramers-Kronig relation as (Portis, 1978):

where

$$\epsilon''(\omega) = \frac{2}{\pi} \int_0^\infty \frac{\omega' \epsilon'(\omega')}{\omega'^2 - \omega^2} d\omega' \quad (2.57)$$

It may be noted that in the relations (2.55) and (2.56), the real and imaginary parts of permittivity are expressed as a function of each other. The solution for these integrals in the microscopic domain is of the form:

where N , m , q and r are the corresponding constants in the atomic domain (Jordan & Balmain, 1968). By substituting eqs. (2.53) in (2.50) we obtain the complex form of electric susceptibility as:



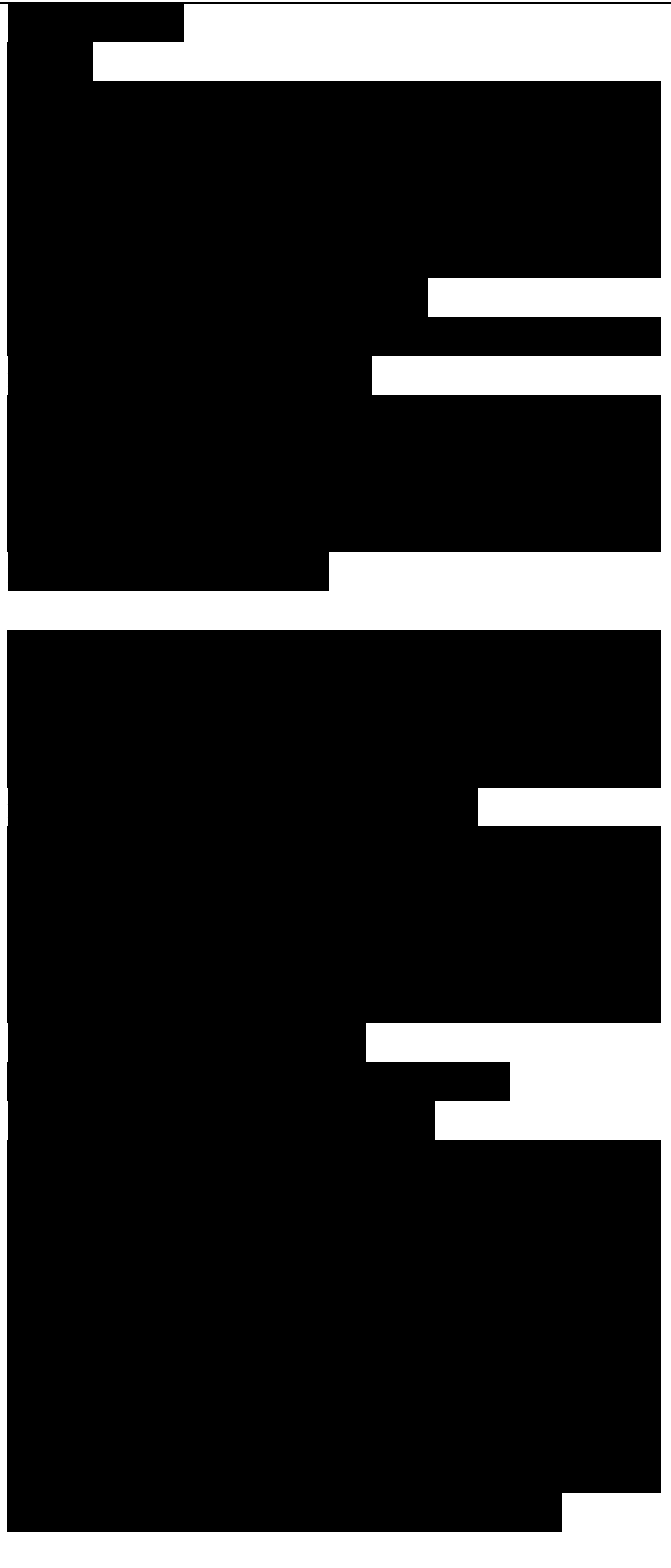
With reference to eq. (2.63), a permittivity ellipsoid (Fig. 2.5) may be visualized with three unequal axes ϵ_1 , ϵ_2 and ϵ_3 . A material defined by the relation (2.63) is said to be biaxial. If $\epsilon_1 = \epsilon_2$, the general ellipsoid becomes an ellipsoid of

Figure 2.5 The permittivity ellipsoid for a biaxial media

revolution, and the material is identified as a uniaxial one. Finally the ellipsoid reduces to a sphere when $\epsilon_1 = \epsilon_2 = \epsilon_3$, and the material is obviously an isotropic one (Cheng, 1989). A similar reasoning holds for the permeability' tensor as well.

We have so far considered only those media which do not have the crosspolarization effects. It is possible to set up anisotropic constitutive relations where D and B are expressed as bivariate functions of E and H . χ and C are the magnetolectric crosspolarization dyadics (Sihvola, 1995). The materials obeying the relations (2.65) and (2.66) are known as the bianisotropic media. In the special case, where all these are identity tensors the medium is said to be bi-isotropic.

Another important concept with the characterization of the medium is its reciprocity which could be defined analogous to the circuit theory' definition. A medium is reciprocal if the response at an observation point due to the field radiated by a source at a transmitting point is invariant when the transmission and observation points are interchanged. In a reciprocal medium, the permittivity' and permeability' tensors are symmetric for a



plane wave excitation:

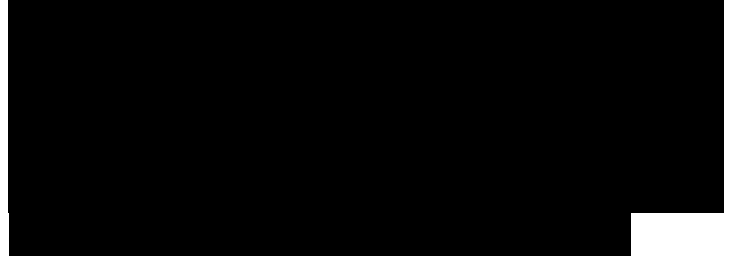
In addition to these, for a reciprocal bi-isotropic medium, the magnetoelectric crosspolarization dyadics are also inter-related:

Materials for which condition (2.68) is not satisfied are known as nonreciprocal materials. For a given polarization, this results in the asymmetry in attenuation and wave velocity' for $\pm N$ (Bergmann, 1982), where N denotes the direction normal to the wavefront.

To conclude, in this section we have presented the general characteristics and broad categorization of materials. A material can be identified as belonging to more than one of these classes. For example, free space is a linear, homogeneous, nondissipative, nondispersive, isotropic and reciprocal medium. Likewise, a medium which is simultaneously bianisotropic and nonreciprocal is classified as a nonreciprocal bianisotropic medium. A theoretical discourse on this class of medium is important in the context of RAM and shall be elaborated upon in Section 2.5. In the next section we propose to set up the wave propagation for some of the most commonly encountered media.

2.4 EM WAVE PROPAGATION

In a typical radar target scenario, the EM waves emanating from the radar travel extremely large distances in free space as compared to the operational wavelength. The waves then strike and are scattered by the target, which may be either conducting or dielectric in nature. The detailed



scattering mechanism however requires analysis of the propagation of EM waves not only over and along the surface but also within the medium. Thus the wave picture that emerges is not only that of free space propagation but also of EM wave propagation within various other media. In general these media, as discussed in Section 2.3, could be linear or nonlinear, lossy or lossless, dispersive or nondispersive, homogeneous or inhomogeneous, isotropic or anisotropic, and even reciprocal or nonreciprocal. The nature of propagation of the electric and magnetic fields at a given observation point within each combination of these media is different. However these characteristics of the medium are not mutually exclusive. Free space for example is not only an isotropic but a linear, homogeneous, lossless and nondispersive medium as well.

In this section we therefore set up wave equations for EM propagation within commonly encountered media. It must be pointed out that the wave equations presented in this section are well known in electromagnetics. Hence we shall desist from deriving these equations. We shall restrict ourselves to stating Maxwell's equation as applicable to each case. The corresponding constitutive relations are also pointed out. This is followed by the wave equation corresponding to EM propagation within the medium. Radar waves travel large distances as compared to the wavelength; hence using the ray picture, it can be assumed that two neighboring wavefronts are always almost parallel. This is idealized by assuming a plane wavefront for the



purpose of the analysis given below. Furthermore it is assumed that for a wave propagating in the z-direction, it is a function of time t, and of the z- coordinate only. A similar condition holds for the propagation along the x- and y- directions.

2.4.1 Free Space Propagation

Propagation in free space is a very significant fraction of the entire path that the radar waves traverse between the source and the observation radar. Since there are no charges in free space, $J=0$, and $p= 0$; the Maxwell equations given in eqs. (2.1) through (2.4) are accordingly modified to The constitutive relations for free space are given in eqs. (2.36) through (2.38). Following a few simple steps of vector calculus operations on eqs. (2.69) through (2.71), and by appropriate substitution of constitutive relations, one obtains the wave equation corresponding to the electric field propagation in free space (Jordan & Balmain, 1968),
(2-73)

The wave equation for the magnetic field propagation similarly follows from eqs. (2.69), (2.70) and (2.72),
(2.74)

The assumption of plane wave propagation along with the wave equations (2.73) and (2.74) makes it possible to define the characteristic impedance of free space as
(2.75)



which is approximately equal to 377 Ω .

2.4.2 Propagation through a Homogeneous Medium

The wave equations for free space propagation can be readily extended to the case of a lossless homogeneous dielectric medium. Such a medium can be considered as a charge free, nonconducting one, where $\sigma = 0$. The constitutive relations for such a medium are already stated in eqs. (2.41) through (2.43). The corresponding wave equations are

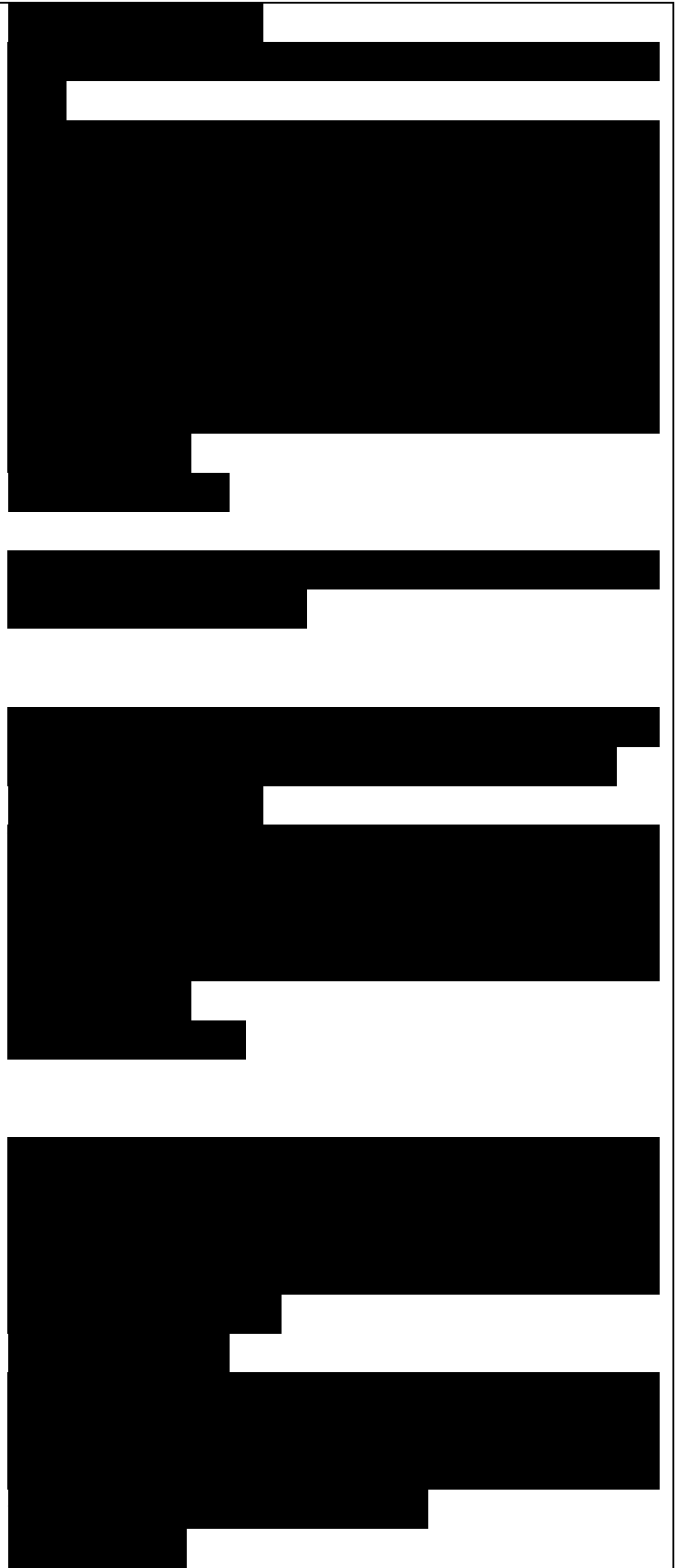
The characteristic impedance of a medium is obtained as

Finally, the velocity of propagation in a lossless homogeneous dielectric is

If the medium is conducting in nature; the conductivity is of finite non-zero value. The constitutive relations are once again given by eqs. (2.41) through (2.43). and the corresponding wave equations obtained are

The solution of the second-order differential equations (2.80) and (2.81) is facilitated by adopting a phasor form for all the EM field vectors. The Maxwell equations (2.1) through (2.4) can be written for a conducting medium as

The phasor forms have been obtained by replacing each differentiation with respect to time with $j\omega$. The wave equations (2.80) and (2.81) can similarly be written now as



where γ is the propagation constant of the wave in a conducting medium. From eq. (2.86), we get

The propagation constant thus is a complex parameter symbolically denoted as $\gamma = \alpha + j\beta$ (2.89)

in which α is the attenuation constant, and β the phase constant or the wave number. Comparing equations (2.88) and (2.89), one obtains (Ramo et al., 1994):

At this point we recall the complex form (2.53) for the permittivity. If the ratio ϵ''/ϵ' is significant, it is said to be a lossy dielectric. On the other hand, if $\sigma \gg \omega\epsilon'$ (OS

the conducting current density is much larger than the electric displacement current density', and such materials are called conductors.

2.4.3 Propagation through an Inhomogeneous Medium

One often encounters a situation where the medium of propagation is not uniform. If one considers a large volume of a bulk medium, it is possible that it consists of distinct layers. This may be due to the variation of density' within a class of material itself. The atmosphere is one such example, where the layers in the vertical direction decrease in density. Yet another example is polyurethane foam (PUF). PUF is essentially a generic material, where the variation in density is controlled by the porosity within. From an EM perspective



this is equivalent to a change in the properties of the medium, such as the permittivity, permeability etc. with respect to location. The constitutive relations for the inhomogeneous medium, consistent with the general form (2.33) through (2.35) are therefore expressed as

For a lossy inhomogeneous nonconducting medium where there are no charges and current sources, eq. (2.95) reduces to $J=0$. Starting with the phasor form of the Maxwell equations (2.82) through (2.85), the equation for the wave propagation through the inhomogeneous medium may be obtained as (Brekhovskikh 1960)

If the variation of the properties of the medium in space is sufficiently small, the last term on the LHS of eq. (2.96) can be neglected. The form of wave equation is then akin to eq. (2.86):
where

The magnetic field vector is derived in an analogous manner, and is given as
$$\nabla^2 \mathbf{H} = -\mathbf{J} - \nabla \times \nabla \times \mathbf{H} \quad (2.99)$$

It is customary' to characterize the layers of inhomogeneity as linear, exponential, inverse square profile etc.. Solutions to the wave equations for these special profiles are well known (Wait, 1970).

To conclude, equations have been set up in this section to determine the fields for EM wave propagation in the various commonly encountered media. The field at a given



observation point is shown to be affected by the intrinsic EM parameters of the medium. This discussion is relevant in the context of RAM where the primary motivation is to reduce the EM energy in the direction of observation.

2.5 EM PARAMETERS FOR RADAR ABSORBING MATERIALS

The absorbing medium, as the name suggests, "absorbs" energy when an electromagnetic wave propagates through it. This often results in significant reduction in EM energy scattered in the direction of the radar. In this section we study the EM parameters which effectively make a material medium absorbent in nature.

2.5.1 The Loss Tangents

We start with the Maxwell-Ampere law (2.2), and substitute the constitutive relations (2.41) and (2.43) for a general linear conducting medium to obtain which in the phasor form can be written as

$$\nabla \times H = j\omega X \cdot E + \sigma E \quad (2.101)$$

It follows from eqs. (2.44) and (2.53) that the complex permittivity can be defined as

$$\epsilon = \epsilon' - j\epsilon'' \quad (2.102)$$

where the impressed electric field is assumed to result in electric polarization. Substituting eq. (2.102) in (2.101), we get

In eq. (2.103), the first term constitutes the conduction current and is dissipative in nature. The second and third terms correspond to the dissipative and nondissipative or "stored" components of the electric polarization current,

respectively. It is instructive to denote the dissipative (or the lossy part) and the "stored" components separately as (Plonus, 1978):

The ratio of lossy to stored component is known as the electric loss tangent which is expressed as

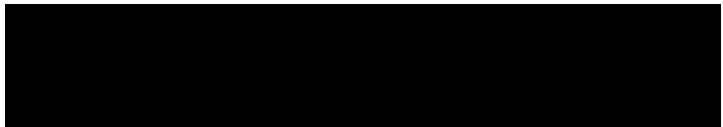
The dissipative energy is said to have been "absorbed" by the medium. Thus for the medium to be an effective absorber, $\tan \delta$ should be as large as possible.

Since the lossy term of the polarization current is frequency dependent, it is possible that $\cos \delta \gg \sin \delta$ beyond a certain frequency. This indeed is the case for dielectric materials where the conductivity is low. For such dielectric absorbers, the electric loss tangent is given by

A magnetic loss tangent is similarly defined as

The absorption however is not the only mechanism by which RAM operate. The reflections at the RAM boundary could be controlled by designing the coatings properly. The principles applied here are those of phase cancellation and impedance matching. These are essentially dependent on the permittivity and permeability of the material, and will be discussed in detail in subsequent chapters.

The discussion so far in this section is applicable to the simple media which constitute most of the conventionally



studied RAM. There are other equally important aspects, such as nonreciprocity, magnetoelectric crosspolarization etc., for the electromagnetic medium which can be utilized to design effective RAM. These materials, of which the class of chirals is just one example, are studied at length to identify the KM wave propagation parameters of interest.

2.5.2 Bianisotropic Materials

Isotropy and reciprocity are two commonly assumed characteristics of the material medium. As already discussed in Section 2.3, and well-elucidated by Post (1962), this by contrast provides a fundamental basis for hypothesizing the existence of a material medium which may exhibit anisotropy and nonreciprocity. The anisotropic materials are in fact a common occurrence; the examples of these are crystals, such as calcite and quartz which exhibit uniaxial anisotropy (Jenkins & White, 1957). On the other hand As₂Se, and Bi₂Te, crystals are biaxial in nature.

The concept of anisotropy can be further generalized to account for the magnetoelectric polarization, leading to the class of bianisotropic materials. Incorporation of nonreciprocity in these media offers the possibility of the nonreciprocal bianisotropic materials. The constitutive relations for the bianisotropic medium are already given by eqs. (2.65) and (2.66). A more convenient form incorporating nonreciprocity and bianisotropy can be written as:

where \mathbf{K} is called the chirality dyadic.

whereas ϵ_{ij} is known as the nonreciprocity dyadic (Sihvola, 1995).

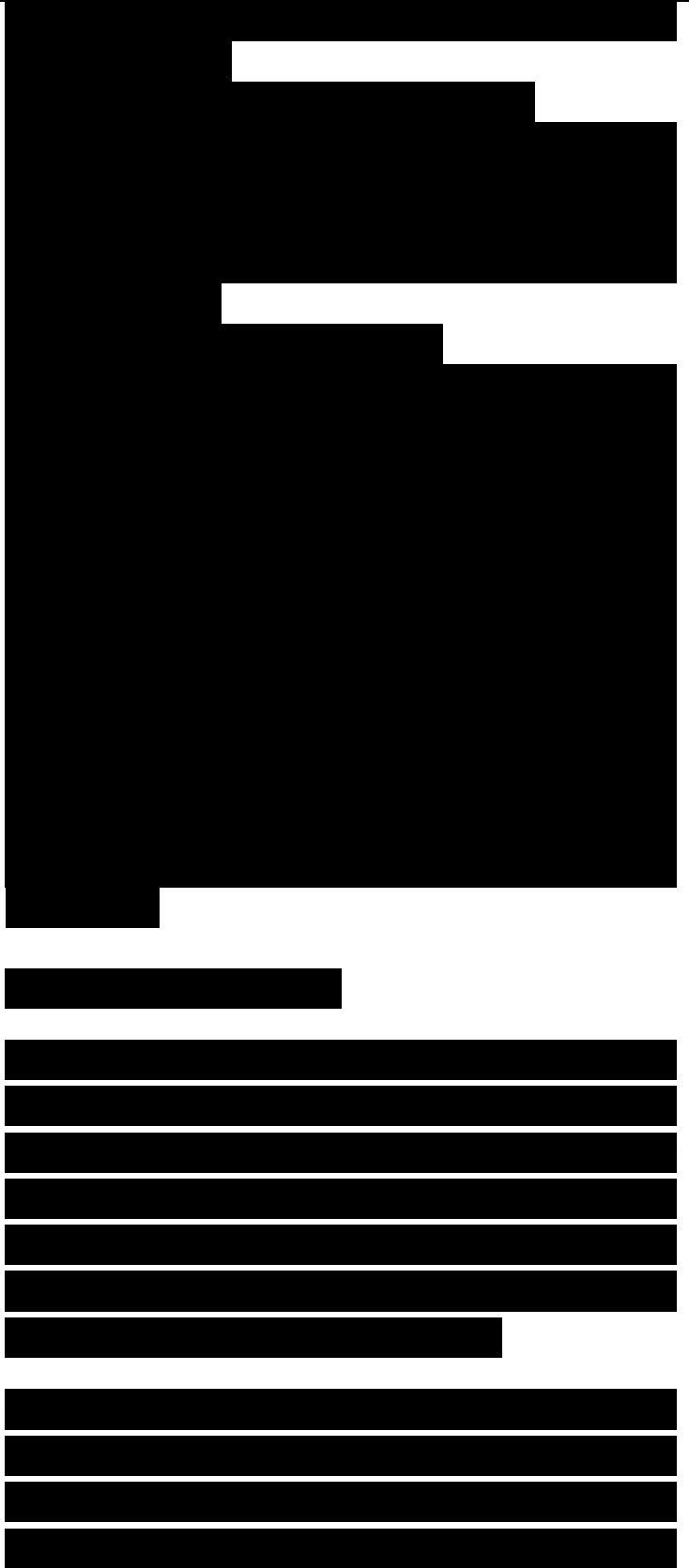
For bi-isotropic materials, the tensors involved in eqs. (2.107) and (2.108) reduce to scalars. Thus the constitutive relations for nonreciprocal bi-isotropic (NRBI) medium becomes

These equations are akin to those derived by Kong (1975). Even though the magnetoelectric coupling is predicted for the NRBI medium on theoretical grounds, the existence of such material itself has been shrouded in controversy. Lakhtakia and Weiglhofer (1994) have provided an elegant mathematical analysis with the help of covariance relations of Post (1962), to argue that such a material cannot exist. This has been disputed by Sihvola (1995) who objected to the assumptions leading to the analysis, and suggested that chromium oxide and the phenomenological Tellegen material could be thought of as examples of the NRBI materials.

2.5.3 Chiral Medium

By setting the condition for reciprocity, that is $\chi = 0$, in eqs. (2.109) and (2.110) we obtain the constitutive relations for the bi-isotropic reciprocal medium. These are commonly known as the chiral media. Thus for a chiral medium the constitutive relations are:

which involve a chirality parameter K in addition to the commonly conceived EM parameters ϵ and μ . This new parameter accounts for the optical activity and circular dichroism observed in the chiral materials.



We digress slightly to explain these phenomena for a better understanding of the characteristics of these materials.

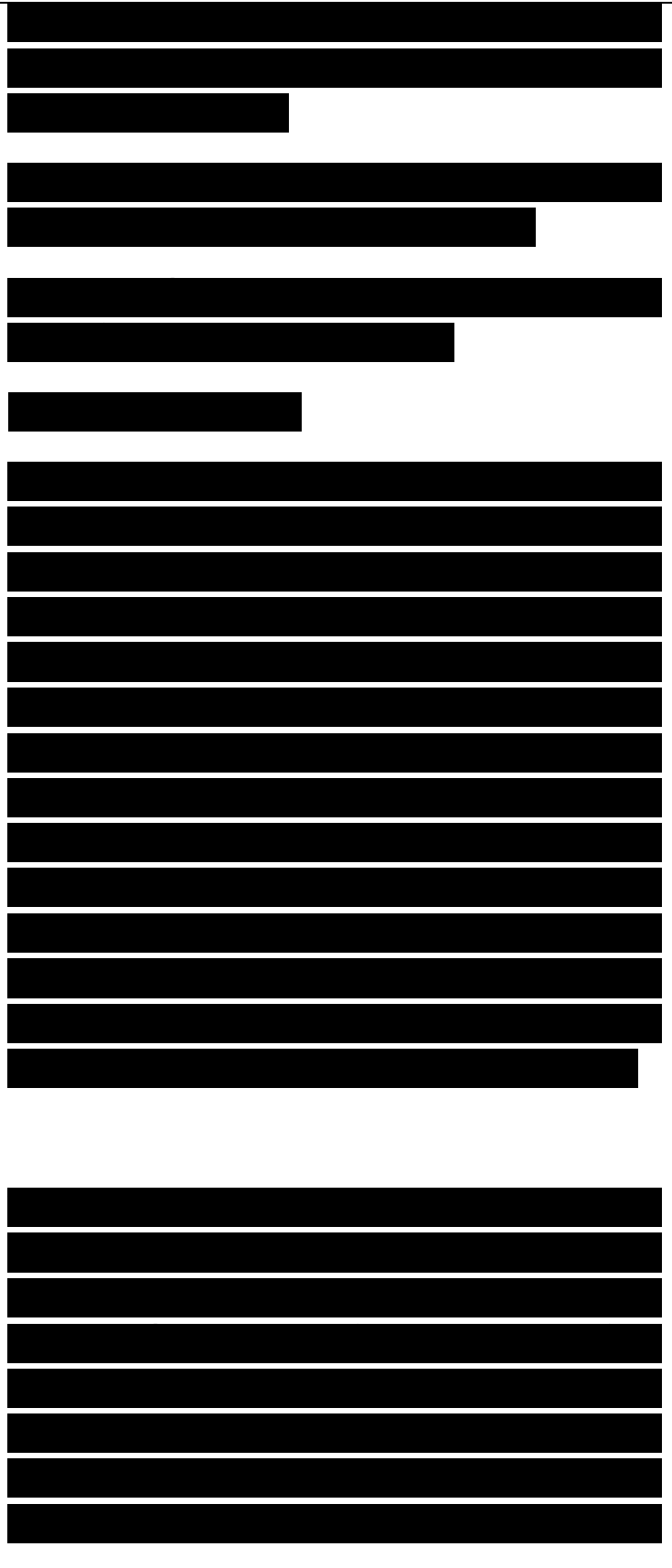
Figure 2.6 Optical activity in crystals The rotation of plane of polarization,

PoP2 \s ith respect to PoPl is a characteristic of optically active crystals.

Opticul Activity

It is widely known that the plane of polarization of a light beam (the plane defined by the propagation and electric field vectors) undergoes rotation due to its traversal within certain crystalline media (Fig. 2.6). This is a reciprocal phenomenon and is called optical activity or rotatory power (Wood, 1964). One commonly encountered medium which shows such a property' is the a-quartz (Lovett, 1989). Sodium chlorate, iodoform, cinnabar, Rochelle salt, and tartaric acid cry stals are some of the other well known optically active materials (Wahlstrom, 1979). The direction as well as the degree of rotation for the plane of polarization are intrinsic properties of these crystals.

The explanation for this optical activity is given terms of the two different circularly polarized light beams (right- and left-circularly polarized, or RCP and LCP) propagating through the crystal. It can be easily proved that only the RCP and LCP modes of propagation are possible within an optically active crystal (Kong, 1975). The incident linearly polarized light thus splits into the RCP and LCP beams as it enters the



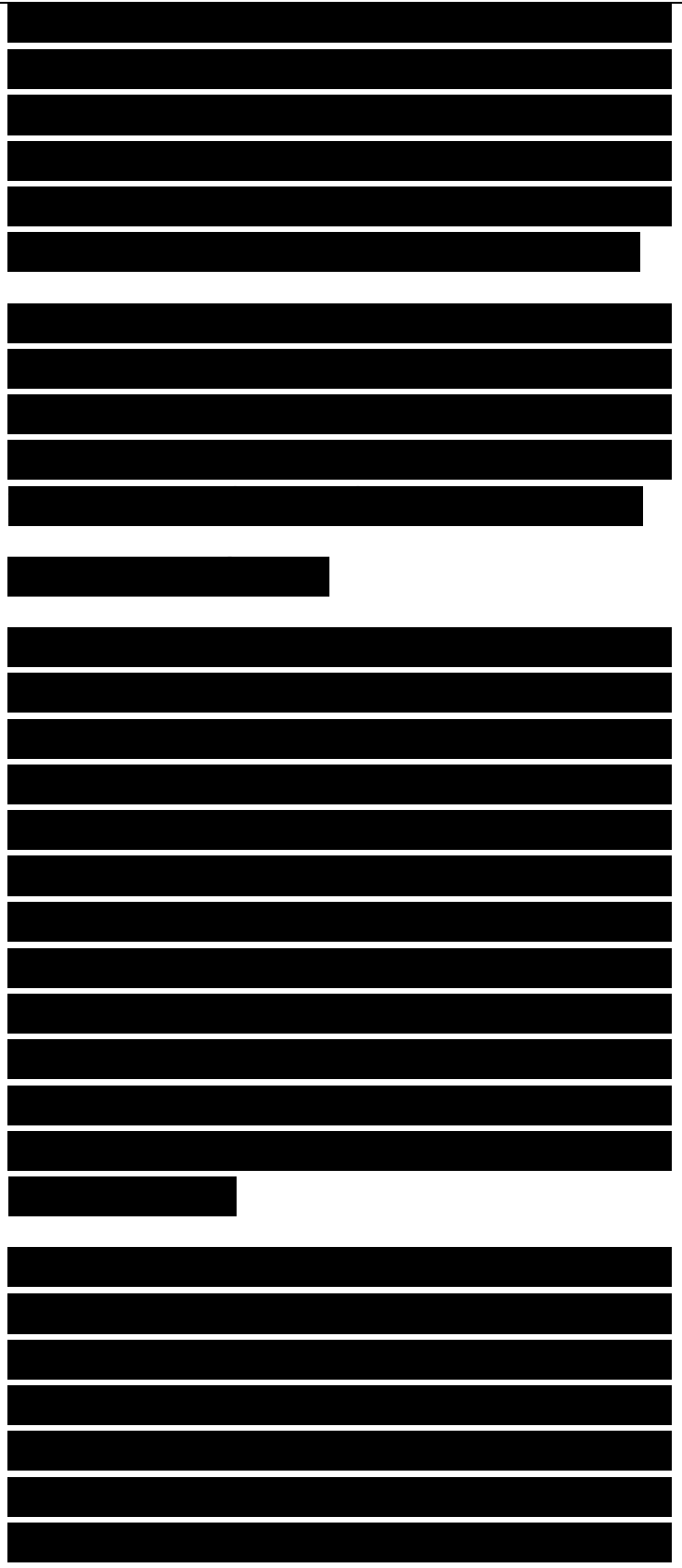
cry stal. Optically active crystals are therefore identified by two separate refractive indices. At the end of the path through the crystal, the two circularly polarized light beams add up once again, but result in a different plane of polarization which is attributed to the unequal values of the two refractive indices.

This rotation is also dispersive in nature, thus implying that the optical activity depends on the geometry of the crystals. It is now possible to identify other composite materials exhibiting such behavior in the microwave region as well.

Circular Dichroism

Dichroism is yet another optical property of crystals where the absorption coefficient is different for light waves with two orthogonal polarizations. A common example of the material showing dichroism is tourmaline (Jenkins & White, 1957). Even if the incident light at the first boundary of the tourmaline crystal is unpolarized in nature, it results in a transmitted wave of one particular polarization at the other boundary. Furthermore, if a second tourmaline crystal which has been rotated by 90° is placed in the path of this polarized light beam, it completely eliminates the transmission of the light waves.

The concept of dichroism can be further extended to optically active crystals which permit two differently circularly polarized modes of propagation. There are two different absorption constants associated with the RCP and LCP modes of propagation within such media. When a linearly polarized light is incident on an



optically active crystal, the two RCP and LCP components within the crystal not only traverse at different velocities, but also are absorbed unequally. The net effect at the transmission boundary is a light beam which is elliptically polarized. This phenomenon is known as circular dichroism.

Wave equations in a chiral medium

The equations for the FM wave propagation through a chiral medium can be derived by substituting the constitutive relations in Maxwell's equations. It is apparent from the literature that there are various versions of the constitutive relations. The discrepancies arise from the argument that the constitutive relations ought to be given for D and H, since E and B are considered to be the "primary electric and magnetic fields." For example, the constitutive relations obtained by Jagard và các cộng sự. (1979) are of the form

$$(2.113)$$

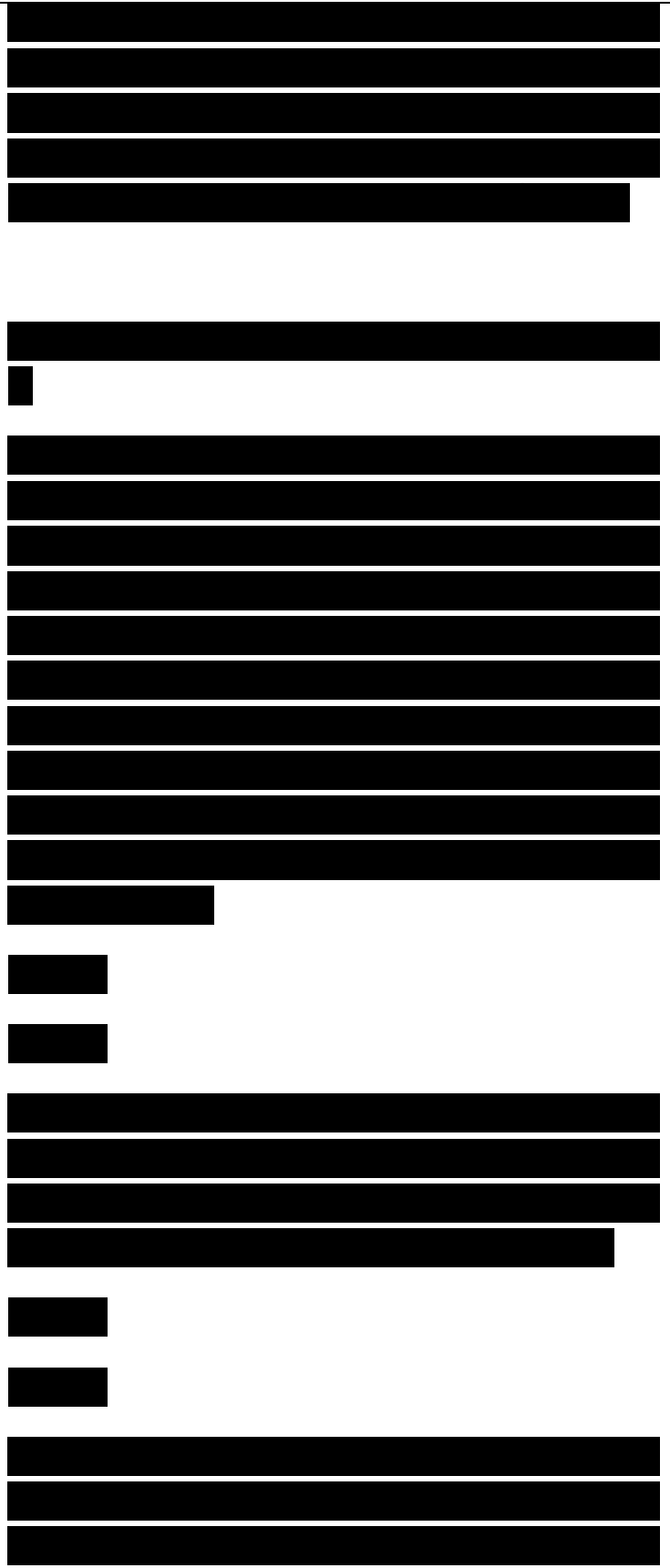
$$(2.114)$$

in which χ is known as the chirality admittance. Yet another form was employed by Jagard and Engheta (1989) to describe Chiroorb™, a reciprocal bi-isotropic chiral medium as

$$(2.115)$$

$$(2.116)$$

The similarity of eqs. (2.115) and (2.116) to the eqs. (2.113) and (2.114) is too close to be commented upon. Obviously, χ refers to



the chirality admittance once again.

A notationally similar form has been presented by Bassiri et al (1988) for a study of dielectric-chiral medium interface.

We rewrite eqs. (2.115) and (2.116) in a form consistent with those given in this book. Observe that eq. (2.118) has been made use of in deriving the constitutive relation (2.117). It is possible to establish a correspondence between the LEM parameters as proposed between the various sets of constitutive relations. Comparing eqs. (2.111) and (2.117) we obtain

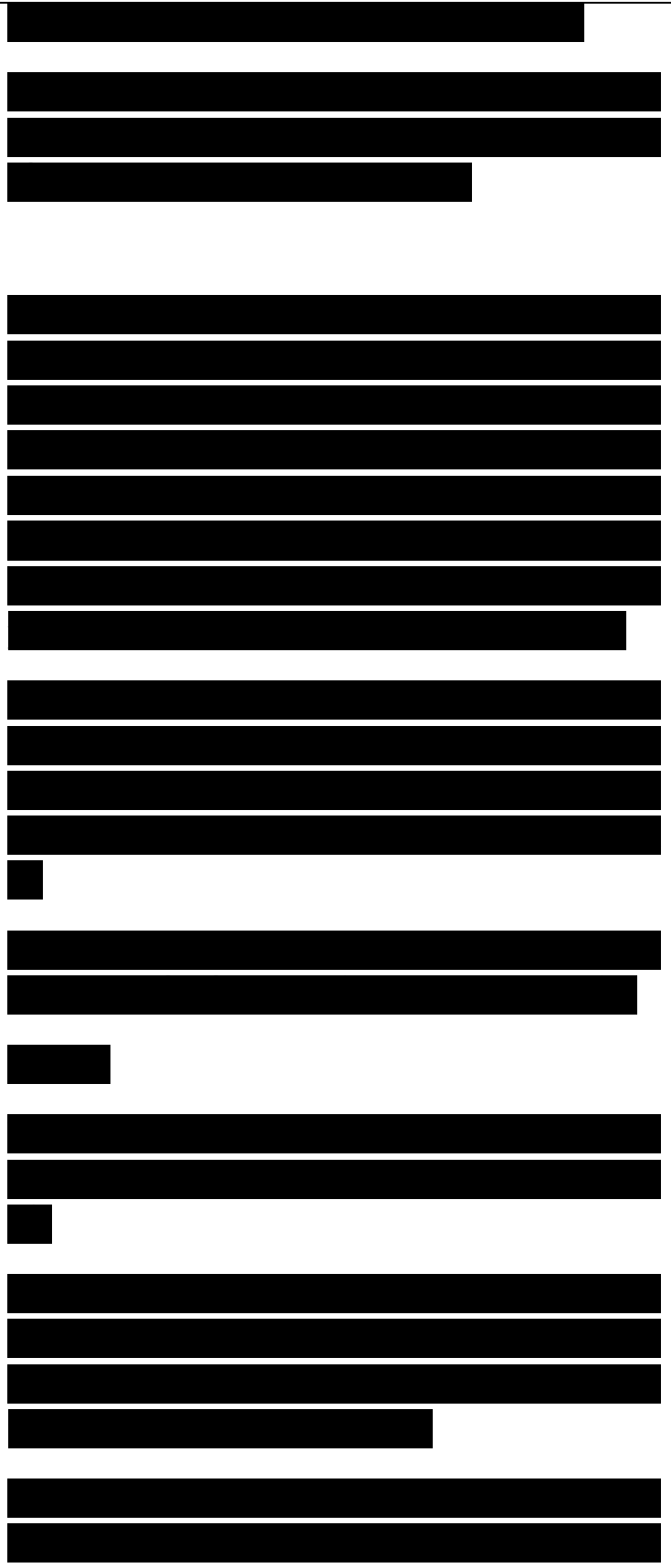
We also mention in passing, that the equivalence (2.119) is dimensionally consistent. Similarly, it follows from the equivalence (2.120) that the chirality parameter K is a dimensionless quantity.

A comparison of eqs. (2.112) and (2.118) shows that under this equivalence permeability remains an invariant.
(2-121)

Relations (2.119) through (2.121) are utilized for writing down a set of transformation conditions

Substituting eq. (2.122) in the eqs. (2.117) and (2.118) yields the constitutive relations (2.111) and (2.112) referred to in the beginning of this section.

To set up the electric field wave equations for the chiral medium, we substitute the constitutive relation (2.111) into the phasor



form of Maxwell's equation (2.82)
$$\nabla \times H = j\omega \epsilon_0 E - j\kappa \nabla \times E$$

In the equation above, we assume that there are no conduction currents, i.e., $J=0$. By rearranging the terms in the constitutive relation (2.112) and substituting in eq. (2.123) above for H , we obtain

By distributing $\nabla \times$ over the terms, and identifying Maxwell's equation (2.83), we get

Further taking the curl of both sides of eq. (2.83), and substituting (2.112), we write

Substituting eq. (2.125) in the equation above, we obtain the wave equation as
$$\nabla \times \nabla \times E + 2\kappa \nabla \times \nabla \times E - \omega^2 \epsilon_0 E = 0 \quad (2.127)$$
 The magnetic field wave equation can be obtained likewise.

$$\nabla \times \nabla \times H + 2\kappa \nabla \times \nabla \times H - \omega^2 \mu_0 H = 0$$

The characteristic impedance of the chiral material is defined as
$$Z_c = \sqrt{\frac{\mu_0}{\epsilon_0}} \quad (2.129a)$$

It is convenient to refer to Z_c as the chirality characteristic impedance or just chirality impedance to distinguish it from the characteristic impedance definition in eq. (2.78). By using the equivalence relations (2.119) and (2.121), one obtains
$$\quad (2.129b)$$

Observe that eq. (2.129b) is similar to the expression derived by Jaggard & Engheta (1989). The wave numbers k_{\pm} , corresponding to the RCP and LCP modes of propagation within the chiral, are given as

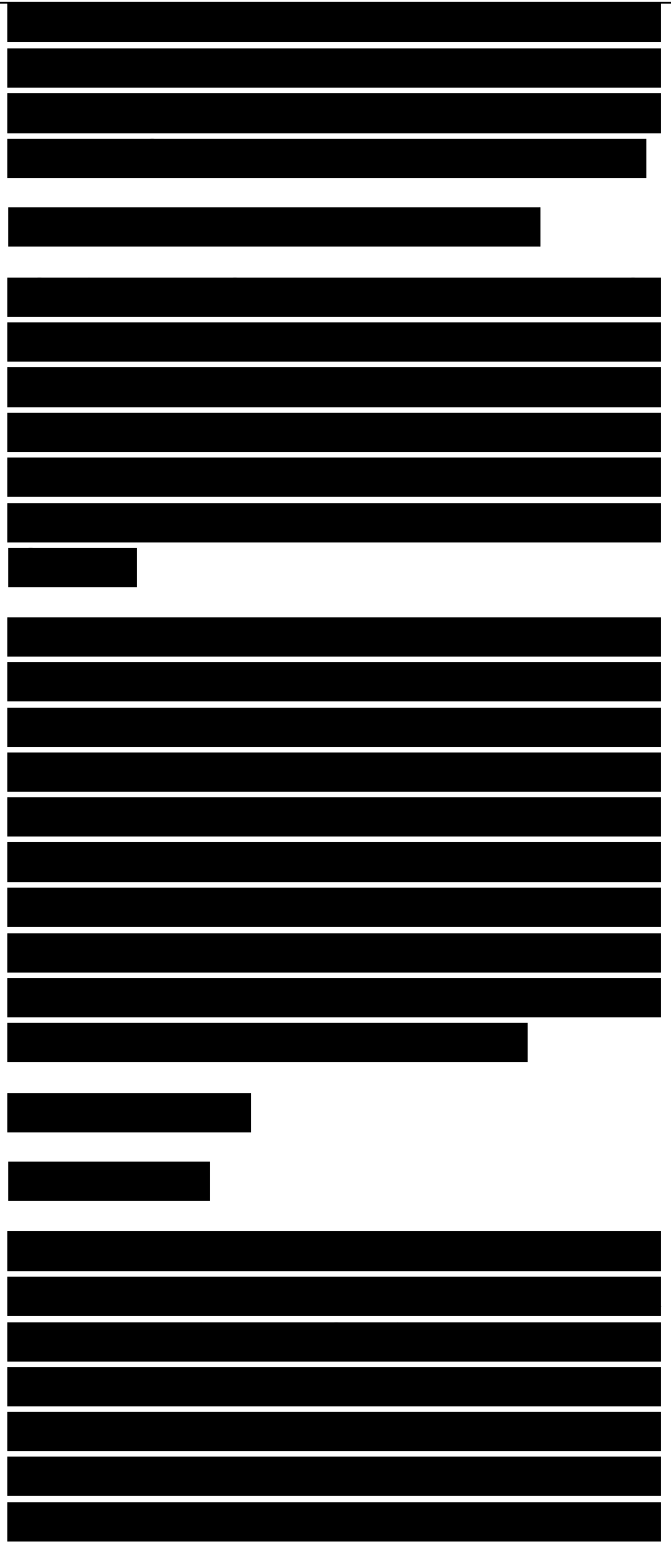
$$k_{\pm} = \frac{\omega}{c} \sqrt{\epsilon - \mu \pm \gamma} \quad (2-30)$$

The inequality of the wave numbers for the two modes of propagation in the chiral medium results in the rotation of the plane of polarization which is analogous to the well known phenomenon of optical activity in the case of crystals. Similarly, the attenuation constant can be shown to differ for the two polarizations due to circular dichroism.

To summarize, EM parameters of interest in the context of RAM are the electric and magnetic loss tangents which are the ratio of the imaginary and real parts of permittivity and permeability, respectively. For a more general class of material, it is possible to hypothesize magnetoelectric coupling. Two electromagnetic tensors called the nonreciprocity dyad and the chirality tensor offer considerable flexibility in the design of such RAM, of which chiral RAM is the most popular example.

2.6 SUMMARY

In order to analyze a RAM, it is necessary to identify EM parameters which help characterize the absorptive properties of the RAM. The starting point for RAM analysis is the Maxwell equations. These equations can be expressed in both the differential and integral forms by making use of Stokes' theorem and Gauss's divergence theorem. The Maxwell equations essentially relate the



four EM vectors E , H , I and B . Using the integral form of these equations, it is possible to obtain boundary conditions for these vectors at the interface between two media. These media could be of entirely different EM characteristics, e.g., a dielectric-dielectric interface or a dielectric-metal interface, as are often encountered in the analysis of RAM coated aerospace bodies.

Although the Maxwell equations consist of apparently independent equations, the two divergence relations can be readily derived from the two curl equations. Furthermore it is possible to express the EM wave propagation equations within a medium with only two EM field vectors, viz., E and H by the use of the constitutive relations. However the constitutive relations for EM vectors are themselves different for the various classes of media. These media can be broadly classified as being (i) linear or nonlinear, (ii) homogeneous or inhomogeneous, (iii) isotropic or anisotropic, (iv) dissipative or nondissipative, (v) dispersive or nondispersive, and (vi) reciprocal or nonreciprocal. Hence the corresponding wave equations for the various media are also different.

In-depth study of the constitutive relations also provide some fundamental results about the general behavior of the EM characteristics of the materials. The Kramers-Kronig relation is one such result

[REDACTED]

[REDACTED]

[REDACTED]

offering insight into the qualitative nature of both the real and imaginary parts of the electric susceptibility. Studies of the constitutive relations over conventional materials show that the absorbed EM energy is dissipated eventually. This is related to the imaginary part of the permittivity. A parameter of interest in the case of RAM is the electric loss tangent. Likewise, the magnetic loss tangent is also a RAM parameter. The reduction of the backscatter which is the essence of RAM on aerospace structures, can also be implemented by phase cancellation. The concept of characteristic impedance is used in the context of RAM design which again is related to the permittivity and permeability of the material.

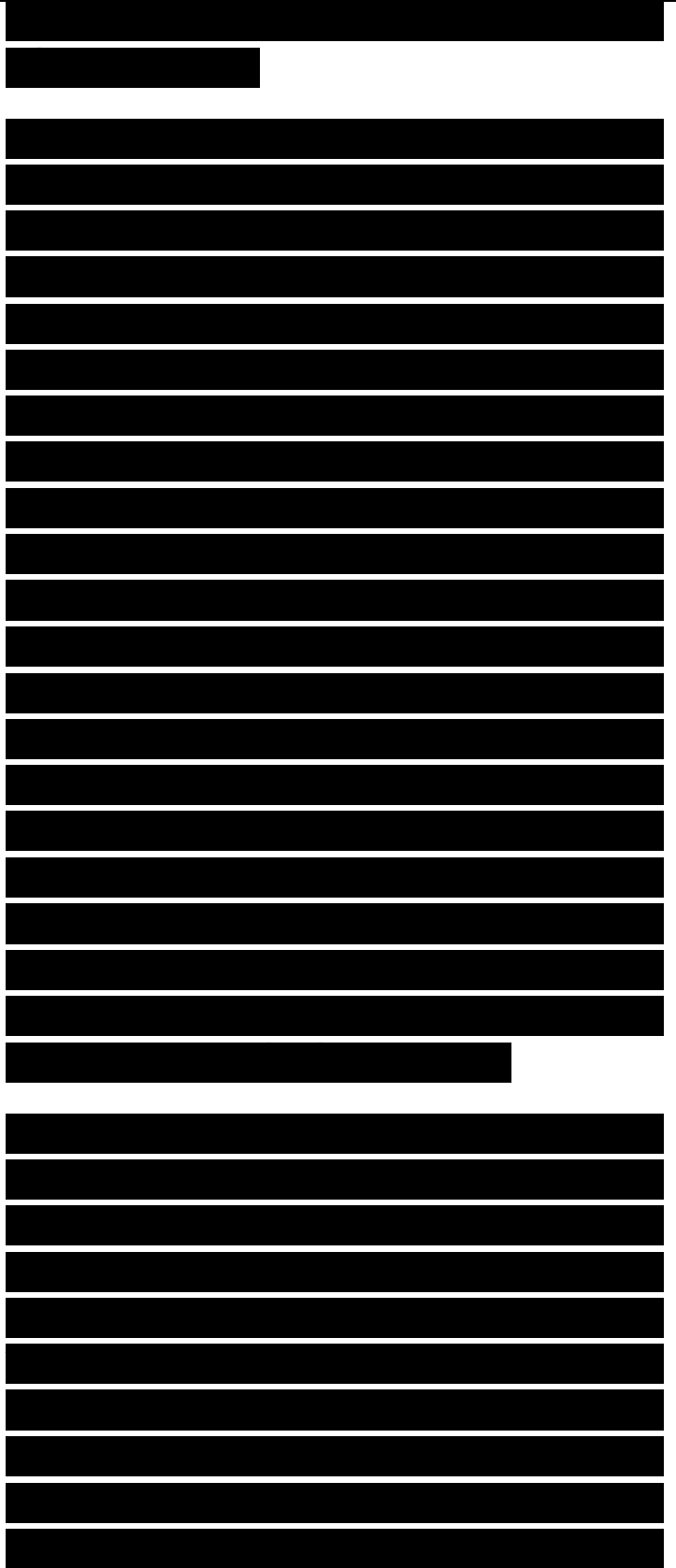
From a theoretical perspective, it is possible to visualize a general class of nonreciprocal bianisotropic media where E and H are functions of both B and D . The corresponding EM parameters relating these general constitutive relations include the chirality and nonreciprocity dyadics which are of the tensor form. The chiral RAM is a special class of this type, which is bi-isotropic and reciprocal in nature. It has also been shown in this chapter that the various constitutive forms proposed in the literature for chiral materials are equivalent.

Từ góc độ lý thuyết, chúng ta có thể hình dung một lớp tổng quát các môi trường bianisotropic không thuận nghịch trong đó E và H là các hàm của cả B và D . Các tham số EM tương ứng thiết lập mối liên hệ giữa các hệ thức cơ bản tổng quát này bao gồm các dyadic chiral và không thuận nghịch ở dạng tensor. RAM chiral là một lớp đặc biệt thuộc loại này, về bản chất nó là bi-isotropic và thuận nghịch. Trong bài báo này, chúng tôi cũng chứng tỏ rằng các dạng hệ thức cơ bản khác nhau trong các tài liệu về vật liệu chiral tương đương nhau.

MATHEMATICAL ANALYSIS FOR RAM ON SURFACES

Fundamental concepts involving the analysis of RAM were introduced in the previous chapter. Various classes of material media were identified and expressed in terms of their constitutive relations. Wave equations were also set up for EM propagation using these constitutive relations within these media. Two important EM parameters namely characteristic impedance of the medium and propagation constant were also obtained in the context of EM wave propagation. It was shown that the complex nature of permittivity and permeability is primarily responsible for electric and magnetic losses, and hence the attenuation within a medium. The finite conductivity of the material also results in electric loss which also is incorporated in the total electric loss. Furthermore, by generalizing the constitutive relations to incorporate magnetoelectric crosscoupling, one obtains a chirality parameter which provides an additional parameter in the design of chiral RAM.

In reality however RAM are rarely studied in isolation, since they are often coated onto other metallic structures to reduce backscatter RCS. This results in a metal-backed dielectric free space interface. It is of interest to study the effects of EM wave incident on such a surface. The boundary conditions derived in Chapter 2, are relevant in this context. In Section 3.1 the reflections at the interface of two media are studied for both normal and oblique incidence; this is extended to multilayered



RAM coatings on planar surfaces.

A planar surface however is often an idealization. In the context of aerospace engineering, the constituent surfaces of a hybrid shape are curved. In the second half of this chapter we discuss EM scattering and diffraction from curved surfaces. Since EM analysis is done with respect to the electrical wavelength, the analytical methods described in the latter part of the chapter are identified as low frequency and high frequency methods. The low frequency methods are essentially grid based. The method of moments (MoM) and finite difference time domain (FDTD) method are the most versatile examples of these. The fundamental principles involved in these analyses are followed by a discussion of their applications including those in RAM coated low frequency scatterers in Section 3.3. High frequency methods are in contrast formulated as an extension of the geometrical optics (GO). The most important amongst these are the geometrical theory of diffraction (GTD), physical optics (PO) and the physical theory of diffraction (PTD). These are outlined in Section 3.4.

3.1 ELECTROMAGNETIC REFLECTIONS AT PLANAR BOUNDARY

In Section 2.2 we have derived the boundary condition for the tangential and normal components of the electromagnetic (EM) vectors. These results can be

các

employed to determine the reflections at an interface between two media. We first study the case of the normal incidence which is followed by the generalization to the relatively more complex case of the oblique incidence.

3.1.1 Normal Incidence

In the context of FM reflections, perhaps the most common example is that of the planar interface between free space and a semi-infinite medium. This can be generalized to the case of normal incidence at a planar interface between any two media as shown in Fig. 3.1. The electromagnetic wave incident at the planar interface is split into a transmitted component in Medium 2 and a reflected component in Medium 1. For the normal incidence, the electric and magnetic field vectors are tangential to the interface. Hence from the Boundary Conditions 1 and 2 in (2.14) and (2.23), we get:

$$E_i + E_r = E_t$$

$$H_i + H_r = H_t$$

where the subscripts i , r , and t are employed to denote EM field vectors corresponding to the incident, reflected and transmitted waves.

We have already defined the characteristic impedance in terms of the intrinsic properties of the medium in eq. (2.78). The characteristic impedance can be employed to relate EM field vectors for the incident, reflected and the transmitted waves (Stratton. 1941):

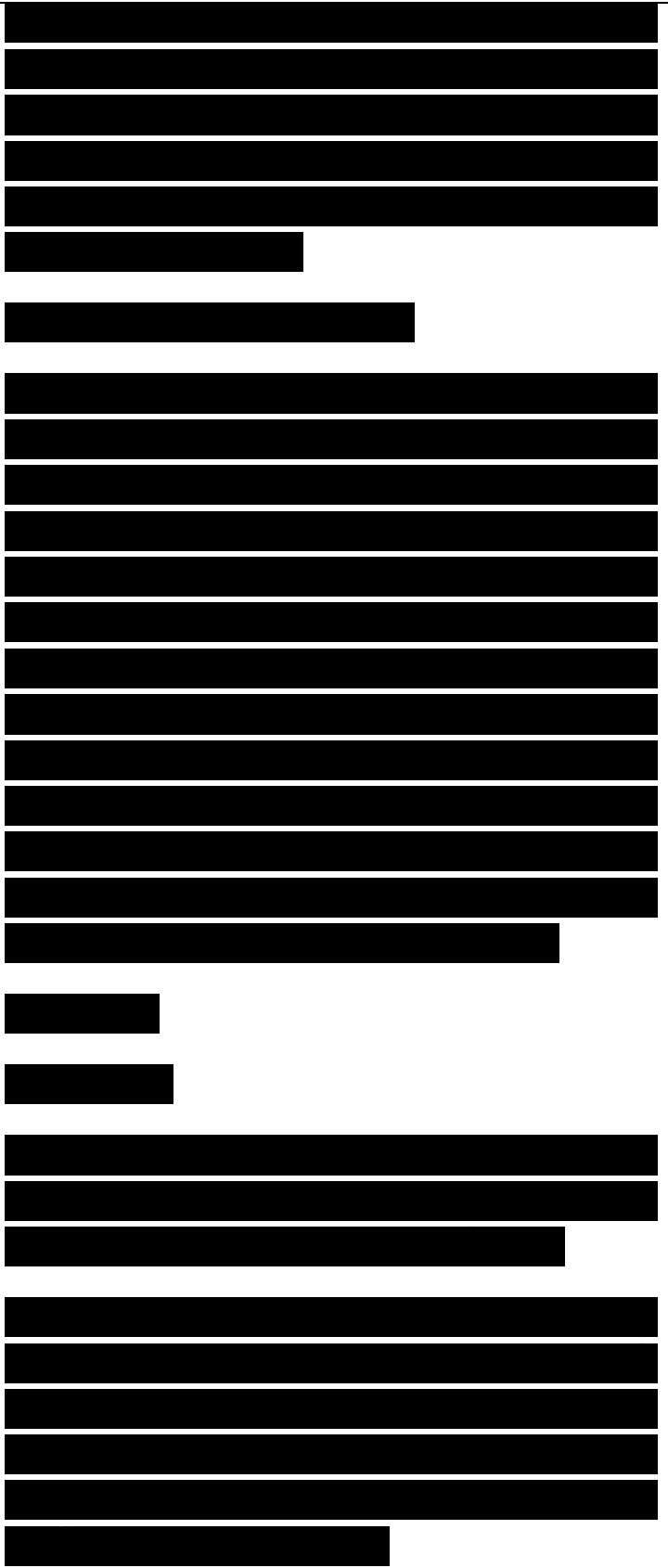


Figure 3.1 EM wave reflection and transmission at an interface between two media

where Z_1 and Z_2 are the characteristic impedances of Media 1 and 2, respectively. Substituting eqs. (3.3) through (3.5) in (3.2), we obtain so that

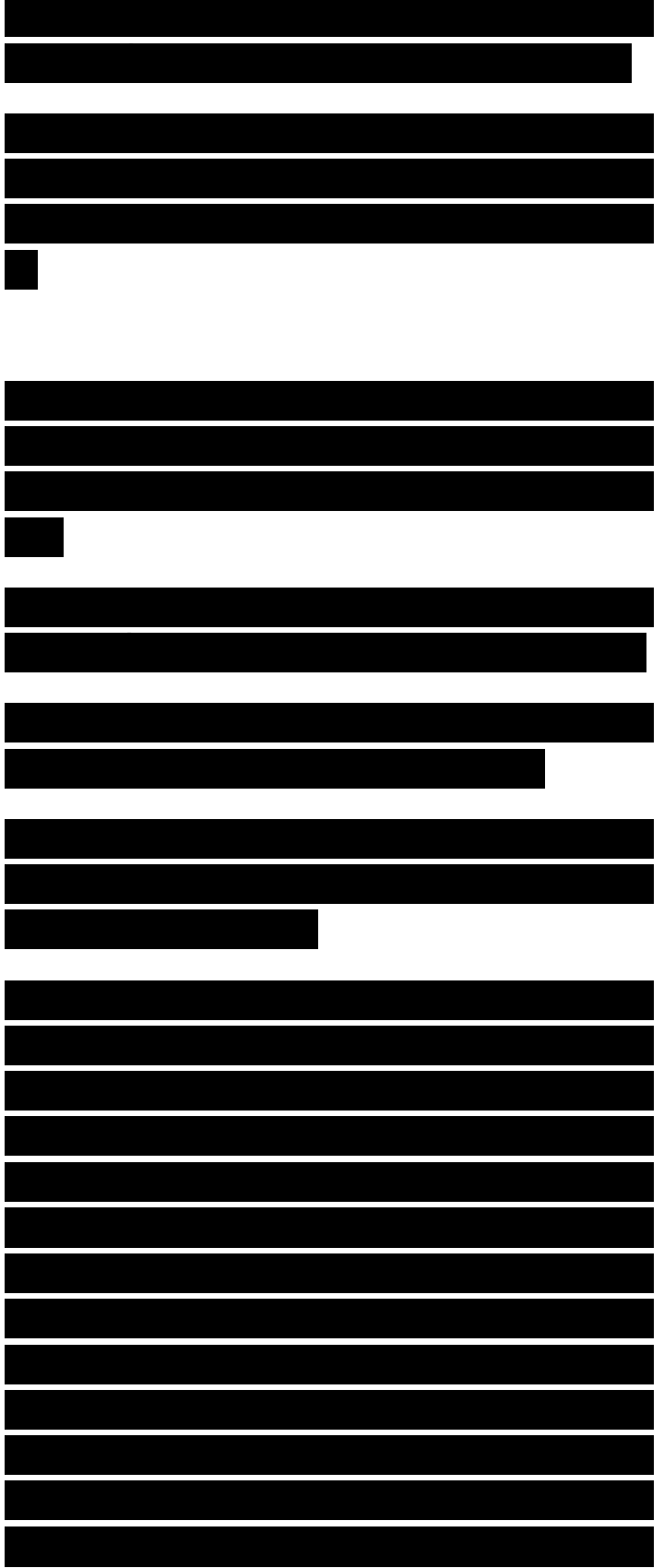
By substituting for E_r in eq. (3.1) with the expression above, and rearranging terms, one obtains the transmitted electric field.

The ratio E_t/E_i is defined as the transmission coefficient at the interface between two media.

Eliminating E_r between eqs. (3.1) and (3.6), the reflected electric field E_r becomes:

The ratio E_r/E_i is called the reflection coefficient and is denoted as ρ which in terms of the characteristic impedances of the two media is:

In the context of RAM, we often encounter situations which can be modeled by a thin flat slab sandwiched between two media. To proceed with this analysis, we first analyze the problem where Media 1 and 3 are idealized as being semi-infinite along the direction of propagation, as shown in Fig. 3.2a. The analysis in such cases is made tractable by drawing upon an analog in the transmission line theory. The transmission line equivalent circuit of Fig 3.2a is represented by Fig. 3.2b where d corresponds to the thickness of Medium 2. One defines an input impedance Z_{in} :



which is the effective impedance as seen by the incident wave at the interface between Media I and 2.

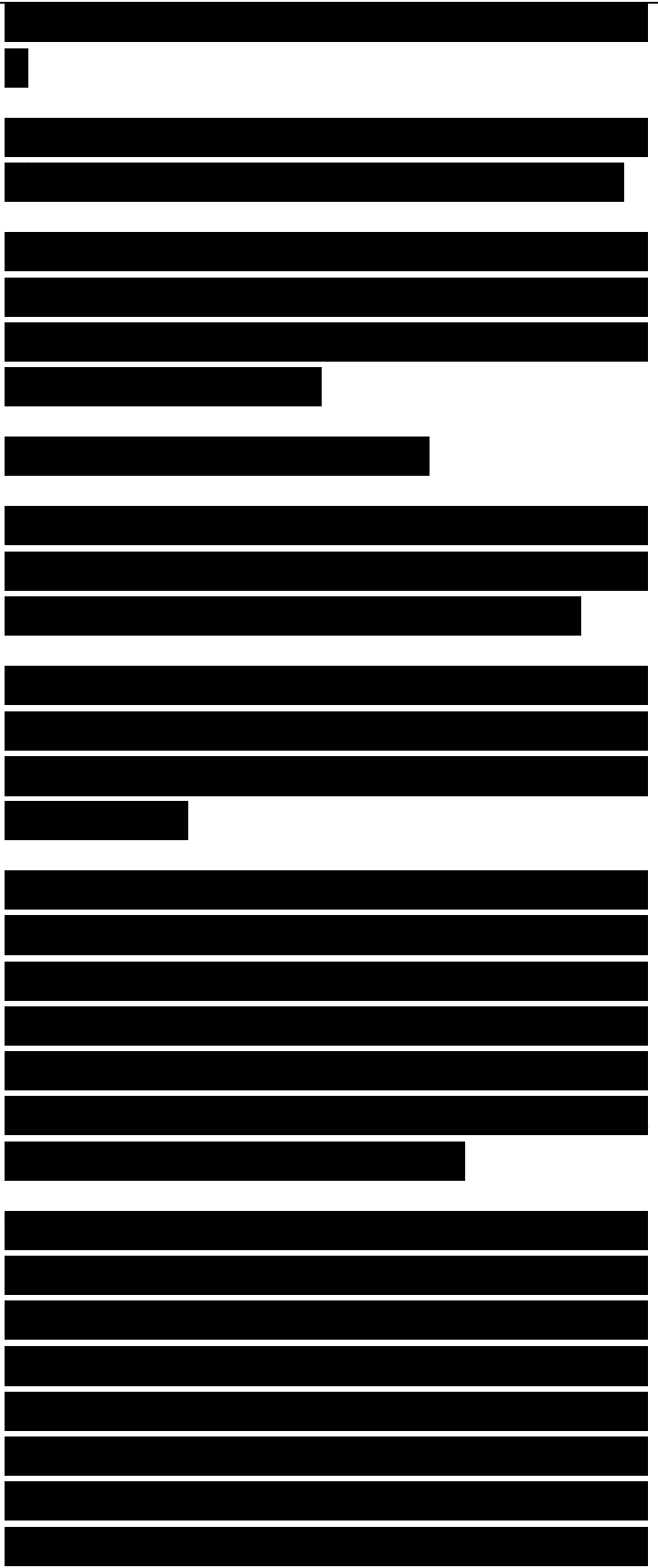
The reflection coefficient at the interface between the Media I and 2 can be obtained by replacing Z_2 in eq. (3.11) by the Z_{eff} obtained from eq. (3.12),
... , Medium 3 Medium 2

Figure 3.2 (a) Schematic and (b) transmission line equivalent circuit for EM wave propagation through a thin slab between two semi-infinite media

If Medium 3 is metallic in nature (Fig. 3.3), the value of its impedance approaches $^{\wedge}zero$. In such cases, the reflection coefficient reduces to

It is possible to select the thickness of the slab so that the numerator in the equation above, and hence the reflection coefficient is zero. Equation (3.14) is one of the fundamental equations for the design of RAM. Thus the condition for zero-reflection at the normal incidence for a slab terminated by a metallic load is given by:

Observe that the propagation constant β is dependent on the angular frequency ω . It follows from eqs. (2.88) and (3.15) that the RAM so designed is effective only in the immediate neighborhood of a resonant frequency. The operational bandwidth of such a RAM can be increased by resorting to multilayered design (Fig. 3.4). For such multilayered structures, Z_{eff} is determined



by taking all the successive layers into account. The input impedance Z_{in} , in fact is a recursive relation, and is a function of the impedances and propagation constants corresponding to each layer encountered by the EM wave. These aspects shall be further elaborated upon in Chapter 4 when we take up the design of broadband RAM.

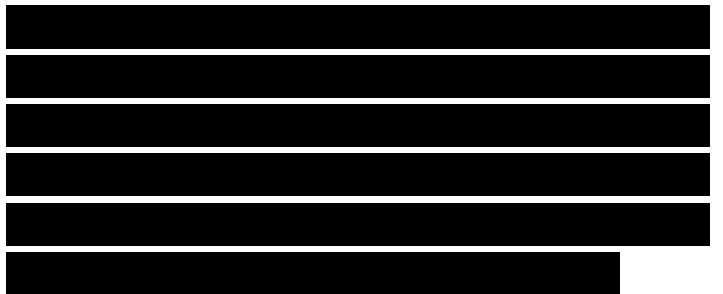
Figure 3.3 A 2-layered RAM coating over a metallic surface
Multilayered

Figure 3.4 A multilayered RAM coating over a metallic surface Equation (3.14) may be extended to analyze such coatings

3.1.2 Oblique Incidence

In the more general case of oblique incidence, (the EM field vectors associated with the ray are not entirely tangential (Fig. 3.5). The tangential components of these vectors are considered for applying the Boundary Conditions 1 and 2 outlined in Section 2.2.

With reference to Fig. 3.5 we define the angle of incidence θ_i , as the angle that the incident ray makes with the surface normal at the point of incidence. The angle of reflection θ_r , and the angle of refraction θ_t , are similarly defined with respect to the reflected and transmitted rays, respectively. The phenomena of reflection is dependent on the local property of the interface. The laws of reflection for EM waves (Stratton, 1941) require that:



1. the incident ray, the reflected ray, and the surface normal be coplanar: and

2. the angle of reflection be equal to the angle of incidence, i.e..

(3.16)

The plane consisting of the incident ray and the surface normal is called the plane of incidence.

Similar to the laws of reflection, the laws of refraction require that the incident ray, the transmitted ray and the surface normal be coplanar. The angles of incidence θ_i , and the angle of refraction θ_t are related to the ratios of the intrinsic EM properties of the two material media.

The ratio defined in (3.17) is also the ratio of the velocity of EM waves inside the two media:

where v_1 , and v_2 , are (he velocity of propagation in Medium I and Medium 2, respectively. Observe that ϵ , μ , f , and ω , can be complex in general, leading to a complex value for eq. (3.17). The velocity of propagation in eq. (3.18), is then interpreted as a complex quantity. It is assumed with respect to Fig. 3.5. that Medium 2 is semi-infinite in extent in the direction of the ray propagation.

The plane of polarization is defined as the plane containing the directions of wave propagation and the electric field associated with it. If the plane of incidence, and the plane of polarization are orthogonal, it is referred to as perpendicular polarization (Fig. 3.6). On the other hand, if the plane of incidence



and the plane of polarization are parallel (Fig. 3.7), the polarization is said to be parallel.

Perpendicular Polarization

In the case of perpendicular polarization, the incident electric field E , is normal to the plane of incidence, and therefore tangential to the interface (Fig. 3.6). However the incident magnetic field H , which is orthogonal to E , must be resolved at the interface to obtain H_{OT} , the component parallel to the plane tangential to the interface. Thus in the case of perpendicular polarization, applying the boundary

Figure 3.6 The reflection and refraction of an EM wave with perpendicular polarization at an interface.

conditions for the tangential components of the electric and magnetic fields leads to:

Substituting eqs. (3.3) through (3.5) in eq. (3.20b), we obtain $E_i \cos \theta_i = E_r \cos \theta_r + E_t \cos \theta_t$,

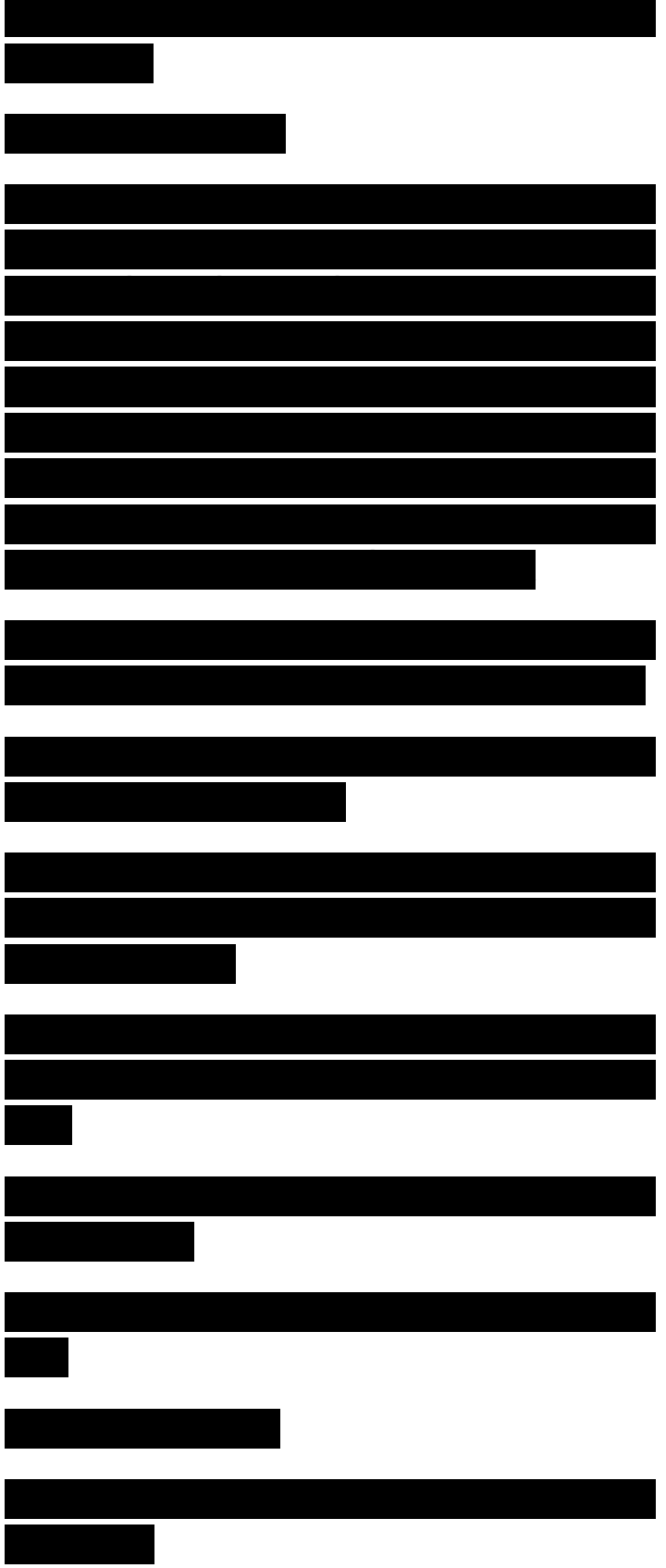
Thus the perpendicular polarization reflection coefficient p_L for the oblique incidence is derived as

We obtain the cosine of the angle θ_t , from Snell's law (3.17)

Figure 3.7 Reflection and refraction at the interface

Parallel polarization

and substitute in eq. (3.22) to derive p_L as a function of θ_i ,



Parallel Polarization

When the electric field is parallel to the plane of incidence, the incident electric field E , is in general resolved to obtain its tangential component along the interface (Fig. 3.7). In contrast, the incident magnetic field H , is now aligned with the interface. Thus the Boundary Conditions 1 and 2 (Section 2.2) yield

$$E_i \cos \theta_i - E_r \cos \theta_r = E_t \cos \theta_t,$$

By a treatment similar to that applied for the perpendicular polarization case above, we obtain the parallel polarization reflection coefficient p_{\parallel}

Figure 3.8 A multilayered RAM coating over a metallic surface. The perpendicular and parallel polarization cases can be treated by extending eqs (3.27) and (3.29), respectively!

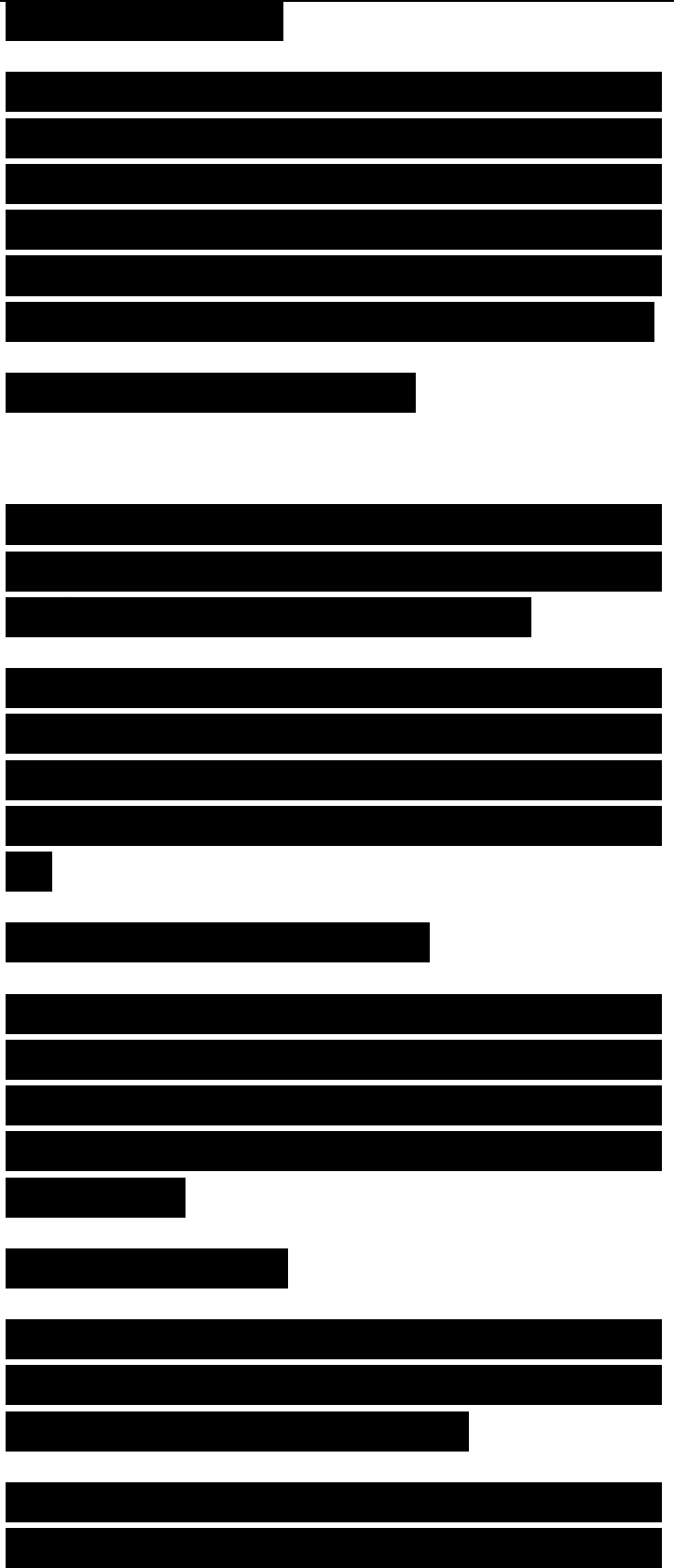
3.1.3 Multilayered RAM Coatings

For multiple layers of RAM (Fig. 3.8), we treat the general problem of oblique incidence. The concept of impedance transformation outlined in eqs. (3.12) and (3.13) is extended for the analysis of this problem.

Perpendicular Polarization

The reflection coefficient for perpendicular polarization at the interface between layers 1 and 2, p_{\perp} is obtained as (Klement và các cộng sự., 1988):

where $Z_{1\perp}$ denotes the input impedance for perpendicular polarization between these two layers. This is obtained by the



concept of impedance transformation of successive layers.

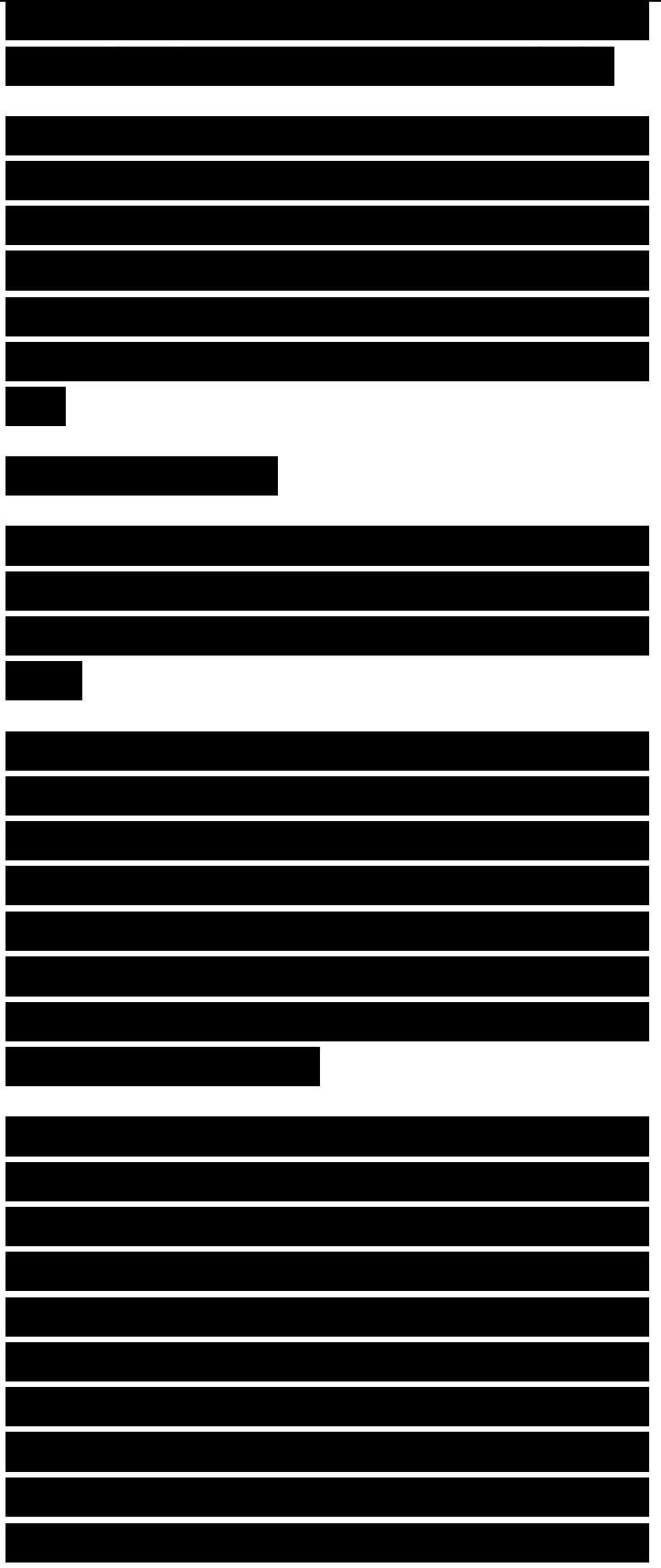
$Z_{i\pm}$, in the equation above denotes the input impedance at the interface between the Layers 2 and 3. Obviously this concept can be generalized to any number of layers, for which expressions similar to (3.28) may be obtained by recursion.

Parallel Polarization

The corresponding expressions for the reflection coefficient, and the input impedance for parallel polarization at the interface between Layers 1 and 2 may be derived as:

We draw the attention of the reader to the fact that in a typical RCS scenario. Layer I represents free space whereas the multiple layers of coatings on the aerospace target begin with Layer 2 (Fig. 3.8). Hence the perpendicular and parallel reflection coefficients at the interface between Layers I and 2 are of interest in the determination of the EM backscatter.

A second point to be noted here is that the expression given in eqs. (3.27) and (3.29) appear to be interchanged as compared to that given in some recent books. However a discerning reader might have observed that we have derived these formulae from first principles, i.e., from the Boundary Conditions 1 and 2. Our definitions for perpendicular and parallel polarizations are similar to those adopted in the other classical textbooks in electromagnetics (Stratton, 1941; Cheng,



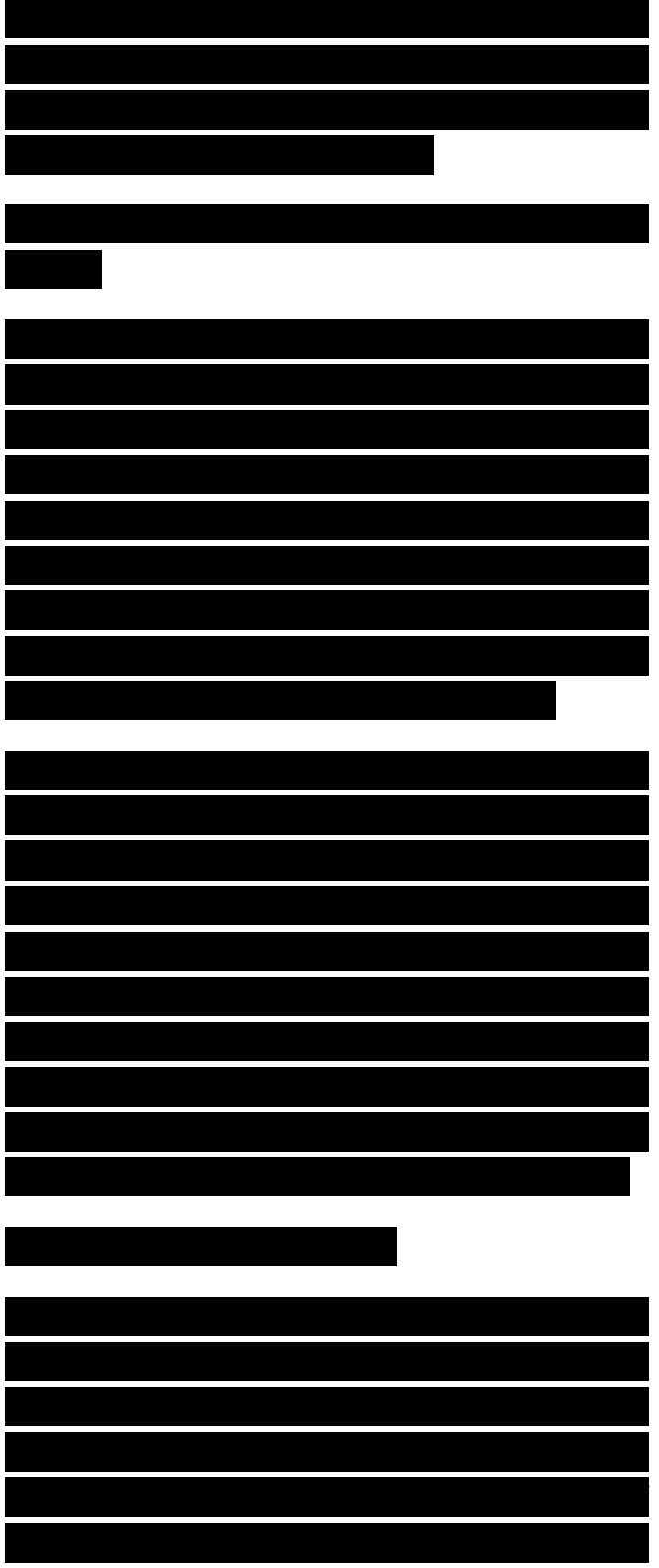
1989). Finally, for the particular case of EM wave incident at an oblique angle on a metal backed RAM coating, eqs. (3.27) and (3.29) reduce to:

3.2 ANALYSIS OF RAM ON CURVED SURFACES

The foregoing discussion is valid for the RAM coatings on flat surfaces in general. The analysis of coatings on curved surfaces is, in contrast, relatively more complex. Two important results derived by Weston (1963) facilitate the RCS reduction of the planar and curved scatterers coated with RAM. However these require profiles of specified geometry and suitable coatings as explained below.

In a typical detection and surveillance scenario, the monostatic radar is in the nose-on direction of the target. Hence from the perspective of incoming fighter aircraft and missiles, it is important to reduce RCS in the backscatter direction. It is convenient to associate a rectangular axis with nose-on direction which for relatively simple shapes is often the axis of rotational symmetry as well. In this discussion we identify this as the r-axis.

If the scatterer, i.e., the aerospace body is rotationally symmetric, the profile or the aspect as seen from any point on the z-axis would be circular. It is also possible to visualize other symmetries with respect to the r-axis. For example, a square cylinder would offer a square profile from the points



on the 2-axis, which has an angle invariance for a rotation of 90° (Fig 3.9a). However, square is not the only shape which offers this angle invariance upon 90° rotation. It can be easily shown that all regular polygons with the number of sides $p = An, n = 1,2,3, \dots$

have this symmetry. For $n= 1$ and 2 , we get a square and a regular octagon (Fig. 3.9b), respectively. In the limit, when the value of n is large, the profile is a circle (Fig 3.9c). Hence profiles such as square, regular octagon, circle etc. are invariant upon a 90° rotation.

For the purpose of discussion in this section we identify and label two materials. These materials which have the property $\epsilon = \epsilon_r$ are identified as RAM1. On the

Figure 3.9 Bodies with a rotational symmetry of 90° . (a) Square, (b) Regular octagon: (c) A circle may be considered as the limiting case of a $4n$ -polygon

other hand, coatings which satisfy the impedance boundary condition $E \cdot (N \cdot E)N = ZN \times H$ (3.34)

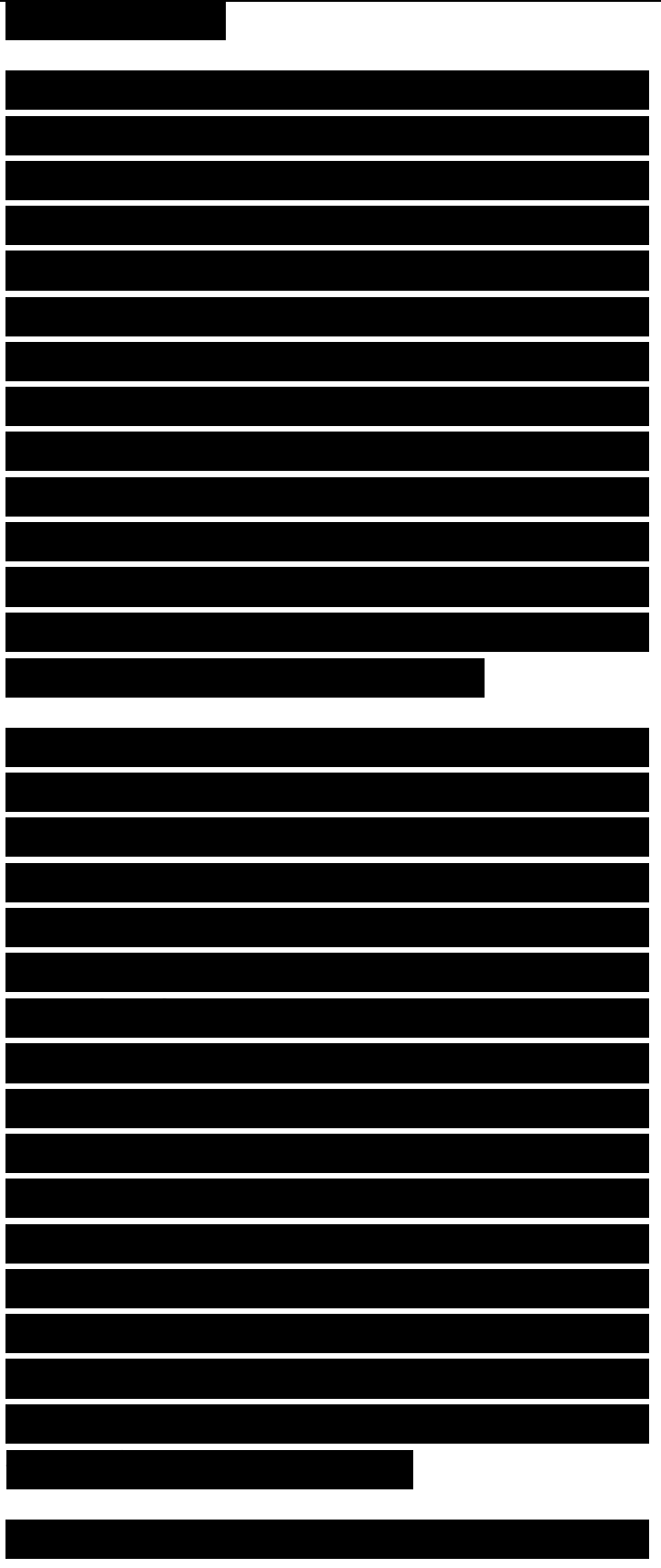
are labeled as RAM2. In the equation above, N denotes the unit outward surface normal.



It has been shown by a rigorous derivation that if the profile of the scatterer has a 90° invariance around a given aspect angle, and (i) the scatterer has been coated with RAMI, or (ii) satisfies the boundary' condition stated in eq. (3.34), then the backscattered field corresponding to that aspect angle reduces to zero (Weston, 1963). This theoretical result is of considerable importance since the conditions outlined tend to reduce the backscattered RCS to a minimum. We proceed to discuss the possible shapes for the scatterer for which the 90° angle invariance is maintained. We also explore the possible existence of the coatings identified as RAMI and RAM2.

Since the results mentioned above place the constraint only on the profile as seen from the z-axis, various shapes are possible for the scatterer. For a square profile, one could think of a cube. However, a square prism, and a square cylinder could also satisfy the 90° angle invariance. Hence all such absorber-coated scatterer shapes can be employed to achieve the null RCS. A similar discussion holds good for the regular octagon. Finally in the case of circular profile, the corresponding shapes could be right circular cone, sphere, spheroid, paraboloid and hyperboloid of revolution. Thus the importance of Weston's result lies in the flexibility' it offers on the scattering shapes for the nose-on RCS reduction.

The coating RAMI has been characterized



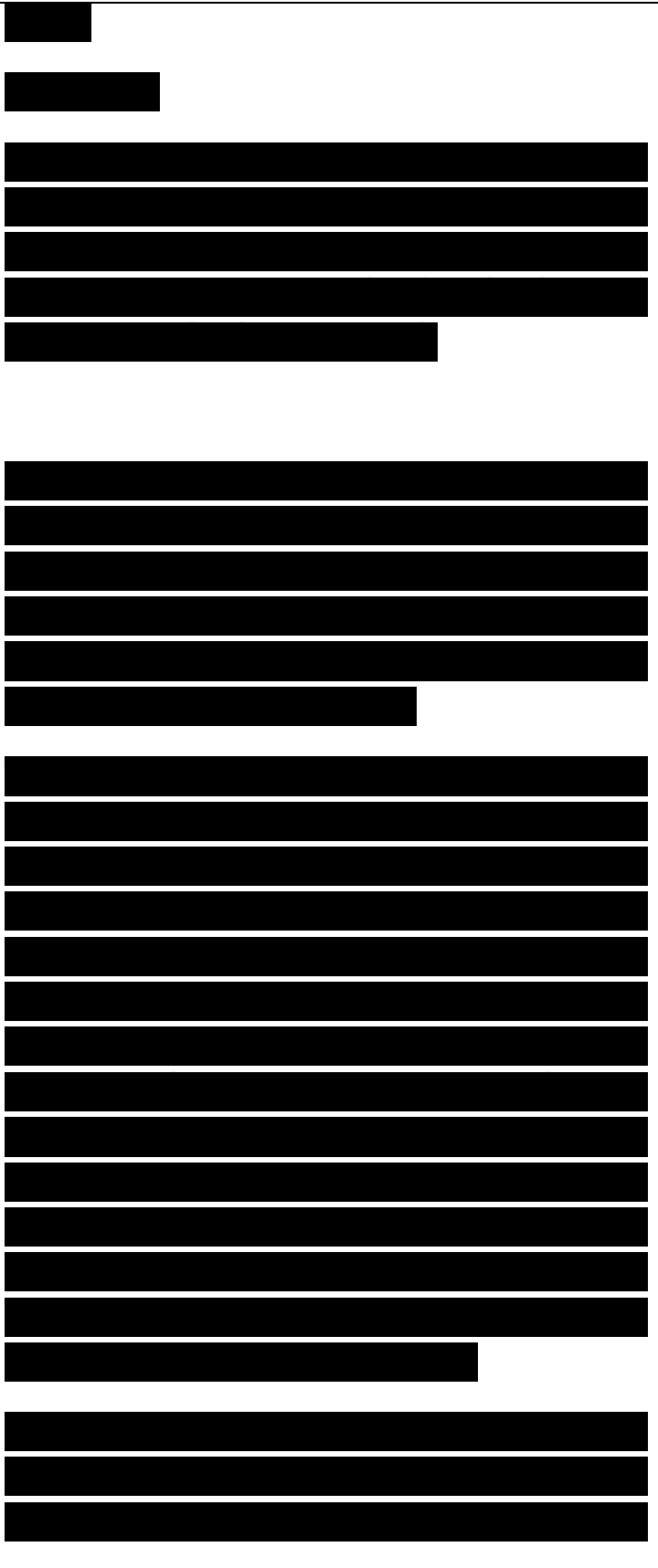
by the intrinsic property
 $H_r = \dots$ (3.35)

It turns out that there are a few absorbers for which eq. (3.35) is valid. They are known as $\epsilon = E$ absorber. The design and fabrication of such absorbers have been discussed in Chapter 4.

For coatings identified as RAM2 the product $(\mu/Y) - \dots - yf''$) is complex and large. The imaginary part of permeability and permittivity μ'' and ϵ'' are also large, implying that these are highly lossy materials. RAM2 are in fact a subset of the class of $\epsilon = \mu$ absorber.

These results are independent of frequency and hence, in principle, are applicable to low-frequency as well as the high-frequency scatterers. For extending these results to general convex surfaces, additional conditions must be satisfied by these curved surfaces. The impedance boundary condition at the surface is shown to be equivalent to the Leontovich impedance boundary condition, which requires that for a smooth convex surface: (a) The two principal curvatures of the surface vary and $n're'' + //''\epsilon' \gg 1$, (c) the spatial variation of ϵ , and $y/$, are negligible, and (d) the spatial variation of the near field exterior to the scatterer is small.

All the comparisons made above are with respect to the wavelength of EM wave propagation within the scatterer. The method of analysis is essentially ray-



theoretic, relying on geometrical optics and geometrical theory of diffraction. The methods outlined by Fock have also been utilized in the high-frequency domain. The results obtained by Weston (1963) can be extended to predict the backscatter RCS for multilayered RAM coatings on smooth conducting convex bodies (Bowman & Weston, 1966). Such scatterers have two components for their backscatter, viz. the specular, and the diffracted field contributions. The specular contribution from an absorber covered body is $|r|^2 cr$. Here r is the flat plate reflection coefficient, and a is the specular reflection. The diffracted field contribution is affected by the shape of the scatterer, its conductivity and the direction of the ray with respect to the axis of the body. A detailed analysis is given by Bowman and Weston (1966).

To summarize, an absorber with a large and complex refractive index significantly reduces the backscattered RCS for convex scatterers. In the resonance and high-frequency region, the main contribution to scattering is from the specular reflections and the creeping waves.

3.3 GRID BASED METHODS

3.3.1 Method of Moments

One of the methods to analyze this class of EM scattering and diffraction problems is the method of moments (MoM) (Harrington, 1968). The MoM is a very versatile and powerful technique which can be applied to linear, planar, as well as three-dimensional problems. The current distribution on the entire structure (including the RAM layer) is treated here

[REDACTED]

[REDACTED]

[REDACTED]

[REDACTED]

[REDACTED]

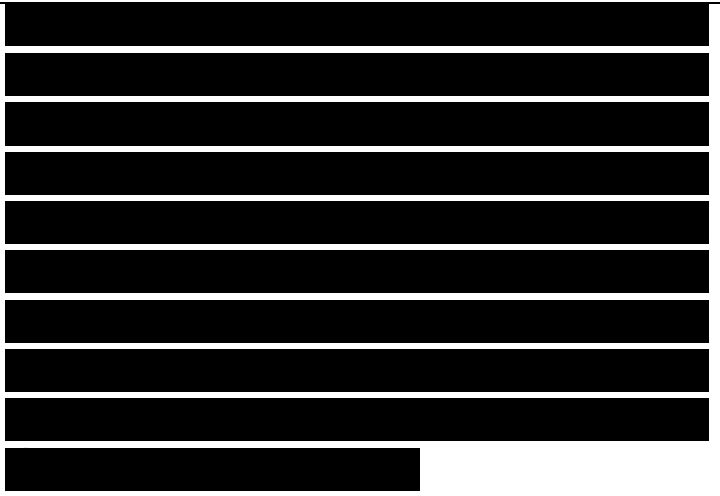
as unknown. The method involves segmentation of the body and choosing suitable basis functions to represent the current on these segments. A set of equations is generated by enforcing the boundary condition with a suitable set of testing functions. This results in a matrix whose order is proportional to the number of segments on which the current distribution is represented. The solution to the problem is found by inverting this matrix.

We now present the formal mathematical structure of MoM. It is assumed that when a source of excitation q is impressed upon a system, it manifests in a response p . These parameters q and p could for example represent the current and voltage of an electrical circuit. The physical parameters p and q can be related by a linear operator L ,

The linear operator L is system dependent. Quite often in the analytical problems, the source q is well-defined but the response p is to be determined. A salient feature of MoM is the hypothesis that it is possible to represent p by a set of linear basis function p ,

$$p = \sum a_n Z_n$$

where a_n are the coefficients associated the basis functions. The basis functions are also known as the expansion functions. It may be recalled that such expansions are not uncommon in electrical engineering. A square pulse signal is conventionally expressed in terms of the Fourier sine series with appropriate coefficients. The basis functions selected are linearly independent,



and are often sinusoidal, step, or triangular in nature.

The substitution of eq. (3.37) in eq. (3.36) results in:

(3.38)

Quite obviously, a_n are not known a priori and must be determined. The MoM overcomes this problem by assuming a set of testing or weighting functions. Just as with the basis functions, the testing functions too must be linearly independent. These testing functions are employed to define the inner product with respect to eq. (3.39)

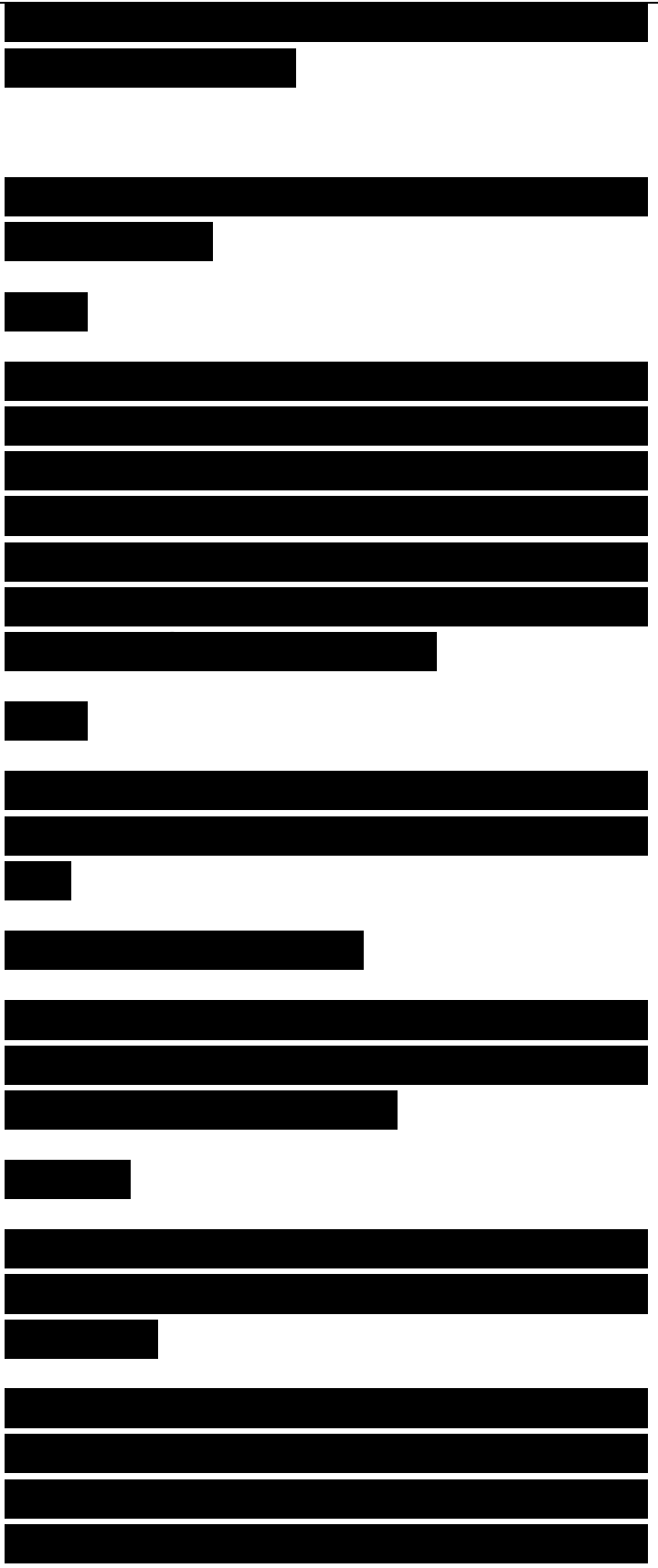
The commutative property of the linear operator permits the above equation to be written as

$$\langle \phi_m, L(\psi_n) \rangle = \langle \psi_n, L(\phi_m) \rangle$$

Equation (3.40) in fact is a set of linear equations which can be symbolically represented in the matrix form, where

Assuming that B^{-1} the inverse of B exists, the set of coefficients associated with the expansion functions can be evaluated from

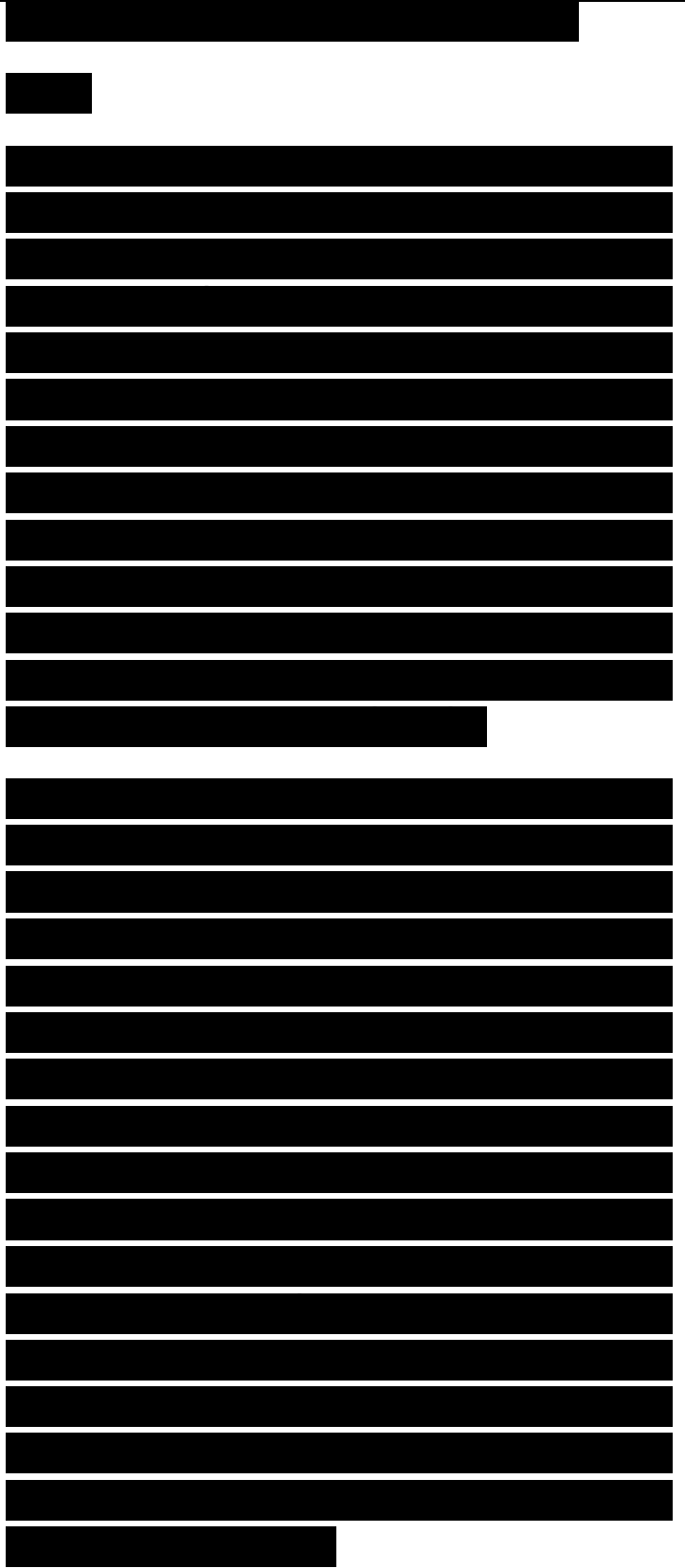
For square matrices, an inverse exists only if the matrix is nonsingular, that is, its determinant is nonzero. A_{nm} is essentially a column vector consisting of n coefficients. The response of the system p can therefore



be expressed as
(3.46)

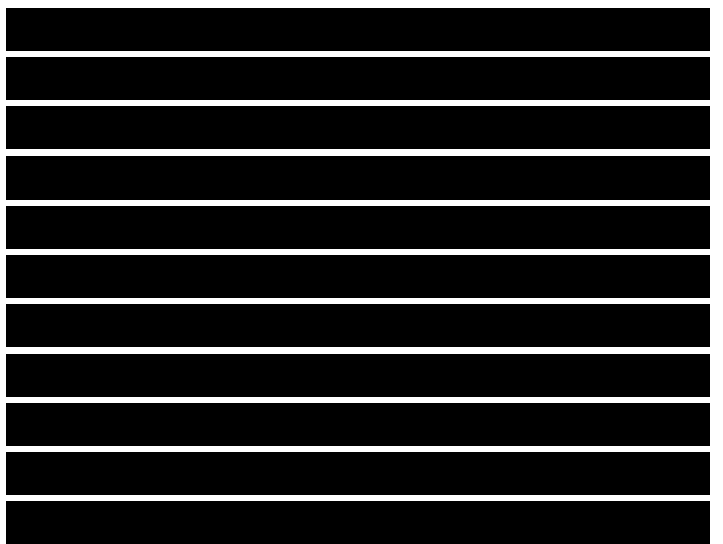
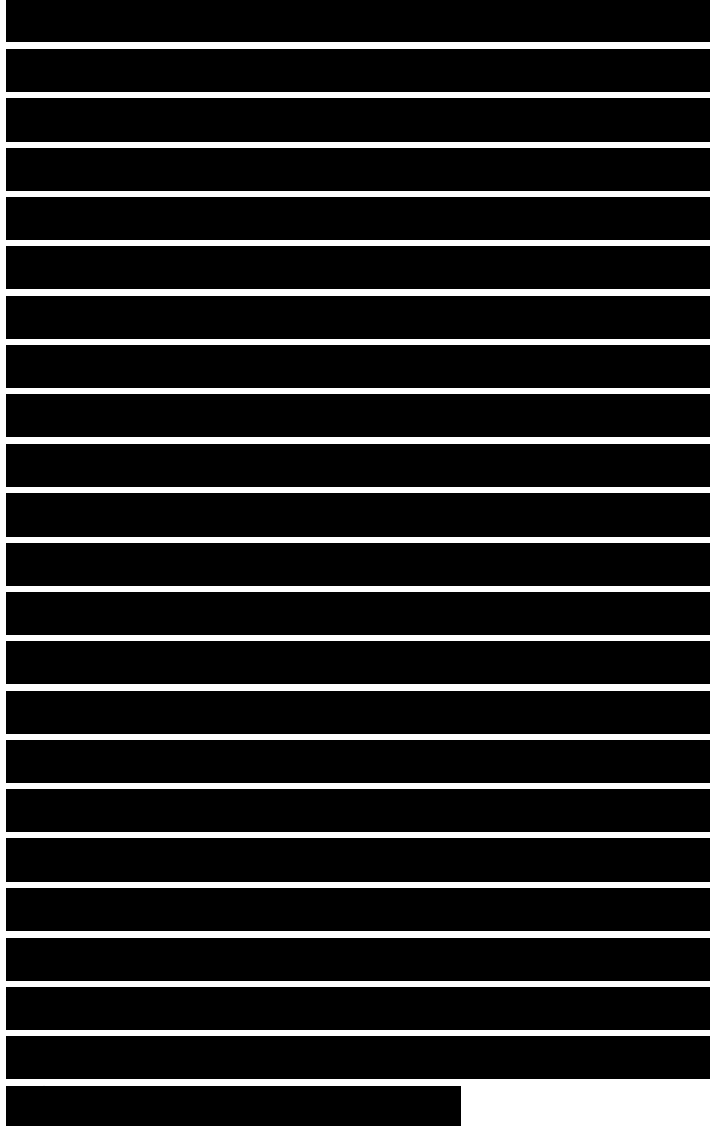
The time required to invert the matrix B and the accuracy of the solution obtained depends on the value of m and n. If the basis and testing functions chosen are the same, the analytical procedure is known as Galerkin's Method (Kantorovich & Akilov, 1964; Silvester & Chan, 1972). This method results in a symmetric matrix, thereby satisfying the reciprocity principle (Moore & Pizer, 1984). If one were to use the Dirac delta functions as the testing functions, this results in a point matching or collocation method which tends to reduce the computational time considerably.

In the context of EM problems, the matrices in eq. (3.41) correspond to impedance, current, and voltage matrices, so that the MoM solution essentially consists of inverting the impedance matrix. In the case of very simple problems, MoM yields exact solutions (Harrington, 1968). However, for the practical EM wave propagation problems, the order of the matrix to be inverted is large, and the solution is found by iterative procedure. The computationally intensive nature is one of the constraints on MoM. Considerable attention is therefore paid to understand the nature of the matrix to be inverted. For example, quite often one identifies the matrix as a Toeplitz matrix, enabling considerable reduction in the computer time required during the iterative procedure.



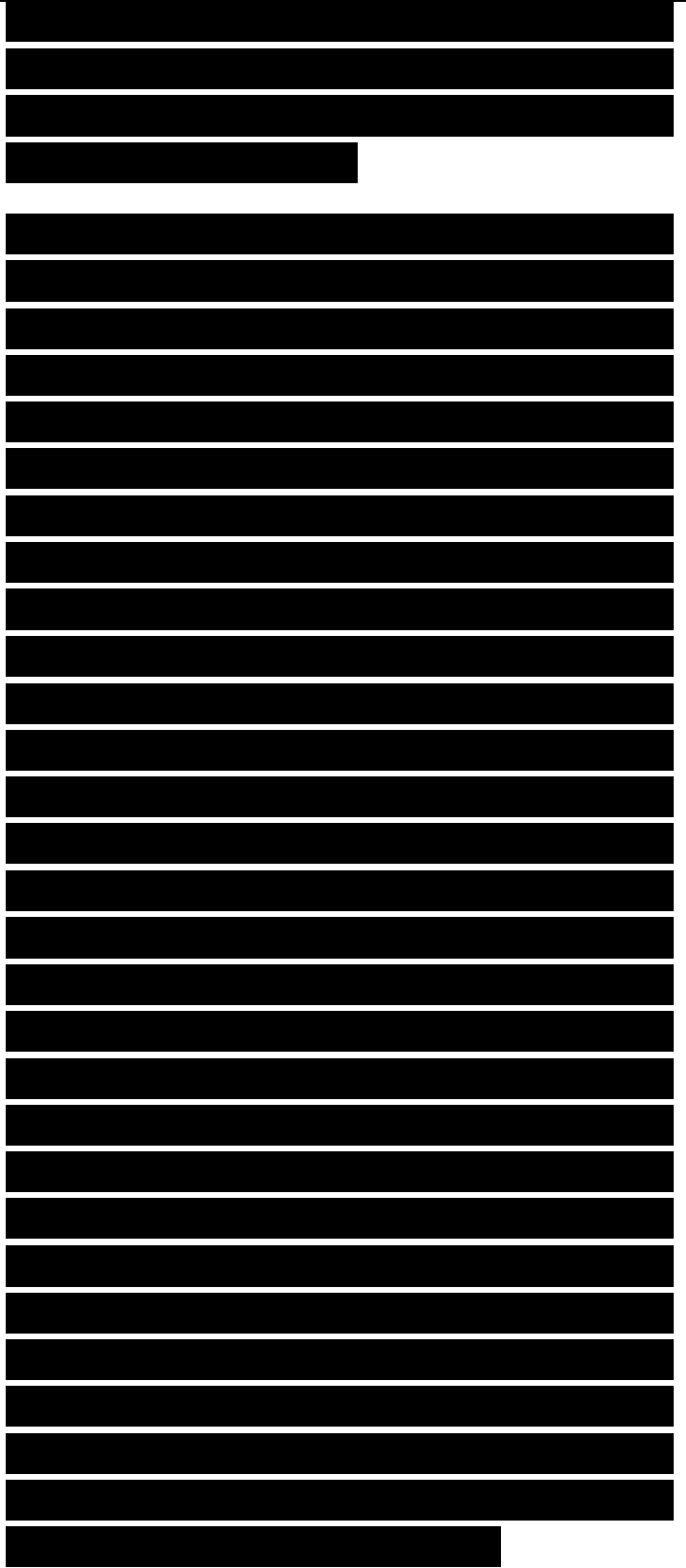
While applying MoM, a body is frequently replaced by a wire-grid model. In the wire-grid model a continuous surface is approximated by a mesh of finely connected thin wires (Newman & Pozar, 1978). Almost all complex surface shapes can be realistically modeled by this approach. However, in order to improve the accuracy of the results, the grid size in the mesh approximating the continuous surface should be small (Richmond, 1966). The successful substitution of a wire-grid for a continuous metallic surface depends upon the fact that, as the grid size becomes smaller compared to the wavelength, the grid supports a current distribution which approximates that on the corresponding continuous surface. This current is only an approximation to the actual current, and as such it can be expected to predict the far fields, but possibly not the near fields. This is due to the fact that the grid supports an evanescent reactive field on both sides of its surface (Lee và các cộng sự., 1976). An actual continuous conducting surface is not capable of supporting such a field.

The accuracy with which a wire-grid model simulates an actual surface depends on the expansion and testing functions, the radius of the wire segments, as well as the grid size. For example, with pulse expansion functions it has been found that a grid-spacing of about 0.1 to 0.2 λ yields good results (Richmond, 1966). In certain cases the grid size can be taken up to 0.25 λ (Lin & Richmond, 1975). Reduction of grid size of the mesh which improves accuracy poses another kind of problem. A finely knit mesh will require the determination of



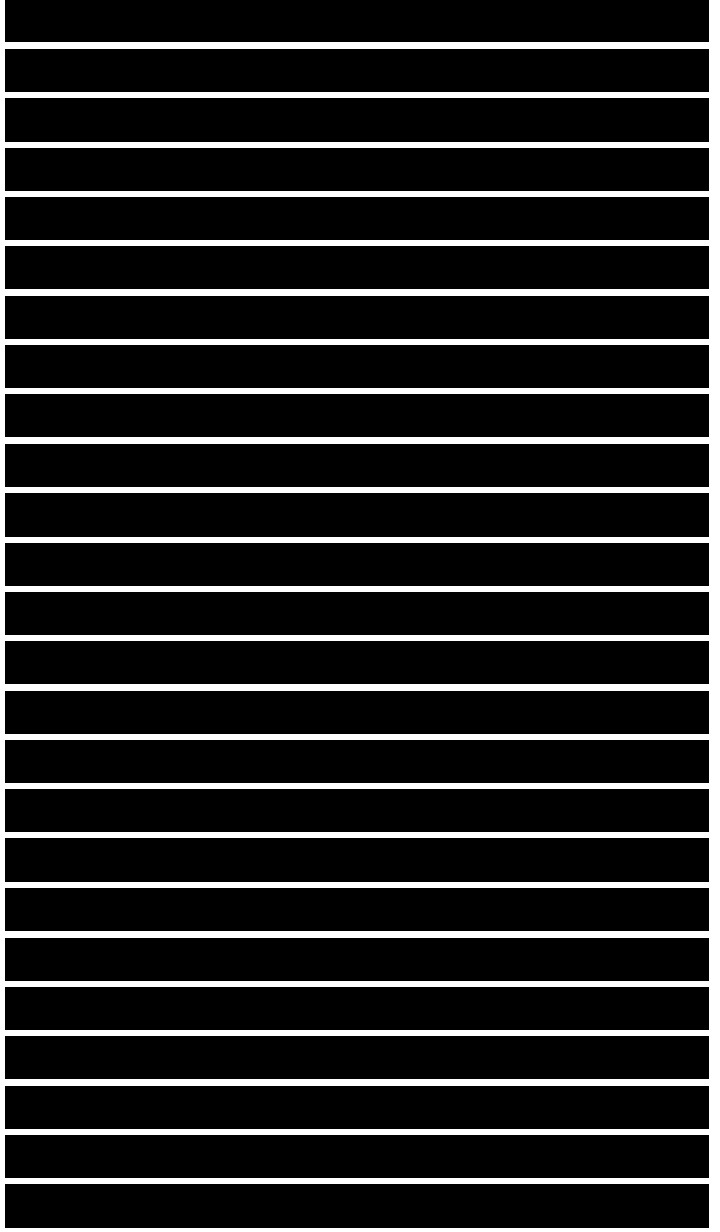
a larger number of unknowns. As a consequence, the order of the matrix will increase, as also the computer time needed for inverting this matrix.

An alternative to the wire-grid model is the surface patch model. Here the surface is treated as continuous and made up of regular small surface patches. However, the current is expressed in terms of two-dimensional basis functions. In this case, the order of the matrix is smaller than the wire-grid model for the same accuracies in the result. In contrast to the wire-grid model, the surface patch models do not allow realistic modeling of complex surfaces. This method has been applied to solving the scattering problems of a flat plate illuminated by a plane wave (Newman và các cộng sự., 1984), bent square plates and canonical problems of cylindrical surfaces and spheres (Rao và các cộng sự., 1982). Once again, the smaller the surface patch, the greater is the accuracy. But a smaller surface patch implies that the order of the matrix is large. There is also a limit to which the size of the surface patches may be increased without sacrificing the accuracy . It has been reported that when the pulse functions are used, failure to allow for variation of the field within each cell limits the maximum usable electrical size of the cells. Appreciable error is expected for $|k| > 2$, in one- or two-dimensions, and $|\xi| > 6$, in the three-dimensional problems, where l is the side of the cell and k is the propagation constant in the material (Hagmann và các cộng sự., 1982).



The MoM is well known to predict reasonably accurate solutions for the class of problems they treat. The applicability of MoM to RAM analysis has therefore been explored extensively (Tremain & Mei, 1978; Medgyesi-Mitschang & Eftimiu, 1979; Sultan & Mittra, 1985). Rogers (1986) applied MoM to RCS prediction of arbitrarily shaped conducting bodies coated with RAM. MoM can also be modified to effectively analyze the shapes used in the construction of anechoic chambers. Yang và các cộng sự. (1992) have developed a periodic moment method (PMM) for the analysis of two-dimensional lossy dielectric scatterers. A CRAY-YMP was employed to determine the reflection and transmission coefficients of periodically distributed wedges illuminated by a plane wave. The grid-like segmentation of MoM is also employed in the spatial network method by Kashiwa và các cộng sự. (1990). The scattering body, an aircraft, is divided into a number of cells of $X/30$ size. In this method, the equivalent circuit of the coated scatterer is constructed in terms of bulk impedances to compute the field patterns.

It is apparent from the literature that MoM is most suitable when the scatterer is electrically small in size. MoM is often thought of as a low-frequency technique because it cannot be applied to bodies that are arbitrarily large in terms of the wavelengths. A body that is large in terms of wavelengths will result in a large matrix. Such a matrix is not only difficult to invert, but also tends to become unstable (Mittra



& Klein, 1975). Thus the review of MoM has clear pointers as far as its application to RAM-coated structures is concerned. The MoM technique can be used satisfactorily only when the dimensions of the structure are of the order of the wavelength, i.e., the radar frequency is low (Medgyesi-Mitschang, 1982). Quite often, the practical scatterers in the Gigahertz range tend to be much larger than one wavelength; for such problems, MoM is not a viable method even with the state-of-the-art computers.

3.3.2 Finite Difference Time Domain Method

An alternate to the Method of Moments within the domain of grid-based methods is the Finite Difference Time Domain (FDTD) method (Yee, 1966). In this method, the scatterer over which EM fields are induced is embedded in a space lattice over

which the finite difference is taken. The starting equations are the Maxwell curl equations in differential form. These equations are then adapted in the finite difference format and rearranged to yield recurrence relations. The finite difference scheme implemented in FDTD is essentially based on one-dimensional Taylor series expansion. Given suitable boundary conditions, the scheme converges to steady state values for the electric and magnetic fields.

Prior to outlining the FDTD method, we give the Taylor series expansion which is

[REDACTED]

[REDACTED]

[REDACTED]

[REDACTED]

[REDACTED]

utilized in finite difference schemes. In the complex (x, y) plane, an analytic function $f(x, y)$ can be expressed by its Taylor series expansion around a given point (a, b)

In the simpler one-dimensional case, the Taylor series reduces to

Substituting $x = a + \Delta x$ in the equation above, we obtain

We denote a function at an arbitrary grid point (u, v, w, n) in the four-dimensional orthogonal space-time (x, y, z, t) coordinate frame as

where $u, v, w,$ and n are assumed to be integers. It follows that: $\frac{\partial f}{\partial x} = \frac{f(u+1, v, w, n) - f(u-1, v, w, n)}{2\Delta x}$

Applying the Taylor series expansion (3.50) in the immediate neighborhood of the space lattice grid point (u, v, w) at the instant n , one obtains

Thus as a first-order approximation of eq. (3.55), we get

Similarly by adding eqs. (3.53) and (3.54) it can be shown that

The derivatives with respect to y and z are identical in form to those in eqs. (3.56) and (3.57). The partial derivatives with respect to time t can be obtained in likewise manner. We recall that in the space-time coordinate frame, the analyses along the

[REDACTED]

[REDACTED]

[REDACTED]

[REDACTED]

[REDACTED]

[REDACTED]

[REDACTED]

[REDACTED]

[REDACTED]

length and time axes are identical. Thus the first derivative of the function ϕ with respect to the time parameter t can be derived as

Equations (3.56) through (3.58) are made use of in the FDTD formulation to convert the partial differential equations into the finite difference equations.

We now recall the Maxwell-Ampere law

The constitutive relations (2.41) and (2.43) for a linear isotropic medium are substituted in the equation above, to get (3.60)

The curl equation (3.60) can be conveniently denoted by its determinant definition

Equating the two sides of (3.61) along the directed components, we obtain

Substituting eq. (3.58) and the partial derivatives with respect to y and z (c.f eq. (3.56)) in eq. (3.62), we obtain a finite difference form as

The value of E_x at time n is assumed to be the average of those at the $(n-\frac{1}{2})$ and $(n + \frac{1}{2})$ instants.

Substituting eq. (3.66) in eq. (3.65), and by rearranging the terms, we get

We therefore obtain the electric field at the time instant $(n + \frac{1}{2})$ as a recursive relation.

[Redacted]

From eqs. (3.63) and (3.64), one can obtain the E_x , and E_y components as:

From the Faraday induction law, recursive relations can be similarly derived for the magnetic field components H_x , H_y , and H_z . The electric and magnetic field values thus obtained are used as the starting point for the next instant. The recursion process is continued till one obtains the steady state.

The FDTD formulation permits spatial variation of the intrinsic parameters of the media. Such inhomogeneities are handled by setting up a lookup table of the permittivity and permeability values at each spatial point of interest.

Spatial segment resolution increases the accuracy of the results predicted by the FDTD method. Typically with 0.1λ length segmentation, one could achieve ± 0.6 dB accuracy, whereas 0.05λ would result in an error margin within ± 0.2 dB (Taflove & Umashankar, 1989).

The stability of the FDTD numerical solution is guaranteed by taking the time interval Δt as (Taflove & Brodwin, 1975):
 $\Delta t < \frac{1}{c} \sqrt{\frac{\epsilon_{min}}{\mu_{max}}}$

Electric and magnetic field determinations in the FDTD formulation are interspaced in the volume. To illustrate, in a given plane of the grid frame, if the electric fields are

[REDACTED]

[REDACTED]

[REDACTED]

[REDACTED]

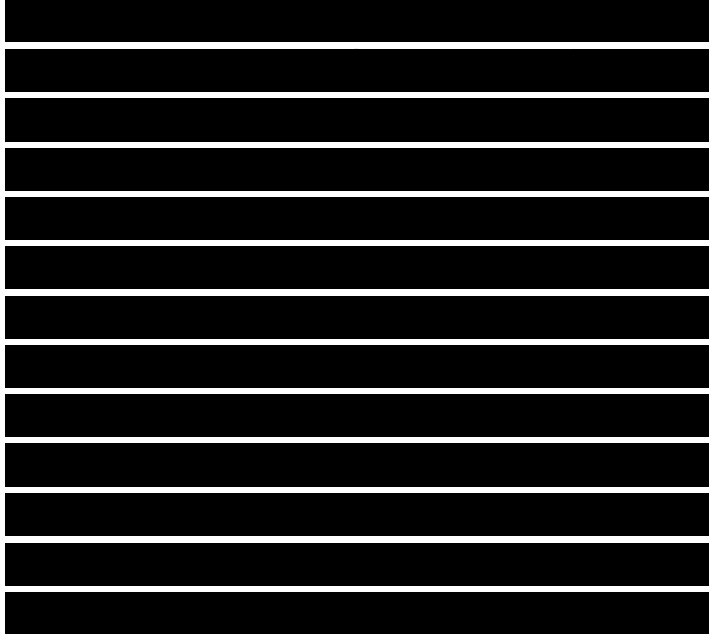
[REDACTED]

[REDACTED]

determined at the grid intersections (nodes), the magnetic fields are determined at the mid points of the grid between two nodes. Similarly, the EM field vectors E and H are also interleaved along the time axis with $\Delta t/2$ time step.

Spatial analysis can be implemented independently for different planes or even different nodes. This makes the FDTD algorithm amenable to parallelization (Brand & Vanewijk, 1994). Such a scheme can be implemented even on parallel computers with a low number of processors. On the other hand, FDTD can be parallelized to the extreme, with a grid intersection node per processor. Taflove and Umashankar (1989) have shown that if there were a Connection Machine with 1,500,000 processors (1.5M machine), the effective performance could be scaled up to 100 GFlops as compared to the 10 GFlops of Cray 3.

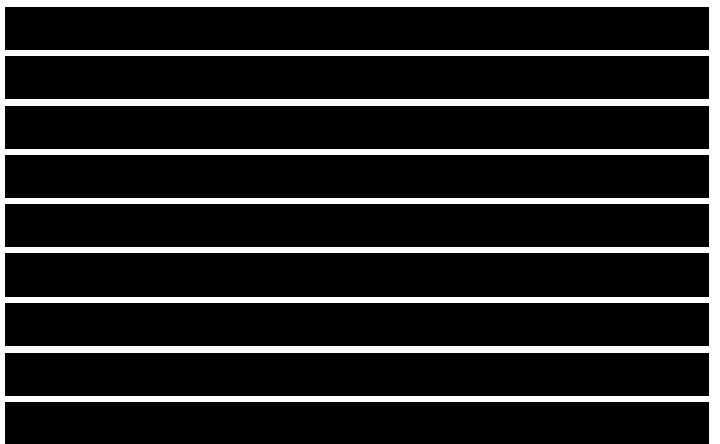
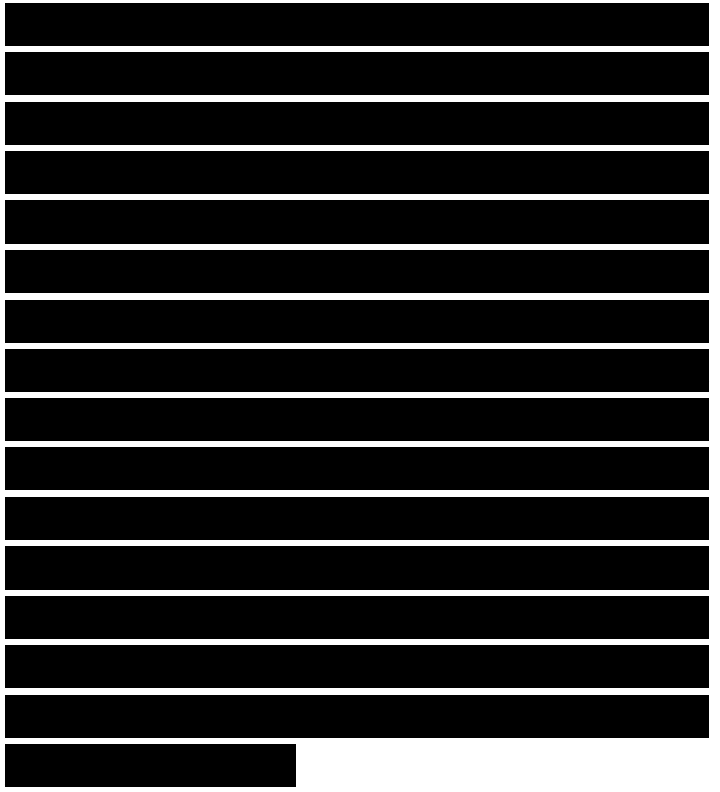
The FDTD formulation often employs the rectangular coordinate system. Hence surfaces with planar shapes have been more amenable to analysis through this approach. Among the simplest of the canonical shapes to be handled has been the square metallic cylinder (Umashankar & Taflove, 1982), which was validated against the results obtained by MoM. A cube of similar dimension, i.e., $ps - 2$, was analyzed for broadside RCS (Taflove & Umashanker, 1983) which once again matched, within 0.2 dB in magnitude and 1° in phase, the results predicted by MoM. Yet another canonical surface, namely the



plate, was analyzed and compared with measurements (Taflove và các cộng sự., 1985) where the theoretical predictions showed agreement within 1 dB and 1° look angle. FDTD under the rectangular formulation has been applied and has predicted excellent results in the case of complex aircraft structures (Taflove, 1995).

It would appear that the FDTD formulation in the rectangular coordinate system is not very efficient for analyzing curved surfaces (Taflove & Umashankar, 1989) for which use of the locally distorted grid (Madsen & Ziolkosvski, 1988), the globally distorted unstructured and body fitted grids (Fusco, 1990) have been explored. The metallic circular cylinder (Fig 5) thus handled, resulted in an accuracy of 1.5%. It is interesting to note that among the first structures to be analyzed by FDTD was a dielectric cylinder (Taflove & Brodwin, 1975). However the accuracy was within 10% which was an order of magnitude worse than that of other contemporary methods.

An alternative approach to the bodies of revolution has been by reformulating FDTD in the appropriate coordinate system (Jurgens & Saewert, 1995). For example, one would analyze the circular cylinder in the circular-cylindrical coordinate system since the right circular cylinder is a coordinate surface of this particular coordinate system (Moon & Spencer, 1971). The FDTD method has been used in conjunction with the Levenberg-Marquardt



nonlinear optimization routine for forward scattering computations of broadband absorbers (Strickel & Taflove 1990). It is also suggested that the use of Connection Machine would enable cost-effective RAM design with efficient higher dimensional searches.

Earlier work by Holland and Cho (1986) on the lines of FDTD employing coarse grids reported reasonable accuracy (within 10%) for RAM coated cylinders. This was essentially a two-dimensional analysis involving no more than 3,125 cells. Yet another variant of time domain analysis conforming to Bergeron's method in three-dimensional space and time was successfully employed to analyze the resonant RAM (Aoto và các cộng sự. 1987).

The characteristics of the time domain pulse waveform as a function of the incidence angle were presented along with the variations of field distribution for the changes in magnetic loss.

How does the FDTD method compare with the MoM discussed above? It has been shown that MoM could be attractive for certain low-frequency problems. But as the operational frequency and thereby the electrical size of the scatterer is scaled up, MoM becomes computationally , whereas FDTD might still be able to solve the problem. The example cited by Taflove and Umashankar (1989) in this context is that of the monostatic RCS of a 30x10x0.65 cm³ flat conducting plate. At 1 GHz, MoM requires a total of 172 triangular patches; inverting a matrix of the order (258x258) is

[REDACTED]

[REDACTED]

[REDACTED]

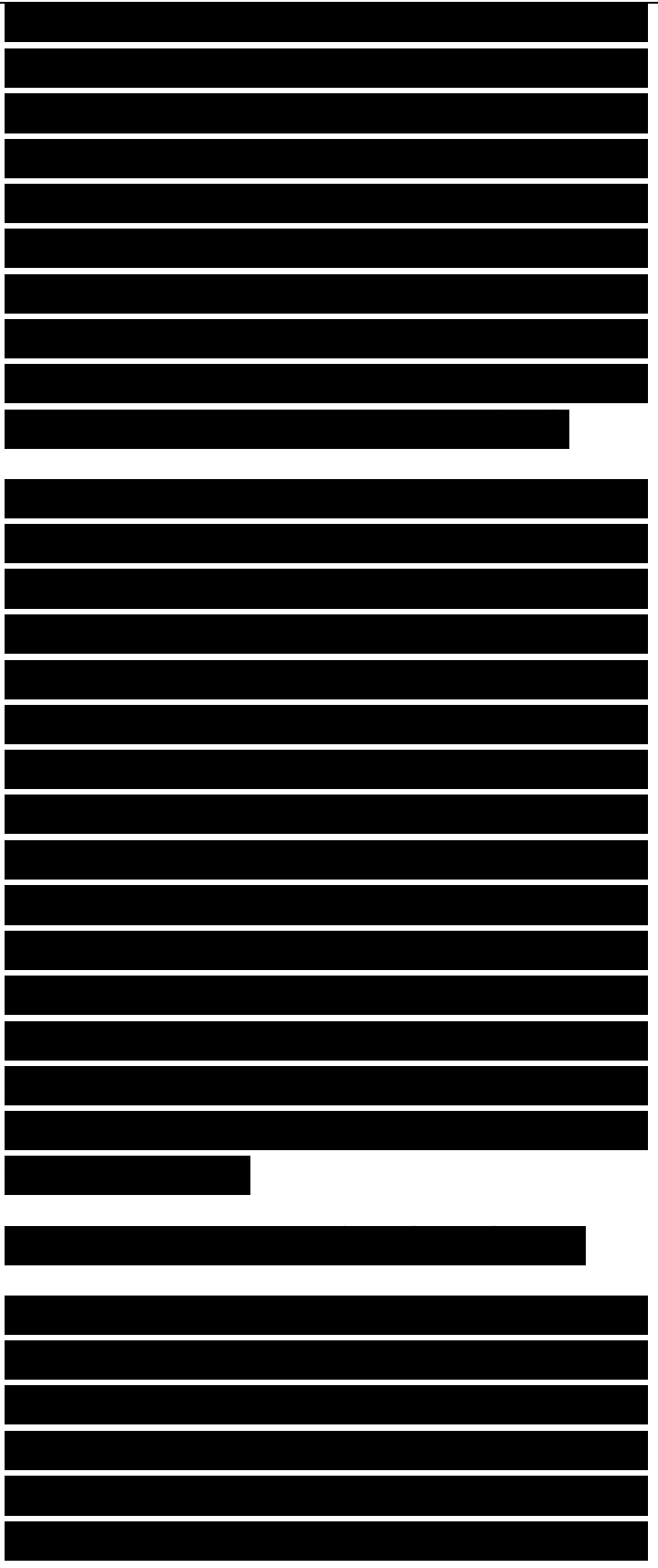
[REDACTED]

computationally feasible. The FDTD method on the other hand, would require the determination of 221,184 unknown field components. However, when the frequency is scaled to 9 GHz, a (4890x4890) order matrix must be inverted, thus eliminating MoM as the method of analysis with present day computers. FDTD still remains a feasible method with the overall cell size of 112x48x18 corresponding to 580,608 unknowns.

It has been suggested that scatterers of the order of 50 X can be handled in the near future with faster concurrent and vector supercomputers than available today. However, at the typical X-band frequency of 10 GHz, 50 X represents 1.5 meters. It must be obvious to a discerning reader that neither MoM nor FDTD can presently treat problems of a practical nature for aerospace applications when the scatterer is electrically large. For such electrically large scatterers one uses an entirely different approach based on high-frequency methods. The ray-theoretic foundation of these methods is described below.

3.4 HIGH FREQUENCY METHODS

Electromagnetic analysis of surfaces is done with respect to the electrical wavelength. One would therefore expect identical behavior for a scatterer of 30 meters at 100 MHz and another one of similar shape scaled down to 1 meter at 3 GHz. The reason for this is that both the

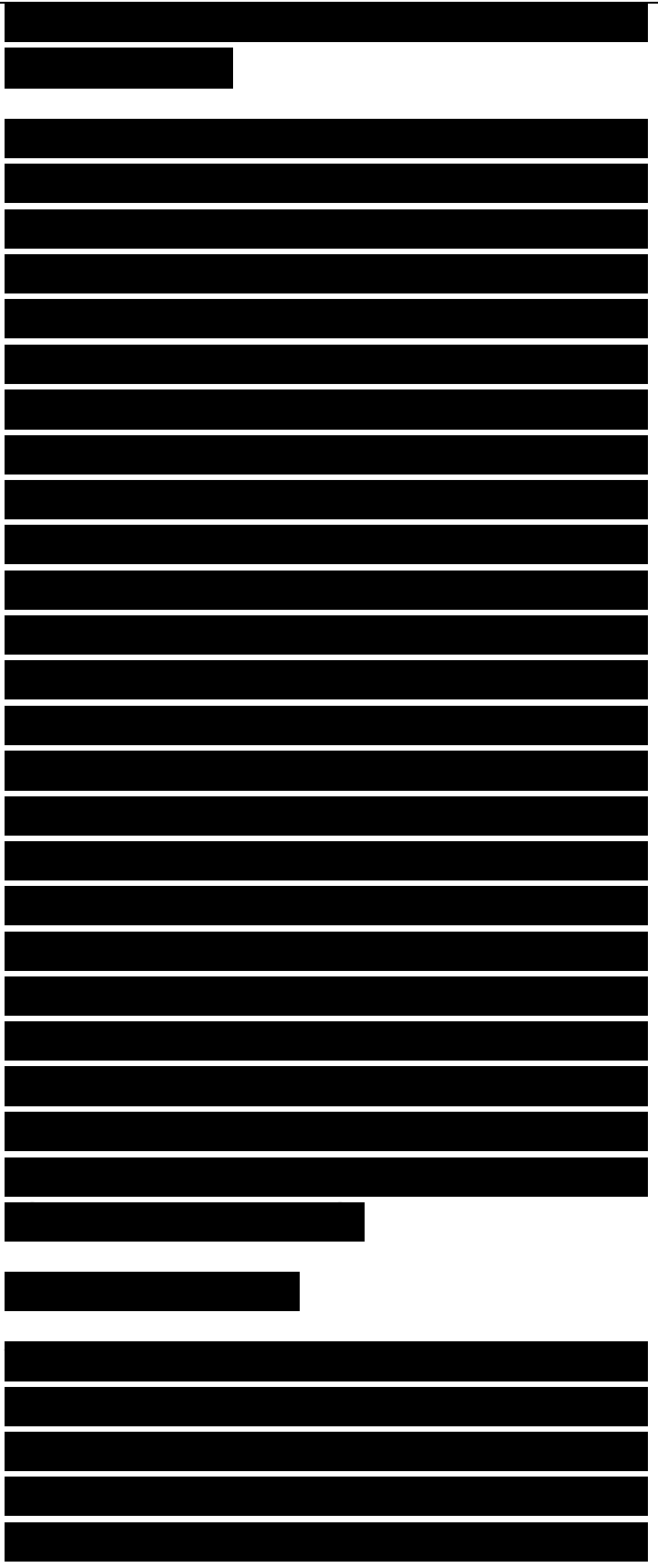


scatterers in terms of electrical size are of 10 X.

It is clear from the discussion of MoM and FDTD that these grid-based methods are constrained by the size of the scatterer. The time taken for volumetric grid analysis increases by a factor of n^3 where n is the increase in the linear dimension of a cube. With the ever increasing use of higher frequencies, the object keeps increasing in electrical wavelength. An aircraft or missile of 10 meters linear dimension corresponds to 1 X, 10 X, and 300 X at 30 MHz, 300 MHz and 9 GHz respectively. All these frequencies are actively used in aerospace applications. However MoM can yield satisfactory results only at 30 MHz. At 10 X only coarse results can be obtained by increasing the grid size, whereas at 300 X, MoM is not a feasible method since it would become computationally intractable. Scatterer much larger than 1 X in linear dimension are said to be in the high-frequency domain. For such high-frequency scatterers, one applies geometrical optics based techniques where the larger the size of the scatterer the more accurate the predicted results.

3.4.1 Geometrical Optics

If the frequency associated with the wave propagation can be considered infinitely large in the limit, as compared to the scatterer, the corresponding wavelengths approach zero. For such scatterers any discernible field variation on the surface



occurs only over large distances. Hence the field behavior is said to be local, in the sense that it depends only on the point of interaction with the HM wave and its immediate neighborhood. For such electrically large scatterers, the wavefront can always be approximated as a plane wave (Jones, 1964),

where $S(r)$ is called the eikonal of the wave. We recall the wave equation (2.76) for the simple media

which in the phasor form is expressed by $\nabla^2 E + \epsilon \mu \omega^2 E = 0$ (3.74)

Substituting eqs. (2.44) and (2.45) in the equation above, we get

$$\nabla^2 E + \epsilon \mu \omega^2 E = 0 \quad (3.75)$$

since

$$p = \epsilon \mu \omega^2 \quad (3.76)$$

Equation (3.72) is substituted in eq. (3.75) above, and upon rearrangement of terms we obtain

$$\nabla^2 E - (\nabla S)^2 E = -j(\epsilon_0 \nabla^2 S + 2 \nabla \epsilon_0 \cdot \nabla S) E - \epsilon_0 \nabla^2 E \quad (3.77)$$

If the wavelength $\lambda \rightarrow 0$, as is the case in the geometrical optics (GO) region, the phase constant $k \rightarrow \infty$, since

The right hand side of eq. (3.77) vanishes in such cases, and we obtain the nontrivial solution

$$(\nabla S)^2 = H, C, \quad (3.79)$$

This is known as the eikonal equation.

The concept of eikonal S can be extended to relate the electric field when transported from one point to another. Consider two eikonals S_1 and S_2 , which is equivalent to considering a ray bundle (or ray tube) at two different points in space (Fig. 3.10). We denote the incremental area at the two eikonals as da_1 and da_2 -

Figure 3.10 Wavefronts at eikonals S_1 and S_2 .

The two radii of curvature along the orthogonal principal directions for the wavefront at the eikonal S_1 , are denoted as r_1 and r_2 . Assuming that the normal distance between S_1 and S_2 is given by s , it is possible to relate the incremental area da_2 and da_1 , on the two eikonals.

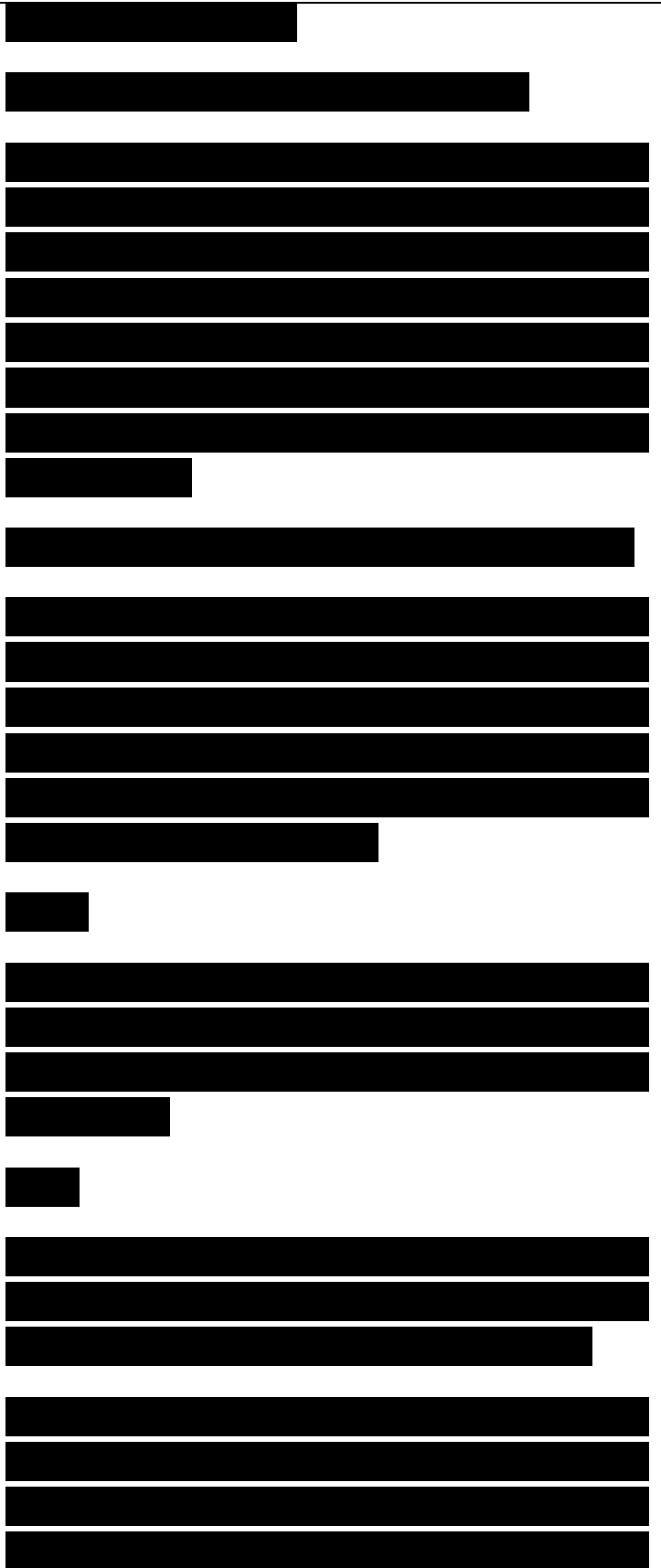
(3.80)

For a homogeneous medium, the electric field at S_2 , due to that at S_1 , can be obtained by the energy conservation principle.

(3.81)

An implicit assumption has been made in eq. (3.81) to incorporate the polarization and phase of the plane wavefront (Pathak, 1992).

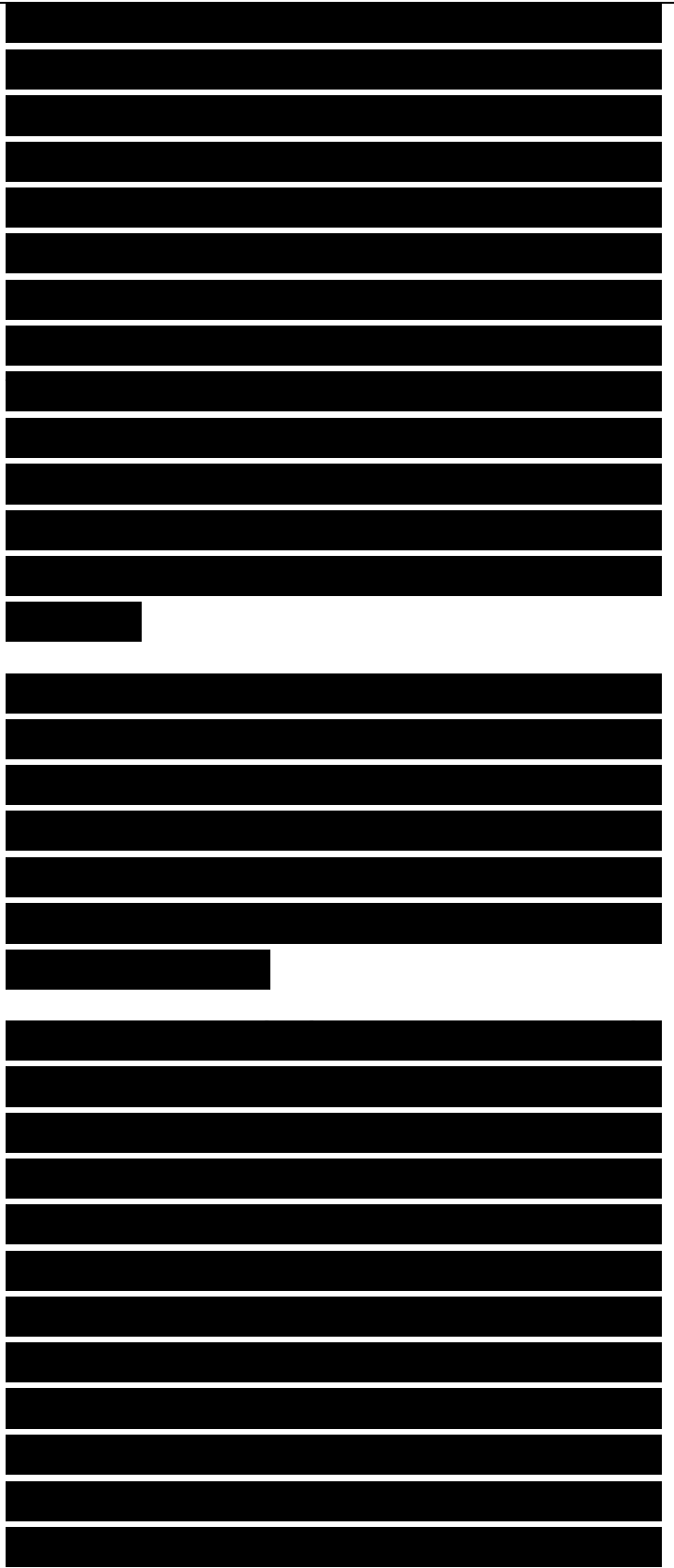
If a point source of radiation S is in the vicinity of an electrically large scatterer, it divides the space surrounding the scatterer in the illuminated and shadow regions (IR



and SR). The regions IR and SR meet at the shadow boundary . SB (Fig. 3.11). Let an observation point, distinct from S, be denoted by Pt in IR. Similarly let an arbitrary point in the shadow region be denoted by Ps. A direct ray can be invariably drawn from S to P,. Reflected ray(s) can also be shown to exist between S and P|. In contrast, for the point Ps in the shadow region, only refracted ray(s) can exist between S and Ps. In many practical applications, however, for example when the scattering is metallic, refracted rays do not exist. These concepts of IR, SR and

Figure 3.11 A point source in the vicinity of an electrically large scatterer divides the neighborhood into the illuminated and shadow regions denoted by IR and SR. respectively.SB, and direct, reflected and refracted rays can be extended to the case of a plane wavefront incident on a scatterer (Fig. 3.12).

It is well known that EM waves traverse in a straight line in free space or in any other linear homogeneous medium. The laws of reflection and refraction have been discussed in Section 3.1.2. The point of incidence on the surface is known as the specular point in the context of reflection. The specular point exists even for normal incidence. In order to determine the exact path of propagation for these direct, reflected, and refracted rays, one can follow a more general principle of optics called Fermat's principle of least action (or least time). This principle requires that ray



paths corresponding to EM propagation be stationary. That the ray path in free space should be the “shortest path”, and hence a straight line, is a consequence of Fermat’s principle. The angles of incidence and reflection being equal, the restriction regarding coplanarity’ of the reflected ray with respect to the plane of incidence also follows from this principle. In the case of refraction, Snell’s law can be readily derived from Fermat’s principle.

There could of course be multiple reflections (and. or refractions) when a ray propagates from a source to an observation point. For example, the ray path undergoes more than one reflection when it is incident on a dihedral comer. The geometric description of the direction of a ray, which undergoes m successive reflections, can be elegantly expressed in the dyadic form (Comblect, 1976),

$$s_r^{[1-2N_m N_m][1-2N_{m-1} N_{m-1}] \dots [1-2N_1 N_1]} s_{i=1,2,3,\dots} \quad (3.82)$$

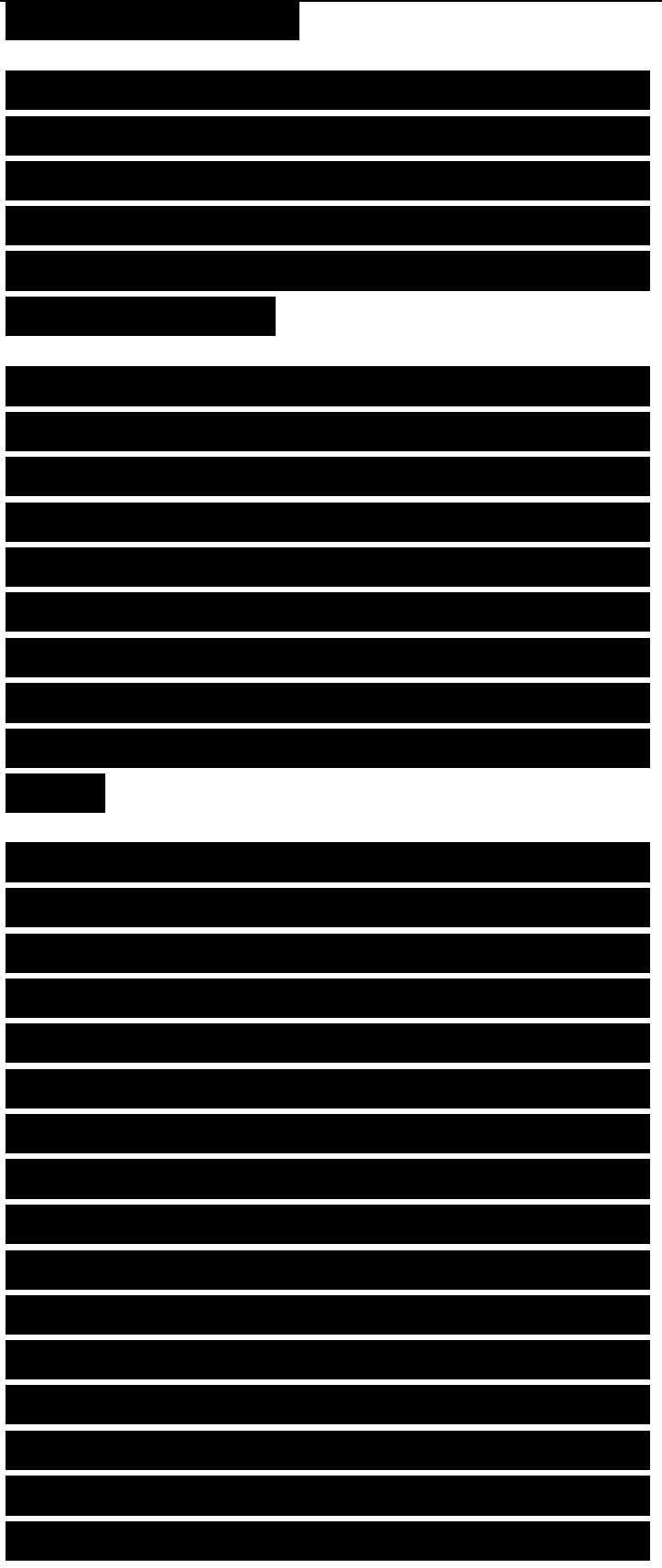
where I is the identity’ matrix, N_w, is the unit outward surface normal vector corresponding to the w-th reflection, and s_w is the unit vector in the ray direction. Similarly the refraction can be written as a dyad:

Observe that in order to generalize this dyadic form to multiple refractions, N in eq. (3.84) must be replaced by N_m corresponding to the i-th refraction. Similarly, the direction of s_w in the denominator also varies and may be denoted as s_{w,m}. It is apparent that s_{w,m} is s_{w,m}. Hence this relation is essentially recursive in nature.

If the scatterer is conducting in nature, GO predicts an accurate field in the deep of the illuminated region. This is the sum of the fields associated with the incident ray and the reflected ray(s). Equation (3.81) may be rewritten for the incident and reflected electric fields as

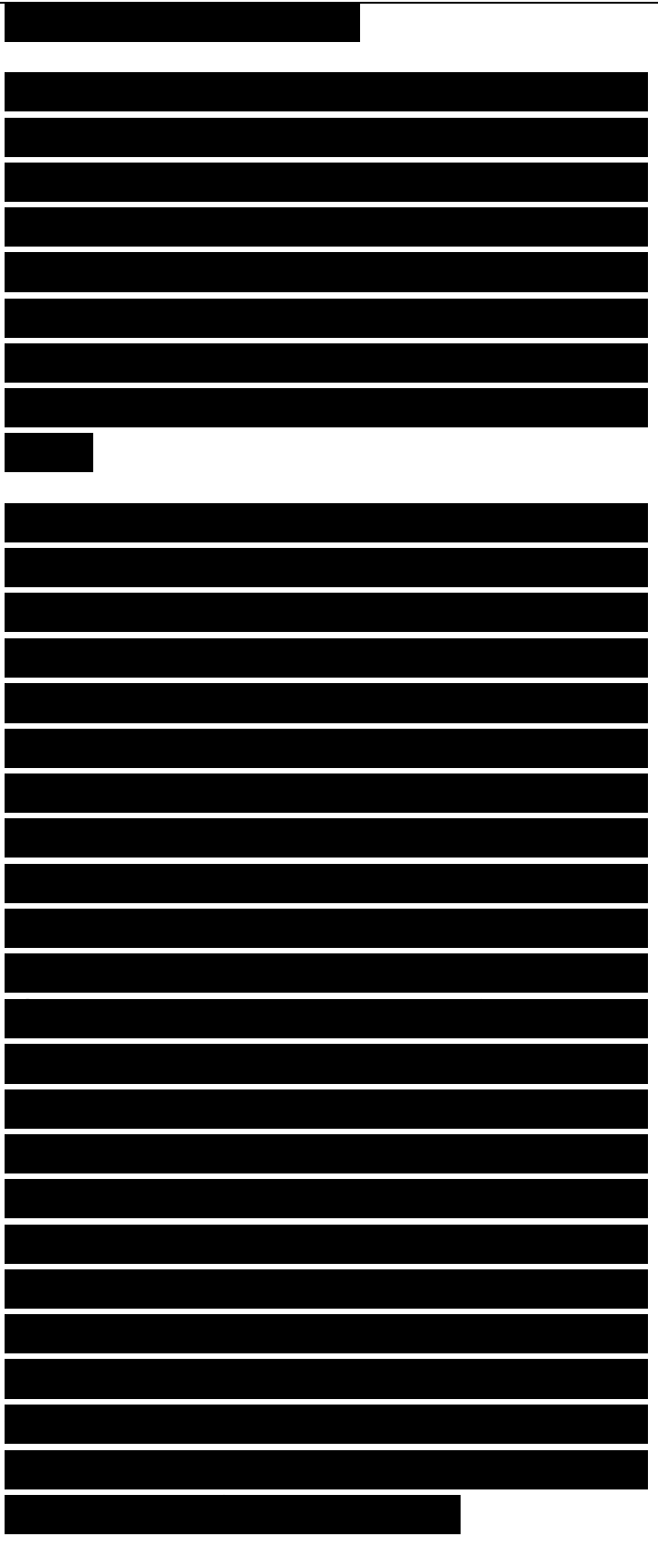
We note that S and P , in eqs. (3.85) and (3.86) are equivalent to S , and S_j in eq. (3.81). The subscripts i and r denote incident (or direct) and reflected ray fields. Further, the sub-subscripts have been dropped for reasons of convenience. Equation (3.86) relates the incident and reflected field at the point of specular reflection through a reflection dyad R as outlined by Pathak (1992).

Moreland and Peters (1966) applied GO to obtain an expression for RCS analyses of spherical and cylindrical coated dielectric shells. Further, by comparing specular and creeping wave contributions they concluded that the latter gave rise to errors in the case of comparatively smaller bodies while its effects are negligible for larger bodies. Earlier solution of a similar problem had been attempted using semi-empirical methods for RCS computations of the spherical and cylindrical scatterers (Swamer & Peters, 1963). The scattered field was approximated as the phasor sum of the field scattered by the air-dielectric interface and that by the equivalent conducting body, which differs from the actual body because of the lens action of the shell.



Alexopoulos (1969) applied GO to obtain the reflected electric field for large spheres ($ka \sim 50$ to 1000 ; a is the radius of the sphere) coated with inhomogeneous dielectrics. A series solution has also been obtained for the backscattering GO computations for bodies of revolution coated with homogeneous RAM to study the effect of curvature on RCS reduction (Arfaev, 1982).

Since GO is based on the assumption that the scatterer is electrically large, it cannot be applied in the low-frequency domain where the scatterers are smaller than the operational wavelength. For the same reason, the scattering results predicted in the resonance region ($X \sim 1$) are not accurate. Furthermore, GO is known to break down at the shadow boundaries and in the vicinity of the sharp edges (Stratton, 1941). Geometrical optics predicts a zero field in the shadow region of a conducting scatterer. This is yet another flaw of GO since in practice there is always a finite field, however small, in the shadow region. These drawbacks of GO are overcome by the introduction of a class of high-frequency asymptotic theories which essentially introduce corrections in the form of diffraction coefficients. The geometrical theory of diffraction (GTD) is one such example which has been extremely popular and also extensively modified to suit the various modeling requirements. Consequently asymptotic theories have found their way into the analysis of RAM as well.



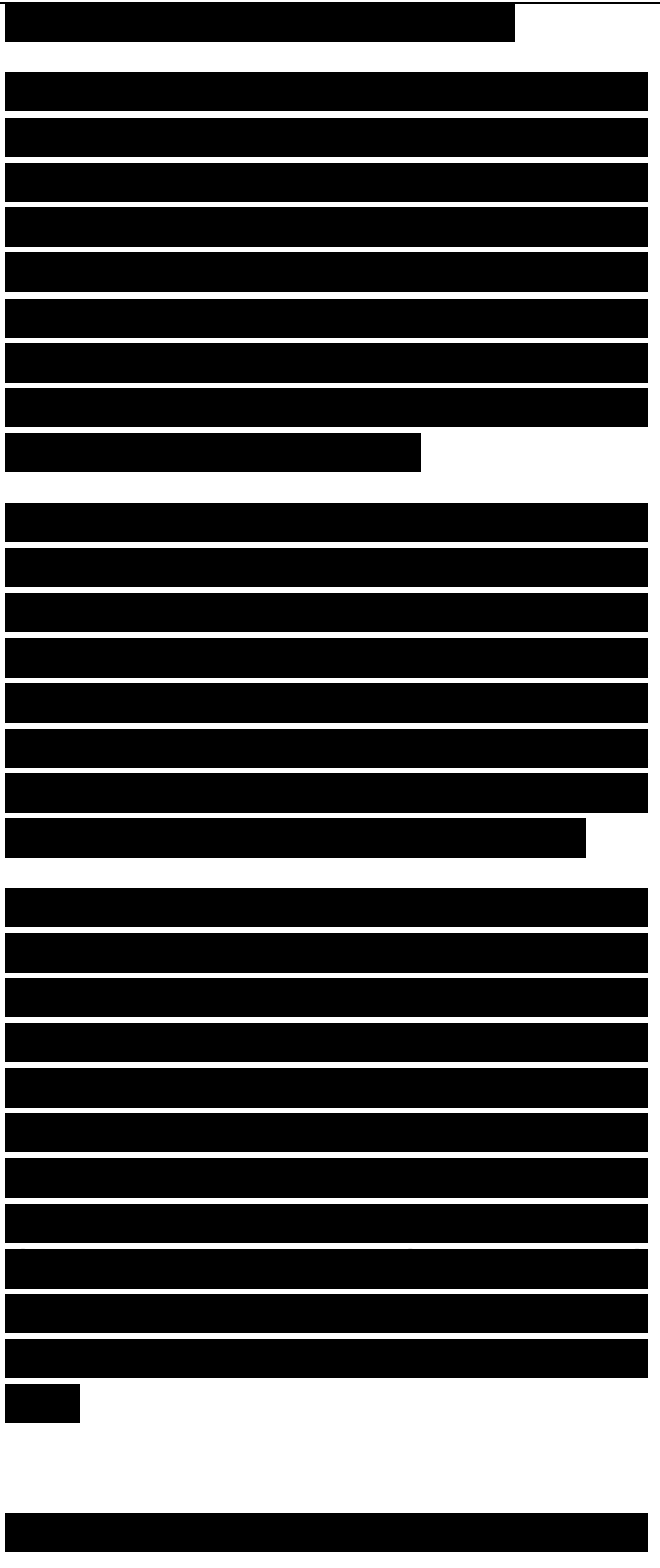
3.4.2 Geometrical Theory of Diffraction

The geometrical theory' of diffraction (GTD) is a modification of the GO formulation, which is well-known and easy to apply. GTD in fact incorporates the phenomenon of diffraction into GO by systematically introducing a set of diffracted rays to which the diffracted fields are associated. Diffraction occurs when a ray strikes any surface of discontinuity, such as an edge (edge-diffraction) or a vertex

Figure 3.13 Various Ivpes of diffraction mcchanism (a) I ip dilTraction. (b) Edge diffraction, and (c) Surfacc diffraction (itip-diffraction), or when it grazes a curved surface (surface-diffraction). The surface-diffraction phenomenon is represented by a ray path, whereas edge- diffraction results in Keller's cone (Bach, 1977), and tip-diffraction leads to volumetric scattering of the rays (Fig. 3.13).

Ray tracing between the source and the observation points constitutes the determination of all surfacc-rays, edge-diffracted rays, and tip-diffracted rays. In general, the edge-diffracted field is larger than the tip-diffracted field but smaller than the surfacc-diffracted field (Bach, 1977). The surface-, edge-, and tip- diffracted rays traverse in accordance with the generalized Fermat principle (Pathak và các cộng sự., 1981) which require the rays to be geodesics on the surface or straight lines in free space. The GTD field is therefore given as:

Although, Keller's GTD formulation (Keller. 1962) succeeded in overcoming the

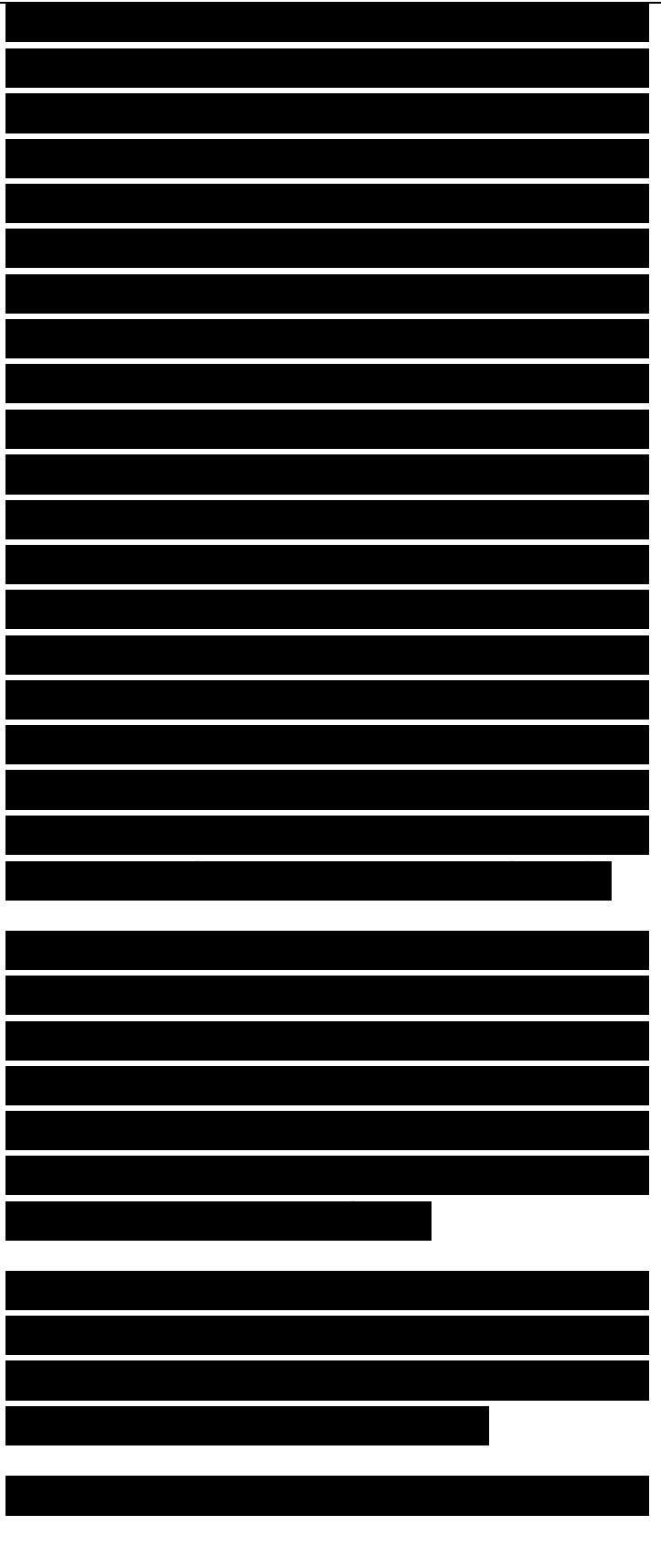


shortcomings of GO, it predicted infinite fields in the transition region (TR), in the immediate vicinity of the SB, and along caustic directions (Mittra, 1977). Much attention was devoted to developing uniform representations (Ahluwalia và các cộng sự., 1968; Kouyoumjian & Pathak, 1974[^] for the diffracted fields in angular regions. In the uniform asymptotic theory' (UAT), the infinities at the TR are annihilated by introducing an additive correction term which has an identical singularity at the TR (Ahluwalia và các cộng sự., 1968). In contrast Kouyoumjian and Pathak (1974) proposed the uniform theory of diffraction (UTD) where the cancellation of infinity is accomplished by a multiplicative factor that goes to zero, precisely at those observation angles where the Keller diffraction coefficients become infinite. All variants of GTD are generically referred to as GTD; among them. UTD is perhaps the most popular.

UTD assumes that the tangential electric field in the aperture is known, so that an equivalent infinitesimal source can be defined at each point in the aperture. Surface rays emanate from this source which is a caustic of the ray system. A launching coefficient is introduced to describe the excitation of the surface ray modes.

In the IR. the incident radiation from the source is treated by GO. In contrast, for a point Ps in the shadow region SR (Fig. 3.14), the UTD field due the source radiator

$$^,(ps) = E,(s,) [D,bS|bS2 + ^nslis2] I— (3.88)$$



where n and b represent the unit principal normal and unit binormal vectors for the geodesic at a given point. The application of the cikonal equation results in a similarity of form between eqs. (3.81) and (3.88). D , and D' , are the soft and hard diffraction coefficients as defined by Pathak (1992).

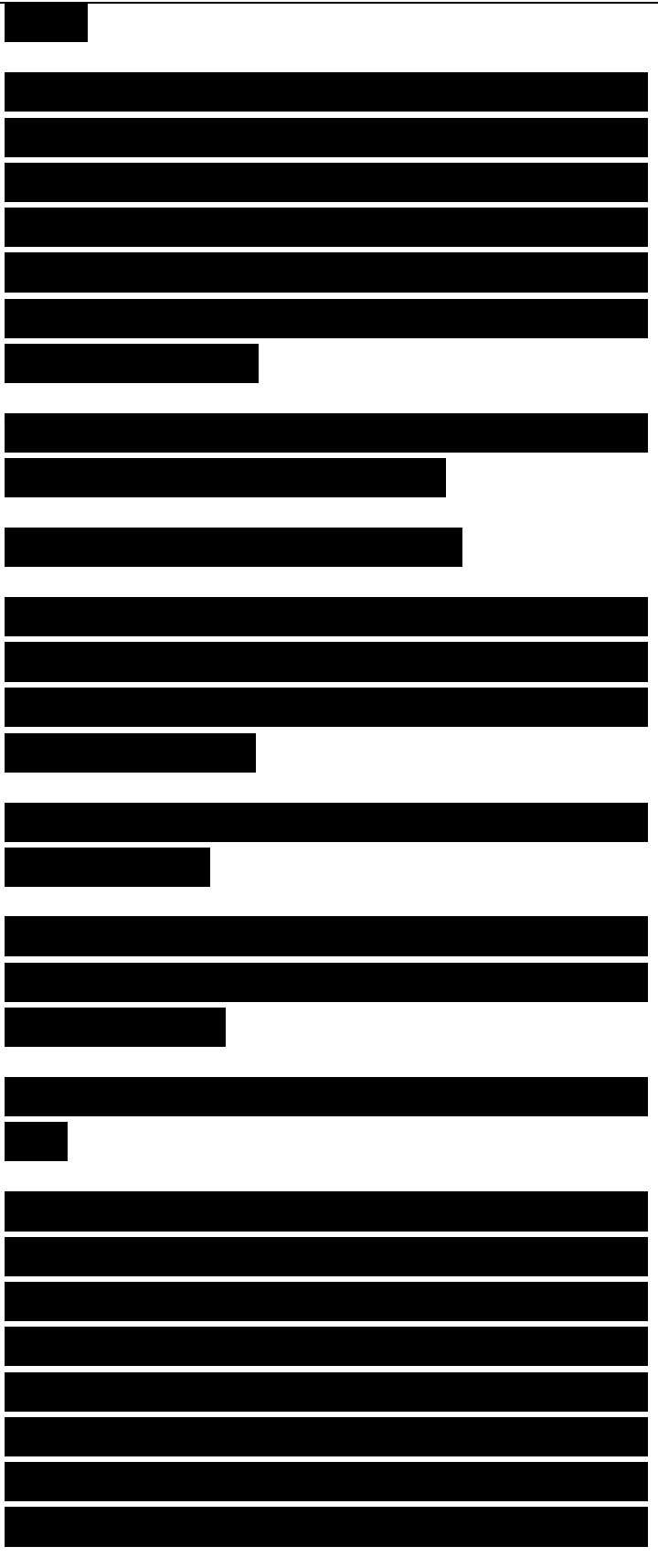
If the scattering takes place from a straight edge, the field in the shadow region has the form

$$F \cdot \hat{e}_s \cdot E(S) \quad (3.89)$$

The edge diffraction coefficient depends on the planes of incidence and diffraction with respect to the incident and edge-diffracted ray directions (Kouyoumjian & Pathak, 1974).

The volumetric scattering due to the tip-diffraction is expressed as where D , is a function of the wave number **besides** the incident and tip-diffracted ray directions (Sikta **và các cộng sự.**, 1983).

UTD has been successfully employed for scattering analysis of simple canonical shapes. The most extensively studied among these is the conducting right circular cylinder for which the predictions matched well (Pathak & Kouyoumjian, 1974) with the exact solution results for radii as small as 0.5λ . The ray analysis for the elliptic cylinder has been treated by Pathak **và các cộng sự.** (1981) where once



again the result matches well with the exact solution (Wait & Mientka, 1959). The radiating source in this case however, is located conveniently at the extremity of the cross-sectional profile. The ray analysis which is the main bottleneck in the application UTD, can

Figure 3.14 The fields in the shadow region of an electrically large smooth convex surface is due to surface diffraction be treated for open cylinders such as the general parabolic cylinder (Jha & Mahapatra, 1992) and the hyperbolic cylinders (Jha và các cộng sự., 1993) in the closed form.

